

**Synthesis of gold and palladium thiolato complexes and their
applications as sulfur dioxide sensors**

by

Busiswa Dyan

DISSERTATION

Presented in fulfillment for the requirements for the degree

MAGISTER SCIENTIAE

in

CHEMISTRY

in the

FACULTY OF SCIENCE

of the

UNIVERSITY OF JOHANNESBURG

Supervisor: Prof. J. Darkwa

March 2008

DEDICATION

To my mother Sibulelo Margaret Dyan, my aunt Duduzile Faith Mokhesi and my siblings

Andiswa Faith Dyan, Mawanda Dyan and Wandile Dyan



ACKNOWLEDGEMENTS

I would like to thank the lord for affording me this chance to study and guide me through the difficulties and challenges I came across during my studies. My sincere appreciation and gratitude to my supervisor, Professor James Darkwa, under whose guidance this research was conducted. I also wish to thank Mr Pierro Benincasa (University of Cape Town) for elemental analysis of samples, Dr Bernard Owaga (University of Johannesburg) for X-ray structural analysis of the complexes reported in this thesis, Mr Philani Mashazi and Dr Richard Moutlouli at Mintek for the Cyclic Voltammetry analysis reported in this thesis. I am grateful to Mintek for their financial assistance during this project. My special thanks are also due to Mr. Frankline Keter, Miss Zandile Hlengiwe Chonco and Mr Leslie Lungisa Maqeba Marareni for their undying support and to my co-researchers from the Inorganic group (University of Johannesburg) for their helpful suggestions during the project. My thanks are also due to the department of chemistry, University of Johannesburg.

ABSTRACT

[AuCl(PPh₃)] was reacted with mixed thiols in the presence of silver(I) oxide, resulting in complexes of the type [Au(SC₆H₄X)(PPh₃)] X= Cl, NH₂,CH₂, forming silver chloride as a by-product. In addition to the above series [Au(SCH₂(C₆H₄)₃(2-C₆H₅(C₆H₄N))] was prepared *via* a different route, where [AuCl₃(2-C₆H₅(C₆H₄N))] was reacted with benzyl mercaptan under reflux in the presence of silver(I) oxide for 3 h, forming silver chloride as a by-product. Palladium complex [PdCl₂(2-C₆H₅(C₆H₄N))] was prepared by reacting [PdCl₂(MeCN)] with 2-phenylpyridine at room temperature for 2 h. All complexes were characterized by ¹H, ¹³C, ³¹P{H} NMR, IR, mass spectrometry and elemental analysis. Characterization of the starting materials [AuCl₃(2-C₆H₅(C₆H₄N))] and [PdCl₂(2-C₆H₅(C₆H₄N))] by single crystal X-ray diffraction confirmed their chemical formula.

All complexes were reacted with sulfur dioxide (SO₂) and the reactions were monitored by electrochemistry and UV-vis spectroscopy. The electrochemical study of the complexes, using cyclic voltammetry (CV) and Osteryoung square wave voltammetry (OSWV), showed one anodic peak, which is due to gold(I/III) and an unresolved peak due to thiolate ligand. Upon bubbling of SO₂ to the complexes, there was an immediate change of colour from clear to yellow, the CV results showing an increase in current of the gold(I/III) peak. UV-vis spectroscopy studies showed a shift of peak from 250-286 nm, upon bubbling of SO₂ to complexes.

TABLE OF CONTENTS

	Page
Title page	i
Dedication	ii
Acknowledgements	iii
Abstract	iv
Table of contents	v
List of Figures	viii
List of Schemes	x
List of Tables	xi
List of Abbreviations	xii
CHAPTER ONE: INTRODUCTION	1
1.1 General metal thiolates	1
1.2. Chemistry and reactions of sulfur and thiols	2
1.3. Metal thiolate and phosphine ligands	6
1.4 Gold thiolate complexes	8
1.5. Gold thiolate complexes as biological models	9
1.6. Luminescence of gold thiolate complexes	12
1.7. Redox behavior of organogold compounds	15
1.8. Palladium thiolate complexes	18
1.9. Metal thiolate complexes as nucleophiles for SO ₂	20

1.10.	Techniques for detection of SO ₂	23
1.11	Fundamentals of electrochemistry	29
1.12	Objectives and rationale of the study	30
	References	31
 CHAPTER 2: MATERIALS AND METHODS		39
2.1.	Materials and Methods	39
2.2.	Instrumentation	41
2.3.	Preparation of starting material	41
2.3.1.	Synthesis of H ₂ AuCl ₄ ·4H ₂ O	41
2.3.2.	Reaction of H ₂ AuCl ₄ ·4H ₂ O with PPh ₃	42
2.3.3.	Reaction of OHC(C ₆ H ₄)OCH ₂ (C ₆ H ₅) with HS(C ₆ H ₄)NH ₂	42
2.3.4.	Reaction of [PdCl ₂ (MeCN) ₂] with 2-phenylpyridine	42
2.4.	Preparation of complexes	43
2.4.1.	Reaction of chloro-triphenylphosphinegold(I) with mixed thiols	43
2.4.1.1.	Reaction of [AuCl(PPh ₃)] with benzyl mercaptan	43
2.4.1.2.	Reaction of [AuCl(PPh ₃)] with 2-aminothiophenol	43
2.4.1.3.	Reaction of [AuCl(PPh ₃)] with 4-Chlorothiophenol	44
2.4.2.	Reaction of tris-chloro-2-phenylpyridine gold(III)	45
2.4.2.1.	Reaction of H ₂ AuCl ₄ ·4H ₂ O with 2-phenylpyridine	45
2.4.2.2.	Reaction of [AuCl ₃ (2-C ₆ H ₅ (C ₆ H ₄ N))] with benzyl mercaptan	45
2.5.	Crystallographic structure determination	46
2.6.	Electrochemistry studies	47

2.7. UV-vis Spectrometry studies	48
References:	49
CHAPTER 3: RESULTS AND DISCUSSION	50
3.1 Synthesis of $[\text{Au}(\text{SC}_6\text{H}_4\text{X})(\text{PPh}_3)]$ X = 4-Cl, NH ₂ , CH ₂	50
3.1.1. Characterization by NMR Spectrometry	51
3.1.2. Characterization by infrared Spectrometry	58
3.2. Synthesis of gold thiolate complexes	60
3.2.1. Molecular structure of 6	63
3.2.2. Synthesis of $[\text{Au}(\text{SR})_3(2\text{-C}_6\text{H}_5(\text{C}_6\text{H}_4)\text{N})]$	67
3.3. Synthesis of palladium(II) complexes	70
3.3.1. Synthesis of palladium(II) thiolate complexes	75
3.4. Electrochemical studies	76
3.4.1. Introduction: An overview	76
3.5. Redox chemistry of gold thiolate complexes	78
3.5.1 Oxidative process of $[\text{AuCl}(\text{PPh}_3)]$	78
3.5.2. Oxidative process of gold(I) and gold(III) complexes	81
3.5.3. Reactions of complexes with sulfur dioxide	85
3.6. Palladium thiolate complexes	92
3.7. Visible and ultraviolet Spectroscopy studies	96
References	100

LIST OF FIGURES

- Figure 1. 1: Examples of thiol ligands
- Figure 1.2: Structural types of transitional metal complexes with dithiolate and phosphine ligands
- Figure 1.3: Gold(I) drugs for the treatment of rheumatoid arthritis: aurothiomalate, aurothioglucose, auranofin.
- Figure 1.4: Structures of Au(III) 2-(dimethylamino)phenyl complexes
- Figure 1.5: Different SO₂ coordination geometries
- Figure 3.1: ¹H NMR spectrum of [Au(SCH₂(C₆H₅)(PPh₃)]
- Figure 3.2: ¹H NMR spectrum of [Au(4-SC₆H₄Cl)(PPh₃)]
- Figure 3.3: ¹H NMR spectrum of 4-hexyloxyC₆H₄N(CH)C₆H₄
- Figure 3.4: IR spectrum of [Au(4-SC₆H₄Cl)(PPh₃)] as a KBr pellet
- Figure 3.5: ¹H NMR spectrum of [AuCl₃(2-C₆H₅(C₆H₄N))]
- Figure 3.6: Molecular structure of [AuCl₃(2-C₆H₅(C₆H₄N))]
- Figure 3.7: ¹H NMR spectrum of [Au(SCH₂(C₆H₅))₃(2-C₆H₅(C₆H₄N))]
- Figure 3.8: Molecular structure of [PdCl₂(2-C₆H₅(C₆H₄N))]
- Figure 3.9: Cyclic Voltammetry of [AuCl(PPh₃)]
- Figure 3.10. Electron-transfer Scheme for K[AuCl₄], [Au(PPh₃)]Cl and [Au(PPh₃)₂]⁺
- Figure 3.11: Cyclic Voltammetry of [Au(SCH₂(C₆H₅)(PPh₃)]

Figure 3.12: Showing the colours of complex before (a) and after bubbling of SO₂ (b)

Figure 3.13: Cyclic Voltammetry of [Au(SCH₂(C₆H₅)(PPh₃))] before and after bubbling of SO₂

Figure 3.14: Osteryoung Square Wave Voltammetry of [Au(SCH₂(C₆H₅)(PPh₃))]

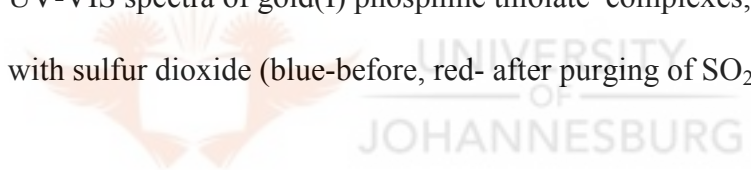
Figure 3.15: Osteryoung Square Wave Voltammetry of [Au(SCH₂(C₆H₅)(PPh₃))]

Figure 3.16: Structure of palladium thiolate complex

Figure 3.17: Cyclic Voltammetry of palladium thiolate complex

Figure 3.18: Cyclic Voltammetry of palladium thiolate complex before and after bubbling of SO₂

Figure 3.19: UV-VIS spectra of gold(I) phosphine thiolate complexes, with sulfur dioxide (blue-before, red- after purging of SO₂)



LIST OF SCHEMES

- Scheme 1.1: Examples of sulfides
- Scheme 1.2: Bonding modes of thioether and thiolate ligands and potentially
- Scheme 1.3: Gold(I) phosphine complex exhibiting interaction between gold(I)---gold(I)
- Scheme 1.4: Redox chemistry of $[\text{Au}(\text{SR})(\text{PPh}_3)]$
- Scheme 3.1: Synthesis of $[\text{Au}(\text{SCH}_2(\text{C}_6\text{H}_5)(\text{PPh}_3)]$
- Scheme 3.2: Synthesis of $[\text{Au}(2\text{-SC}_6\text{H}_4\text{NH}_2)(\text{PPh}_3)]$
- Scheme 3.3: Synthesis of $[\text{Au}(4\text{-SC}_6\text{H}_4\text{Cl})(\text{PPh}_3)]$
- Scheme 3.4: Synthesis of 4-hexyloxy $\text{C}_6\text{H}_4\text{N}(\text{CH})\text{C}_6\text{H}_4$
- Scheme 3.5: Synthesis of $[\text{AuCl}_3(2\text{-C}_6\text{H}_5(\text{C}_6\text{H}_4\text{N}))]$
- Scheme 3.6: Synthesis of gold(III) thiolates complexes
- Scheme 3.7: Synthesis of palladium(II) thiolato complexes
- Scheme 3.8: Electron transfer of $[\text{Au}(\text{SCH}_2(\text{C}_6\text{H}_5)(\text{PPh}_3)]$
- Scheme 3.9. Show possible ways SO_2 could react with the complex

LIST OF TABLES

- Table 1.1: The SO₂ coordination geometry and infrared stretching frequencies
- Table 3.1: Crystal data and structure refinement for [AuCl₃(2-C₆H₅(C₆H₄N))]
- Table 3.2: Selected bond length (Å) and bond angles (°) for tris-chloro-2-phenylpyridinegold(III)
- Table 3.3: Crystal data and structure refinement for **8**
- Table 3.4: Selected bond length (Å) and bond angles (°) for dichloro-bis-2-phenylpyridinepalladium(II)
- Table 3.5: Cyclic Voltammetry data for gold(I) phosphine and gold(III) thiolate complexes before and after bubbling of SO₂
- Table 3.6: Cyclic Voltammetry Data for palladium(II) thiolate complexes. Before and after bubbling of SO₂

LIST OF ABBREVIATIONS

CV	Cyclic Voltammetry
OSWV	Osteryoung Square Wave Voltammetry
[n-Bu ₄ N][BF ₄]	tetrabutylammonium-tetrafluoroborate
SO ₂	Sulfur dioxide
THF	Tetrahydrofuran
CH ₂ Cl ₂	Dichloromethane
CaH ₂	Calcium hydride
UV-vis	Ultraviolet visible spectroscopy
SCE	Standard calomel electrode
FT-IR	Fourier transform infrared
OGC	Organogold compounds



Chapter one

Introduction

1.1. General metal thiolates

Metal thiolates can be generally classified as metal complexes that contain a metal center, usually a transition metal that is bound to a thiolate ligand through the sulfur atom. The thiolato ligand has an organic unit attached to the sulfur. A complex is not a metal thiolate when the sulfur does not have an organic unit. These metal thiolates can be mononuclear; nuclear and even clusters.¹ Metal thiolato complexes are the subject of increasing interest because of their versatile chemistry. Worthwhile topics for study include the potential of thiolate complexes with respect to C-S bond cleavage reactions and desulfurization,² novel structures of coordination complexes³ and the possibility of stabilization of unusual oxidation states. Applications in the study of biological systems⁴ and use in medicine as antiarthritic or cancerostatic drugs⁵ also contribute to the growing interest in these compounds and in particular of gold thiolate complexes.⁶ Generally metal thiolates are prepared from thiols and thiolate ligands bind to a metal through a sulfur atom in the ligand. To understand metal thiolates better, one needs to understand the chemistry of sulfur and thiols.

1.2. Chemistry of sulfur and thiols

Sulfur is the element just below oxygen in the periodic table, and many oxygen-containing organic compounds have sulfur analogs. Thiols, R-SH, are sulfur analogs of alcohols and sulfides, R-S-R, are sulfur analogs of ether. Thiols are named in the same way as alcohols, with the suffix *-thiol* used in place of *-ol*. The -SH group itself is referred to as a mercapto group.⁷ Example of thiols are shown in Figure 1.1.

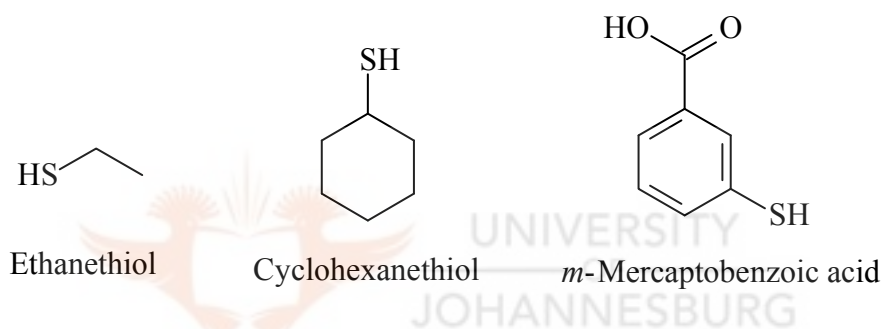
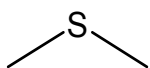
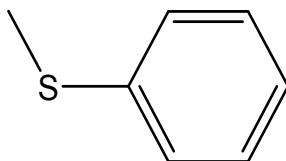


Figure 1.1: Examples of thiol ligands

Sulfides are named in the same way as ethers, with sulfide used in place of ether for simple compounds and with alkylthio used in place of alkoxy for more complex substances.⁷



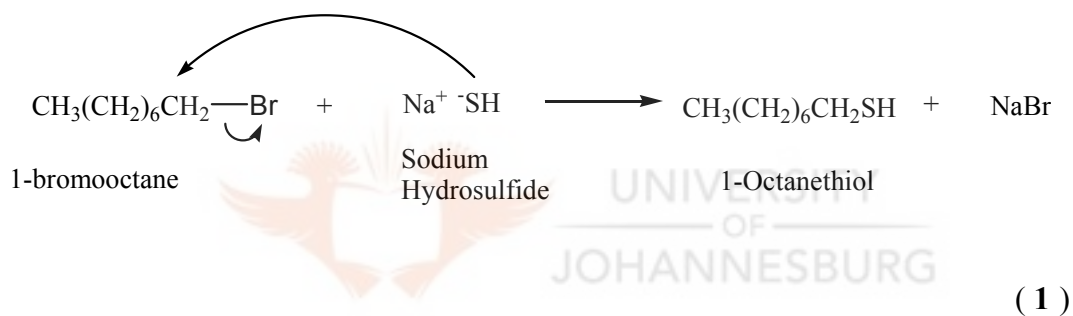
Dimethyl sulfide



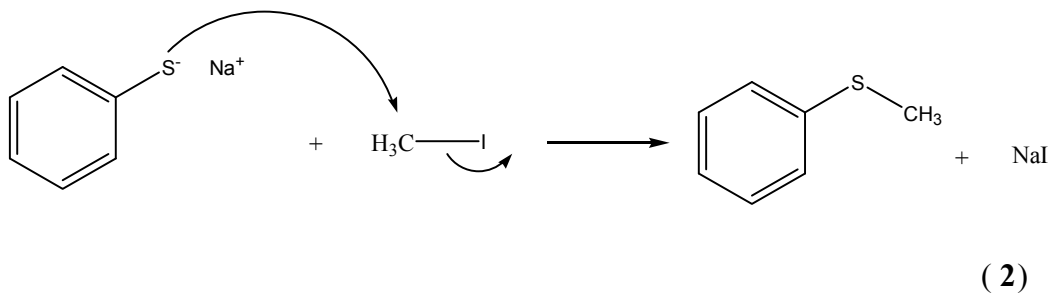
Methyl phenyl sulfide

Scheme 1. 1: Examples of sulfides

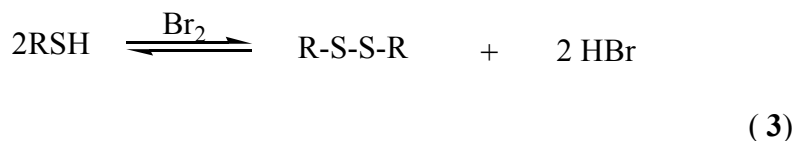
Thiols are usually prepared from the corresponding alkyl halide by S_N2 displacement with a sulfur nucleophile such as hydrosulfide anion, SH^- (equation 1)



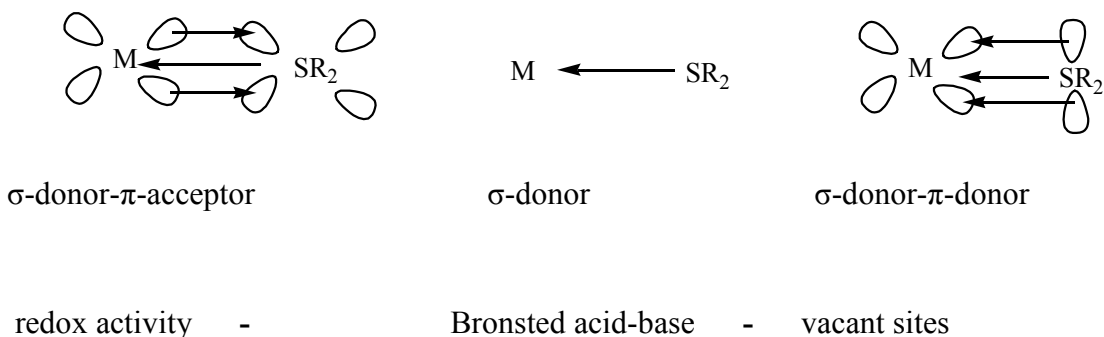
Sulfides are prepared by treating a primary or secondary alkyl halide with a thiolate ion, RS^- . Reaction occurs by an S_N2 mechanism that is analogous to the Williamson ether synthesis.⁷ Thiolate anions are among the best nucleophiles known, so these reactions usually work well. (equation 2)



The most unforgettable characteristic of thiols is their appalling odor. Thiols can be oxidized by mild reagents such as bromine to yield disulfide, R-S-S-R and disulfides can be reduced back to thiols by treatment with zinc metal and acetic acid.⁷ (equation 3)



It is important to elucidate the characteristic features connected with the combination of transition metals and sulfur donors, starting from bidentate dithiolates such as ethane or benzene-dithiolate. These ligands coordinate to biorelevant metals such as Fe, Mo, W, Ni, Co or their group homologues, and the resultant complex fragments are able to bind a large variety of coligands L or L'. It may be noted that L and L' comprise species that are relevant to N₂ fixation, the nitrate-ammonia interconversion, hydrogenases and CO dehydrogenases and the biological sulfur cycle. The coligands can exhibit remarkable electronic flexibility. Scheme 1.2 suggests a few reasons for this flexibility.⁸



Scheme 1.2: Bonding modes of thioether and thiolate ligands and potentially binding

From a biological, but also from a theoretical point of view, it can be anticipated that ligands with biorelevant sulfur donors, i.e. sulfide, thiolate and thioether donors, differ from ligands e.g. such as phosphine or carbon ligands. For instance thioether, thiolate or sulfide S atoms can be expected to act as σ -donor, as σ -donor- π -acceptor, or due to the remaining lone pairs, as σ -donor- π -donor ligands.

The actual bonding modes will depend on the occupation of the metal d orbitals. The variability of the bonding modes also may explain why metal sulfur fragments so frequently exhibit redox activity, Bronsted acid-base behaviour and vacant sites of coordination. These three properties are essential if a molecule **A** is to be activated or stabilized by coordination to a metal sulfur site in order to be transformed subsequently into **B** by addition of protons and electrons according to equation 4. Equation 4 is the most general expression of a typical reductase reaction, stressing the coupling of proton and electron transfer.⁸



The interesting properties that sterically hindered thiols confer to the compounds they form with transition metal complexes have been known for a number of years.⁹ Thus some of these ligands have been employed for the synthesis of species with unusual structures and reactivities.⁹ Of fundamental importance has been the use of thiols as

ligands for the synthesis of different compounds for the modeling of active centers of metalloenzyme, this being particularly true in the case of the nitrogenase enzyme.¹⁰ Hence thiolate complexes continue to attract considerable interest due to the aforementioned chemical properties and structural diversity.¹¹

Given the facility with which thiols can be tuned both sterically and electronically, they have been widely used as auxiliary ligands.¹² The presence of electron-withdrawing groups or substituents with steric requirements favours the formation of mononuclear complexes rather than thiolate bridged oligomers, usually generated by using unencumbered thiols.⁹ Moreover, thiolate complexes are known to undergo chemistry at the sulfur center, including redox and protonation-deprotonation process, which is a plus to traditional chemistry as these complexes are usually centered on the metal,¹³ Hence, our interest in the syntheses and application of thiolate complexes.

1.3. Metal thiolate and phosphine ligands

Transition metal complexes with phosphine ligands have been studied extensively, not only due to their variation in geometric and electronic structures and properties, but also because of their applications in homogeneous or heterogeneous catalysis functions.¹⁴ On the other hand metal thiolates are known to be ubiquitous biological electron-transfer mediators and have been studied for two decades.¹⁵

However, complexes blending both phosphine and thiolate ligands have received attention only in recent years.¹⁶ The earlier studies were mainly in the syntheses of simple

complexes and survey of their properties and a few of these simple complexes have been structurally analysed.¹⁶ Synthesis of metal thiolate phosphine complexes such as $(\text{Et}_4\text{N})[\text{Co}(\text{SPh})_3(\text{PPh}_3)]^{17}$, $[\text{Co}(\text{SPh})_2(\text{CH}_2)_3\text{PPh}_2]^{18}$ [$\text{L} = \text{Ph}_2\text{P}(\text{CH}_2)_3\text{PPh}_2$] and $[\text{Ni}(\text{SC}_2\text{H}_4\text{SC}_2\text{H}_4\text{S})\text{PR}_3]^{18}$ have been reported. Products from the reactions of Ni^{2+} , edt^{2-} and PR_3 ($\text{R} = \text{Ph}, \text{Et}$) in MeOH , have also been isolated. Surveying the studies on metaldithiolate-phosphine complexes, the structural types can be divided into those shown in (Fig. 1.2).

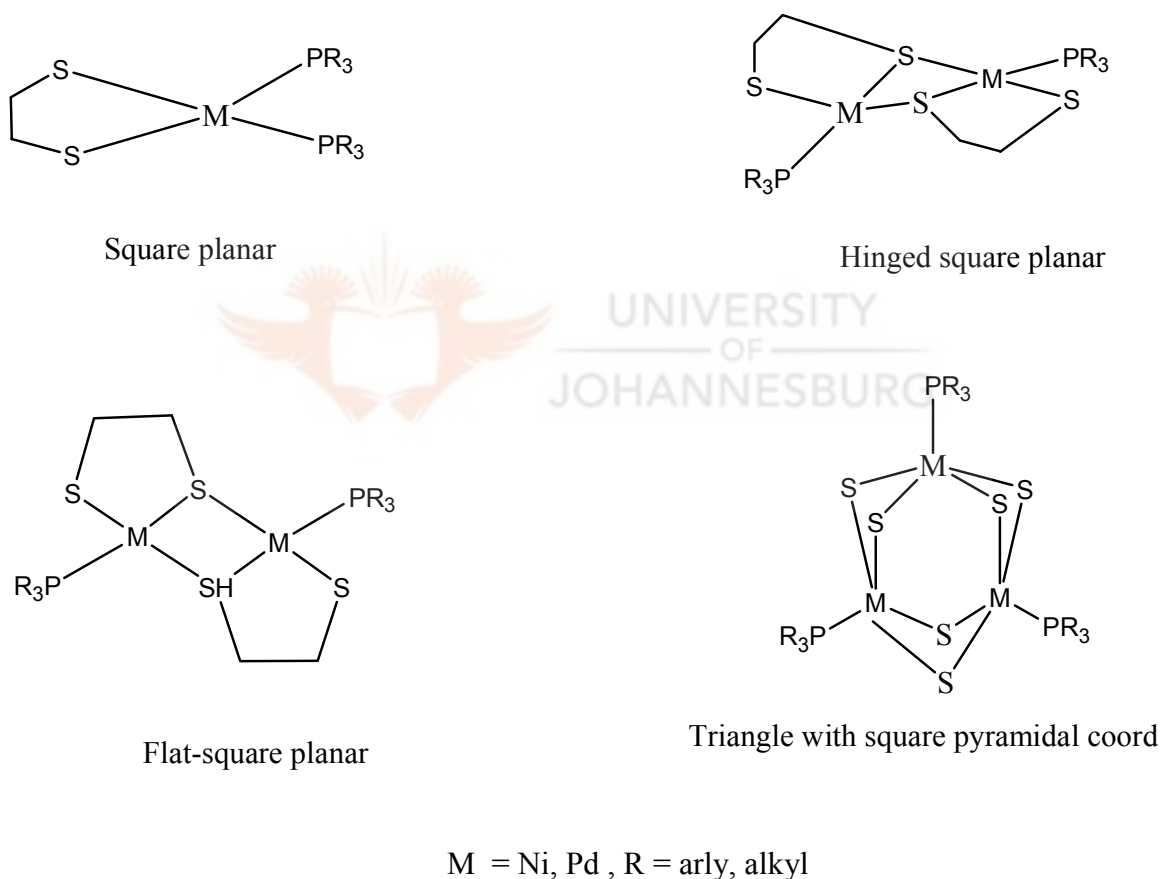


Figure 1.2: Structural types of transitional metal complexes with dithiolate and phosphine ligands

All the complexes with hinged square-planar geometry have shorter Pd-Pd distance than those with flat square-planar complexes. But they are longer than those of the corresponding hinged square-planar nickel complexes, due to the larger atomic radius of the palladium. The dihedral angles for the hinged square planar complexes vary with the change of central metal atoms, thiolate ligands and R substituent of the phosphine ligands.¹⁹

1.4. Gold thiolates complexes

Gold thiolates are an extremely important class of gold compounds. Complexes of the type Au(SR) or AuL(SR) (R = alkyl, aryl), L = neutral donor ligand).²⁰ Thiols function as the key connectives between the surface of bulk gold and the substrate films in self-assembly monolayer (SAM).²¹ The high affinity of gold for the heavy chalcogen elements (sulfur, selenium and tellurium) allows the synthesis of many Au-S preparations from gold salts and thiols or thiolates.²² Most of the thiolate compounds are thermodynamically unstable relative to gold metal and organic disulfides. Many gold(I) thiolates (AuSR) (R = alkyl, aryl) and ancillary ligands gold(I) thiolates complexes, AuL(SR) (R = alkyl, aryl L = neutral donor ligand,) are known to aggregate either *via* intermolecular aurophilic contacts(*i.e.* Au-Au closed-shell interaction) or intermolecular gold-sulfur coordination (Au---S) depending on the electronic or steric nature of the substituents. These interactions lead to interesting supramolecular structures often associated with intriguing photophysical properties.²⁰

Theoretical work has predicted that gold---gold contacts should be particularly strong with sulfides or thiolate substituents,²³ but structural data does not always follow this pattern because Au-S contacts are also able to compete efficiently and a delicate balance between the two types of interactions often lead to unexpected results.²⁴ In the design of a structural pattern, crystal engineering, other weak forces can be combined with gold---gold/gold---S interactions and in recent attempts to incorporate hydrogen bonding have been particularly successful.²⁵

Ligands which offer both thiolate and carboxylate functions have been shown to be instrumental in the construction of multidimensional arrays of gold(I) complexes.²⁶ Other systems probed successfully in this context were those based on hydroxyphosphine/phosphinate,²⁷ imidazole/imidazolate and phosphinophenol/phosphinophenolate gold complexes.²⁸



1.5. Gold thiolate complexes as biological models

Gold(I) compounds with phosphine ligands or sulfur-containing ligands are most commonly used in the treatment arthritis. However, very little is known about how gold compounds perform their functions in *vivo*, despite the fact that numerous studies have been carried out in this area. Some studies suggest that the interaction of the gold(I) center with thiol or disulfide linkages in biomolecules may play an important role.²⁹

Gold(I) thiolate complexes such as aurothiomalate, aurothioglucose (Fig. 1.3) have been used as antiarthritic drugs since the 1920s.³⁰ More recently these compounds have been supplemented by phosphine complexes, eg. Auranofin, which was approved for clinical use in 1985.³¹ Coordination of gold(I) with phosphine ligands stabilizes the oxidation

state of gold against disproportionation to gold(0) and toxic gold(III) whilst allowing exchange reactions with biological ligands. A series of compounds have the general formula $[\text{Au}(\text{SR})(\text{PPh}_3)]$ where R is an alkyl group and SR a diverse range of ligands such as thioglucose, acetylated thioglucose, and 2-mercaptoethanol.³² Complexes of this type are monomeric, two co-ordinate, linear species and generally nonionic and lipophilic and therefore readily absorbed after oral administration. The triethylphosphine complexes are found to have the optimum pharmacological activity.³²

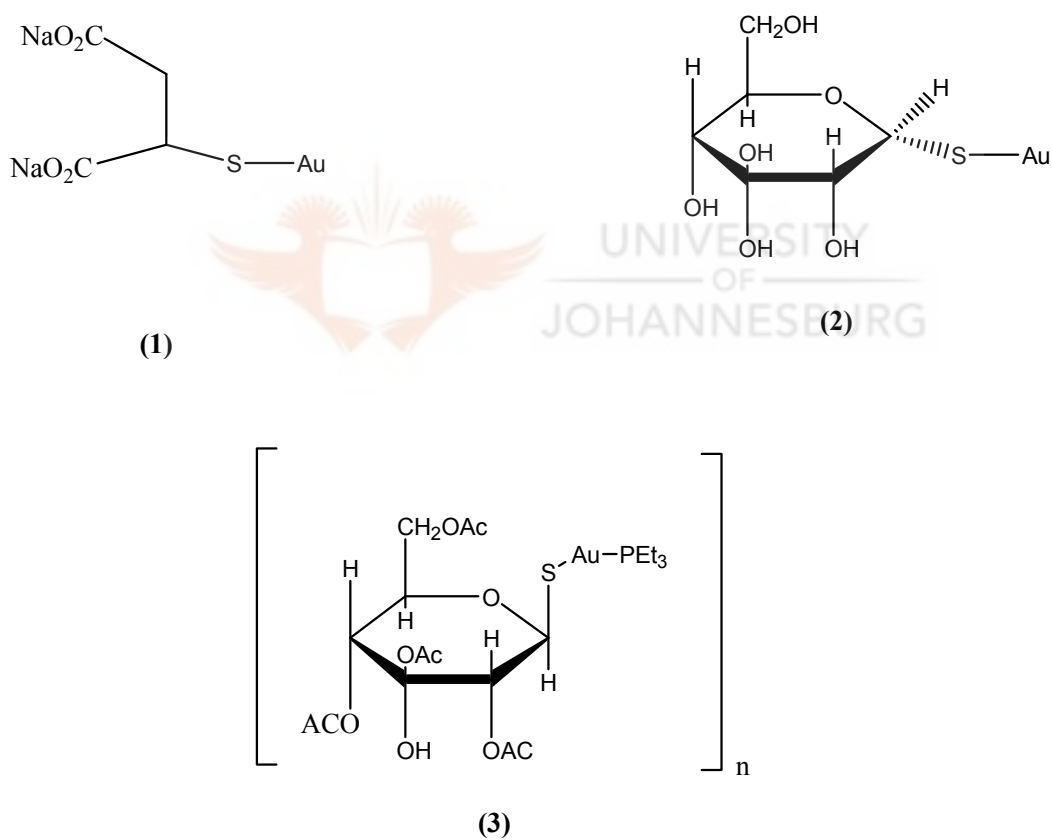


Figure 1.3: Gold(I) drugs for the treatment of rheumatoid arthritis: Aurothiomalate (1), Aurothioglucose (2), Auranofin (3)

In contrast to the extensive studies on gold(I) thiolate complexes, studies on the biological chemistry of gold(III) complexes are substantially fewer, primarily because of their reactivity. As gold(III) is isoelectronic (d^8) with platinum and likewise forms square planar complexes, it is therefore tempting to speculate that such complexes would have similar anti-tumor activity to cisplatin.³² Gold(III) are not reactive. In order to stabilize the gold(III) oxidation state in a reducing biological milieu, mononegative bidentate ligand, (damp(2-[(dimethylamino)methyl]phenyl) (Fig. 1.4) and two monodentate anionic ligands e.g. Cl or acetate or bidentate ligands such as oxalate and malonate (Figure 1.4) have been used.³³

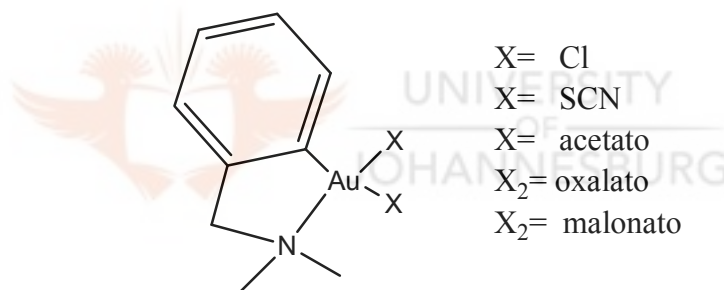


Figure 1.4: Structures of Au(III) 2-(dimethylamino)phenyl complexes

The damp ligand forms part of a five-membered chelate ring in which the nitrogen of the amine group and the carbon of the aryl ring bond to the metal resulting in the Au(III) being stabilized by the σ -bonded carbon. The monodentate ligands are readily hydrolysed and are available for substitution.³⁴

Laguna and co-workers³⁵ reported the synthesis of gold(I) and gold(III) complexes with the 1-methyl-2-sulfanyl-1,2-dicarbido-*closo*-dodecarborate ligand incorporating an *o*-carboarane moiety. A few novel gold(III) thiolate complexes have been reported with interest focusing on synthesis and structures, where a series of 2-phenylpyridine Au(III) compounds were reacted with various thiolato ligands.³⁶ Using both monodentate (SCN⁻) and bidentate (thioacetic acid, thiosalicylic acid, 2,3-dimercapto-1-propanolate, *meso*-2,3-dimercaptosuccinate) thiolate ligands a new series of gold(III) thiolate complexes have been synthesized.³⁶ Henderson *et al.*³⁷ also recently reported that certain gold(III) complexes containing the chelating thiosalicylate (tsc) dianionic ligand showed high to very high antitumour activity against P388 Leukemia cell.³⁷ It is noteworthy that there are some gold(III) complexes containing xanthate ligands have been reported by Laguna and co-workers.³⁸



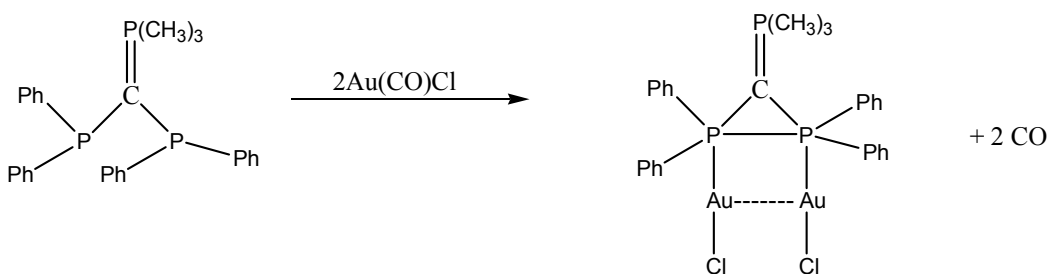
Certain platinum(II) thiosalicylate complexes have also shown high antimicrobial activity. This suggests that this class of complexes offer potential development of antitumor agent.³⁹ The use of gold compounds in the treatment of rheumatoid arthritis is thought to depend on the binding of gold at the sulfur-containing amino acid residues.⁴⁰

1.4. Luminescence of gold thiolate complexes

Gold(I) complexes containing phosphine or thiolate ligands exhibit interesting photochemical and photophysical properties.⁴¹ Luminescence is generally assigned as phosphorescence.⁴² The nature of luminescence in gold compounds is not clearly

understood.⁴³ It is thought that the aurophilic interaction of closed shell attraction plays a role. Of particular interest is the relationship between the observation of emission and the presence of weak bonding interactions between neighbouring gold centre in solid state; evidence for a weak bond between gold atoms is provided by gold(I)---gold(I) separation, where the gold(I)---gold(I) distances are about 2.8-3.0 Å.⁴⁴

Such a short distance indicates significant aurophilic attraction between the two gold(I) atoms. These bond distances are less than the van der Waals radius of 3.4 Å. The energy of gold(I)---gold(I) aurophilic attraction existing in the solid state and solution is estimated to be 30-60 kJ/mol.⁴⁴ This estimate is based upon the observation that coordination of a bis(phosphine) molecule to two Au-Cl fragments alters the ground-state conformation of the phosphine ligand as a result of a gold---gold interaction. (Scheme 1.3).⁴⁵



Scheme 1.3: Gold(I) phosphine complex exhibiting interaction between gold(I)---gold(I)

When aurophilic attraction is present, gold(I) complexes will exhibit luminescence. Luminescence of several binuclear phosphine gold(I) thiolate complexes have assigned to

metal-center (MC) ($d_z^2\sigma$ - $p_z\sigma$), in several binuclear gold(I) phosphine thiolate complexes, however the emission is attributed to the gold to thiolate or sulfur metal charge transfer (MLCT) transition.⁴⁴ Charge-transfer transition is when an electron is moved from orbital of the ligand to orbital of the metal. The transition is classified as a ligand to metal charge transfer (LMCT) transitions. In some complexes the charge migration occurs in the opposite direction, in which case it is classified as a metal to ligand charge transfer (MLCT) transition.⁴³

In binuclear gold(I) complexes, phosphines differ from thiolates in bonding nature. Phosphine ligands provide lone pair electrons to contribute the dative bond from P to Au. However thiolates as anions prefer a covalent bonding between the S and Au atoms to coordinating. These different electronic properties will change the luminescent properties when thiolates are introduced into the phosphine gold(I) complexes, $[\text{Au}_2(\text{PPh}_2)_2(\text{SC}_4\text{N}_2\text{H}_3)_2]$, to form gold (I) phosphine thiolate complexes.⁴³

In contrast to the related gold(I) and the isoelectronic platinum(II) compounds, which are known to show rich luminescence properties, luminescent gold(III) compounds are rare, with very few exceptions that emit at room temperature in solution.⁴⁶ The reasons for lack of luminescence in gold(III) species are probably the presence of low-energy d-d ligand field states and the electrophilicity of the gold(III) center. The presence of a non-emissive low-lying d-d state would quench the luminescence excited state by thermal equilibration or energy transfer.⁴⁷

Coupling of strong σ -donating alkyl ligands to gold(III) should render the metal center more electron rich, with additional advantage of raising the energy of the d-d states, which would result in enhanced luminescence by increasing the chances of populating the emissive state for the construction of organometallic materials.⁴⁸ Despite the fact that alkynyl complexes of gold(I) and the isoelectronic platinum(II)⁴⁹ are known and have been shown to display rich photoluminescent properties.⁴⁶

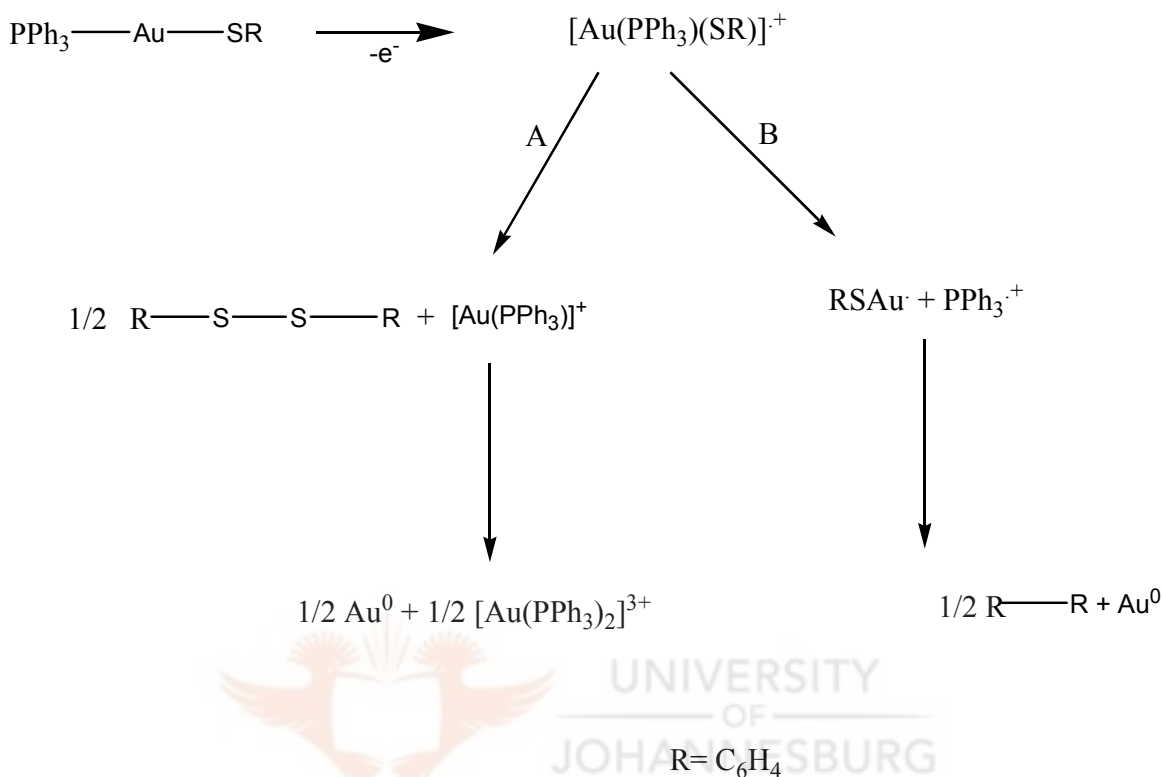
1.5. Redox behavior of organogold compounds

Compounds with single gold atoms are classified according to the oxidation state of the metal: gold(I), gold(II), gold(III) and gold(V). Gold(I) and gold(III) compounds are the most stable, while the oxidation state gold(II) is very rare.⁵⁰ Oxidation state gold(V) is found in the fluoride complexes AuF_6^- and AuF_5 . Most of the mononuclear organogold compounds (OGC) described up to now contain the metal in the oxidation state gold(I) and gold(III), although there is a large number of clusters containing gold-gold bonds, in which one cannot assign an oxidation state to any particular metal atom.⁵¹

As a metal, gold differs from other metals in that dissolved oxygen does not oxidize it, either in acidic or in alkaline aqueous media, unless there is a ligand capable of coordination with gold. This is why gold is considered the most noble metal. However, in the presence of such substances as cyanides or phosphines, accompanied with halide ions, the oxidation of gold proceeds easily and stable compounds of monovalent gold $[\text{Au}(\text{CN})_2]$, $[\text{AuClPPh}_3]$, are formed. The coordination number of gold(I) is usually two. There have been few studies on the electrochemical behavior of OGC.⁵¹

The first concerns the cathodic reactions of sandwich dicarbonyl complexes of gold, namely $((3)-1,2-B_9C_2H_{11})_2Au(Et_4N)_2$ and $((3)-1,2-B_9C_2H_{11})_2AuPPh_3Me$.⁵² These complexes are reduced reversibly in two single-electron steps that correspond to consecutive processes gold(III)/gold(II) and gold(II)/gold(I). It is better to measure electrochemical potentials of OGC using platinum, gold or glassy-carbon electrodes. The data obtained on platinum or gold electrodes are almost similar.⁵¹

The electrochemical oxidation of gold(I) chlorides was reported to proceed as an irreversible two-electron process leading to derivatives of trivalent gold. On the contrary, results obtained by Rakhimov *et al.*⁵³ indicate that the oxidation and reduction waves of all OGC should be considered as single-electron process.⁵³ Consequently, the electrochemical oxidation of these compounds does not cause any changes of the gold oxidation state. Thus, one can suggest two alternative ways for the electrochemical oxidation of OGC to take place.⁵¹



Scheme 1. 4: Redox chemistry of [Au(PPh₃)(SR)]

From this Scheme 1.4 it is very difficult to make an unambiguous choice between these two mechanistic pathways of electrooxidation. It should be expected that the contribution of one or the other pathway of this reaction depends on the nature of the organic radical and the degree of coordination of the triphenylphosphine to the gold atom. Only the fact that the reduction of the triphenylphosphine cation-radical is observed by cyclic voltammetry (CV) would confirm that the oxidation proceeds by path **B**. The closeness of

the oxidation potentials of the OGC to that of free triphenylphosphine (1.24 V in acetonitrile, silver chloride reference electrode) gives indirect evidence of path **B** operating, while the closeness to the oxidation potential of the respective organic anion would indicate the probability of path **A**.⁵¹

1.6. Palladium thiolate complexes

Considerable interest has been shown recently in the properties and reactions of metal complexes of ligands containing sulfur donors.^{54a} Several complexes of palladium with aliphatic and aromatic monothiols (RSH) were prepared by Mann and Prudie,^{54b} who considered them to be S-bridged high molecular weight polymers of general formula $[\text{Pd}(\text{SR})_2]_n$. A similar formula was proposed by Jensen^{54c} for the corresponding nickel compounds. Other examples of nickel- and palladium-thiolate complexes have since been reported.^{54d}

Hayter and Humiec reported that the palladium complexes of higher aliphatic thiols (e.g. for $\text{R} = n\text{-Pr}$) were probably S-bridged hexamers.^{54e} The complexes of Platinum and Palladium with $\text{C}_6\text{F}_5\text{SH}$ also appears to be polymeric.^{54b} A mercaptide ion often retains its tendency to form S bridges even in the presence of other groups capable of coordination, but in these cases the extent of polymerization is often restricted to the formation of dimers. However, Ruiz *et al.*^{54f} have prepared several monomeric nickel(II) and palladium(II) complexes of bidentate ligands containing both amine and thiol groups e.g. $\text{NH}_2\text{C}_2\text{H}_4\text{SH}$. Some of these complexes readily form S-bridged trinuclear species in the presence of free ions.

No complexes of palladium(II) with the ligands $\text{HS}(\text{CH}_2)_n\text{SH}$ appear to have been isolated, but studies of the equilibria in mixtures of Ni^{2+} and $\text{HSC}_2\text{H}_4\text{SH}$ have shown the existence of the species $[\text{Ni}(\text{SC}_2\text{H}_4\text{S})_2]^{2-}$ and $[\text{Ni}_2((\text{SC}_2\text{H}_4\text{S})_3)]^{2-}$, the latter probably having a structure with S bridges.^{54f} The redox chemistry of Pd is dominated by two-electron conversions between palladium(0), palladium(II) and palladium(IV) species.⁵⁵ Mononuclear palladium(I) complexes are rare because disproportionation to palladium(II) and palladium(0), is usually thermodynamically and kinetically favorable.⁵⁶ The palladium(III) oxidation state is unusual but is stabilized by appropriate donor atoms as demonstrated by the isolation of some mononuclear palladium(III) complexes.⁵⁷

The trivalent oxidation state in dinuclear palladium and platinum complexes is stabilized by forming metal-metal bonding and the facile redox reaction between divalent and trivalent oxidation states can proceed without changing the bridging structure of the dinuclear complex. Thus platinum(II/III) and palladium(II/III) systems may show reactivity and functionality characterization of the facile redox reactivity.⁵⁸

Several dinuclear complexes of the $[\text{Pd}(\text{bridge})_4\text{Pd}]$ (bridge = $(\text{C}_6\text{H}_4)\text{CHN}(\text{C}_6\text{H}_4)$) type have been synthesized and structurally characterized.⁵⁶ Some of which have been electrochemically investigated in order to probe the generation of $[\text{Pd}^{\text{III}}(\text{bridge})_4\text{Pd}^{\text{III}}]^{n+}$. Complexes $[\text{Pd}(\text{form})_4]\text{PF}_6$ (Form = $(p\text{-CH}_3\text{C}_6\text{H}_4)\text{CHN}(p\text{-CH}_3\text{C}_6\text{H}_4)^-$), but concludes that both palladium atoms in this seemingly palladium(II), palladium(III) are divalent and the odd electron occupies a ligand – based MO^3 .⁵⁸

1.9. Metal thiolate complexes as nucleophiles for SO₂ reactions

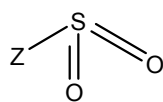
Metal thiolates can behave as nucleophiles. They have been investigated as SO₂ scrubbers.⁵⁹ The SO₂ released into the environment is usually from the combustion of coal and other fossil fuels and the roasting of sulfide ores. Coal based power generators and automobiles are, however, the major contributors to SO₂ pollution.⁵⁹ The contribution from power generators can be reduced by using scrubbers which can absorb the SO₂ before it is emitted into the environment. Although, the efficiency of scrubbers currently in use is not good enough for the total removal of all emitted SO₂.

Efforts directed towards solving this problem have led to the reactions of metal complexes with SO₂ and isolation of SO₂ complexes in order to establish their efficiency as scrubbers and to find possible ways of converting SO₂ to less harmful products. The ability of metal thiolates to absorb sulfur dioxide is another potential application for metal thiolate complexes. Researchers are interested in the ability of metal thiolate sulfur, to absorb sulfur both reversibly and irreversibly and its kinetics.⁶⁰ In these complexes the sulfur dioxide can either bind to the metal or to the sulfur atom of the thiolate ligand. The former interaction seldom leads to reversible absorption of sulfur dioxide, whereas the latter invariably gives products that easily release sulfur dioxide gas; presumably because the sulfur dioxide interaction is generally weak.⁶¹

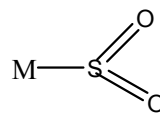
Nickel thiolato complexes $(\text{Ni}(\text{dppe})(\text{S}(\text{C}_6\text{H}_3\text{RS}))$ ($\text{R}=\text{H}, \text{Me}$) are some of the complexes that reversibly bind SO_2 molecules. In these complexes the Ni-SR functionality provides an excellent example of the nucleophilicity of the metal thiolates.⁶² The ability of these complexes to effectively reversibly absorb SO_2 gas is influenced by the substituents on the thiolato ligand. Aryl substituents are found to enhance the reversibility while the alkyl substituents do not enhance reversibility.⁶³ For example the reversibility of SO_2 absorption was observed for complexes $(\text{dppe})\text{Ni}(\text{TDT})$ and $(\text{dppe})\text{Ni}(1,2\text{-BDT})$ (dppe = diphenylphosphine; TDT = toluenedithiol, BDT = 1,2-benzenedithiol) but was found that SO_2 does not bind to the metal when alkyl analogues were used.⁶⁴

In addition a report by Fazlur-Rahman and Verkade⁶⁵ has shown that dithiolato platinum(II) compounds are readily methylated at one of the sulfur sites. This illustrates that the sulfur sites in these complexes are nucleophiles. Another report shows that the presence of phosphine ancillary ligands in metal thiolato complexes reduces the nucleophilic properties of these compounds.⁶⁶ This prompted Darkwa *et al.*⁶⁷ to combine phosphine and organochalcogenides as ligands for nickel, in an effort to get the nucleophilic balance for reversible absorption of SO_2 . The result was the reversible absorption of SO_2 by $\text{Ni}(\text{dppe})(\text{BDT})$ (dppe = bis(diphenylphosphino) ethane; BDT = 1,2-benzenedithiol), proposed to occur *via* pyramidal SO_2 binding to the nickel.⁶⁷

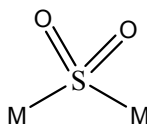
Five different SO_2 coordination geometries have been established by X-ray crystallography. They are coplanar MSO_2 (Figure 1.5), pyramidal MSO_2 , bridging MSO_2M , O, S- bonded SO_2 and SO_2 -ligand bound complexes.⁶⁸



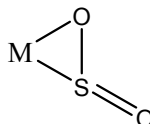
Pyramidal
Z = metal, ligand or
main group
(a)



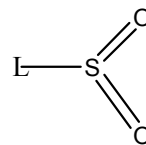
Co-planar
(b)



Bridging
(c)



O,S- bonded
(d)



SO₂- ligand bond
(e)

Figure 1.5: Different SO₂ coordination geometries.

According to Kubias it is possible to determine the SO₂ geometry by means of the SO₂ stretching modes. Only the modes with dipole moment change perpendicular to the surface are active as predicted by the surface selection rule.⁶⁹ Since two strong bands due to SO stretching are normally present in all the spectra of all SO₂ complexes. The free SO molecule is extremely reactive, but the SO can be stabilized by complexation in some.⁷⁰ The position of free SO stretching vibration is located at 1123 cm⁻¹ but when complex to Mn in a bridge structure the stretching SO can be detected at 1045 cm⁻¹, while the complexation to Fe atoms which leads to a threefold coordination with SO stretching at 1107 cm⁻¹, thus shifting the band center to lower wave numbers upon complexation.⁷¹

The ranges in which the $\nu(\text{SO})$ fall for each geometrical type known for transition metal-SO₂ complexes are shown in Table 1.1.

Table 1.1: The SO₂ coordination geometry and infrared stretching frequencies.

Coordination geometry	Observed ranges for $\nu(\text{SO}) \text{ cm}^{-1}$
M ₂ SO ₂ pyramidal	$\nu_a=1237-1150, \nu_s=1065-990$
M ₂ SO ₂ coplanar	$\nu_a=1303-1250, \nu_s = 1130-1051$
M ₂ L-SO ₂ ligand SO ₂	$\nu_a=1317-1210, \nu_s= 1135-1051$
M ₂ SO ₂ M bridging	$\nu_a=1237-1137, \nu_s = 1068-978$
M ₂ SO ₂ S,O-bonded	$\nu_a=1157-1107, \nu_s= 984-873$

The ranges for pyramidal M₂SO₂ and bridging M₂SO₂M are nearly identical. This is not very surprising since in both instances the SO₂ is S bound and the interaction with the metal(s) is of the bent variety. Therefore differentiation between geometries is not usually possible on the basis of infrared evidence alone, but knowledge of the stoichiometry and molecular composition of a complex could easily clarify the situation.⁷²

For both the symmetrical and unsymmetrical stretching modes to be active they have to be under C_s symmetry, where the SO₂ is tilted toward the surface in the molecular plane, leading to the two oxygen atoms not equivalent.⁷⁰ The observed bands show that the wave numbers fit either the symmetric mode of a pyramidal one-fold or the symmetric mode of a bridging twofold coordination, namely the range between 980 and 1029 cm⁻¹. A useful spectral feature to differentiate between these two structures could be the

wagging mode, which should be active for the pyramidal geometry only. This mode however, is located at wavenumbers around 680 cm^{-1} .⁷¹

In electrochemical experiments this spectral feature is difficult to access due to the strong light absorption of the window material (CaF_2). Another window material such as ZnSe with a wider transparency irreversibly contaminates the electrode and no spectroscopic signal is detected. In the present case, there is no spectroscopic evidence which allows the distinction between one-fold pyramidal and the bridging coordination, since the band center wave number for the symmetric SO_2 vibration is located in the same range.⁷¹

In general, pyramidal MSO_2 complexes are reactive towards oxygen in solution to give sulfates. Examples of such complexes which form sulfates in solution are $[\text{RhCl}(\text{PPh}_3)_2(\text{SO}_2)]_2$, $\text{RhCl}(\text{PPh}_2\text{Me})_3(\text{SO}_2)$ ⁷² and $\text{Ir}(\text{SPh})(\text{CO})(\text{PPh}_3)_2(\text{SO}_2)$,⁷³

Which are pyramidal MSO_2 as suggested by $\nu(\text{SO})$ at 1155 and 1030 cm^{-1} .⁷¹

Coplanar MSO_2 complexes normally do not form sulfates. However $\text{OsHCl}(\text{CO})(\text{Pcy}_3)_2(\text{SO}_2)$ ⁷⁴ and $\text{RuCl}_2(\text{PPh}_3)_2(\text{SO}_2)$ ⁷⁵ which possess coplanar MSO_2 has been reported to form sulfates. Thus it is clear that a compound's metal- SO_2 geometry is in itself not a limiting factor in the ability of the compound to undergo the sulfate reaction, although complexes with pyramidal MSO_2 appear to have by far the greatest propensity to form sulfates.⁷¹

1.10. Techniques for detection of sulfur dioxide

Sulfur dioxide (SO₂) gas in the global atmosphere is a major source of acid rain. Sulfur dioxide is a toxic gas for human health. In view of these environment and safety concerns, the development of sulfur dioxide sensors is very important. Several methods and instruments are available to monitor SO₂ levels. The continuous methods for determination of SO₂ in process streams are based on expensive conventionally UV or IR spectrometry instrumentation techniques in which the gas must be conditioned before analysis.⁷⁶

Monitoring of SO₂ using solid electrolytes such as K₂SO₄^{77a}, β-Al₂O₃^{77b}, ZrO₂^{77c} and Nasicon^{77d} by solid state electrochemistry techniques have been demonstrated. All the solid-state sensors are operated at high temperature and a reference gas is required. The feasibility of applying surface acoustic wave (SAW) or quartz crystal microbalance (QCM) for the detection of subnanogram levels of particles and of SO₂ in air has been investigated with respect to mass loading, temperature and the pressure changes.⁷⁸ Chemiresistors or transducers coated with phthalocyanine derivatives to detect SO₂ were proposed by Barger *et al.*⁷⁹ The selectivity of both methods is poor due to the presence of any vapour in the gas stream which changes the resistance of the thin film.

Atmospheric pressure ionization mass spectrometry (APIMS) has been developed to determine atmospheric SO₂ by Thornton *et al.*⁸⁰ using chemical ionization mass spectrometry (CIMS). Thornton *et al.*⁸⁰ have used radioactive nickel-63 for an electron source to produce secondary ions. They continuously added SO₂ as an internal standard.

Their detection limit was < 1 pptv in micro-second integration time, which indicated that the sensitivity of the CIMS technique was strongly dependent on water vapour in the air and the necessity of a dryer in the inlet was suggested especially for marine boundary layer measurements.⁸¹

One technique of increasing importance in such application is passive Fourier transform infrared (FT-IR) spectroscopy. This method utilizes a portable emission spectrometer to measure infrared spectra representative of chemical vapours of interest across a potentially large volume of atmosphere in the field-of-view (FOV) of the spectrometer.⁸²

The passive measurement is based solely on the collection of the naturally occurring infrared radiance with this FOV. While providing the ability to monitor an area with a path length up to a few kilometers in length, these infrared remote sensing measurements retain the chemical selectivity inherent in infrared spectroscopy.⁸² The development of several commercially available instruments suitable for use in open-air applications has also helped to make the passive FT-IR remote sensing technique a viable option in a variety of environment monitoring scenarios. Despite these advantages of passive FT-IR spectrometry, there are key challenges that must be addressed before widespread implementation becomes possible.⁸²

First among these is the difficulty in obtaining a representative background spectrum for use in removing the background, or non-analyte emission profile present in all spectra. Frequent temperature variations, changes in wind direction and speed and varied background composition all contribute to make collection of such a representative

background extremely difficult at best. Although several possible remedies to this problem have been suggested, all require the collection or generation of some form of background spectra and involve the subsequent analysis of absorbance.⁸³

The determination of SO₂ is fraught with a number of difficulties, irrespective of the analytical methodology employed. Achieving the required selectivity and sensitivity for low-level detection in a complex matrix, dictates the use of considerable procedural, classical and interpretative skill on the part of the analyst to ensure accuracy. Routine analysis as increasingly demanded by environmental authorities, will require implementation of instrumental techniques capable of high throughput analysis.

Electrochemical systems have long been proffered as a solution to decentralized testing for many species, given the low cost of the instrumentation, the promise of user accessibility through simple dipstick sampling and the potentially favorable economics of their operation.⁸⁴ The redox properties of SO₂ are such that the analyte can be reduced or oxidized so SO₂ should be readily amenable to electrochemical detection.⁸⁵ As such this technique as a method of SO₂ detection deserves to be given better attention than it currently enjoys.

1.11. Fundamentals of Electrochemistry

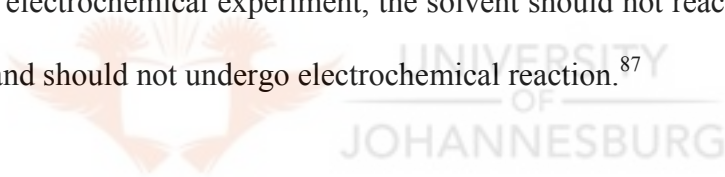
Electrochemistry may generally be defined as the study of chemical reactions to produce electric power or alternatively, the use of electricity to effect chemical process or systems. Thus, electrochemistry techniques are simply the interplay between electricity and chemistry, namely the measurements of electrical quantities, such as current, potential, and charge and their relationship to chemical parameters.⁸⁶ The use of these electrical measurements for analytical purpose has found a wide range of applications in industrial quality control, biomedical analysis and environmental monitoring.

Cyclic Voltammetry (CV) is a most widely applied electro analytical technique for examining the nature or route of an electrochemical reaction. In detail its popularity stems, among others from its relative experimental simplicity and ability to offer a rapid location of redox potentials of the target electro active species and convenient evaluation of the effect of the media on the redox processes. The experiment allows one to scan the potential of a stationary working electrode in an unstirred solution back after reaching a certain value. The resulting current-potential plot is termed cyclic voltammogram.⁸⁷

The electrochemical cell, typical three-electrode is the most commonly used for electrochemical experiments. Three-electrode electrochemical cell consists of (i) the working electrode (WE), (ii) the reference electrode (RE) and (iii) counter electrode (CE). The working electrode (WE) is where the electrochemical reaction of interest takes place and provides high signal to noise characteristics and reproducible response. The

selection of the WE depends on the redox behavior of the target analyte and the background current over the potential region investigated.⁸⁷

The reference electrode (RE) has a characteristic of constant potential which is taken as a reference or standard potential against other electrodes in the cell. The counter electrode (CE) is included to complete the electrochemical circuit and in modern potentiostat instruments, it is used to eliminate polarization of the reference electrode. The choice of the solvent together with the supporting electrolytes needs to be considered for an electrochemical experiment. The choice of the solvent is based upon the solubility of the analyte and its properties such as conductivity, electrochemical and chemical inertness. Therefore in an electrochemical experiment, the solvent should not react with the analyte or its products and should not undergo electrochemical reaction.⁸⁷



1.10. Objectives and rationale of the study

Nickel thiolato complexes (Ni(dppe)(S(C₆H₃RS))(R=H, Me) are some of the complexes that reversibly bind SO₂ molecules. In these complexes the Ni-SR functionality provides an excellent example of the nucleophilicity of the metal thiolates.⁶² The ability of these complexes to effectively reversibly absorb SO₂ gas is influenced by the substituents on the thiolato ligand. The coordination chemistry of ligands incorporate both thiolate and tertiary phosphine donor ligands as their combination is likely to confer structures and reactivities that favour SO₂ binding on their metal complexes.⁶⁰ Because of the ability of metal thiolates to absorb sulfur dioxide as another potential application of metal thiolates which is sulfur dioxide sensors. Therefore in an effort to develop new SO₂ sensors, synthesis of new gold(I) and gold(III) thiolate complexes, and their palladium(II) analogues, were embarked upon:

- (i) to find simple routes for the synthesis of Palladium(II), Gold(I) and Gold(III) thiolate complexes with pyridine and phosphine ancillary ligands
- (ii) To study the reactions of the compounds synthesized with SO₂ using electrochemistry and spectrochemical techniques and identify if they reversibly absorb SO₂

The work described in this dissertation employed two electroanalytical techniques, cyclic voltammetry (CV) and Osteryoung square wave voltammetry (OSWV). They were used in redox of palladium(II), gold(I) phosphine and gold(III) thiolate complexes and their reactions with SO₂. The results of this study are reported in the rest of this dissertation.

References:

1. R. M. Moutloali, *M.Sc dissertation*, University of the North, South Africa. **1998**.
2. F. E. Massoth, *Adv. Catal.*, **1987**, 27, 265.
3. I. G. Dance, *Polyhedron*, **1986**, 5, 1037.
4. E. I. Steifel, *Prog. Inorg. Chem.*, **1997**, 147, 147.
5. W. E. Smith, J. Reglinski. *Perspec. Bioinorg. Chem.*, **1991**, 1, 183.
6. O. Crespo, F. Canales, M. C. Gimeno, A. Laguna, *Organometallics*, **1999**, 18, 3142.
7. J. McMurry, *Fundamental of Organic Chemistry*, 4thed, Cole publishing company, **1998**, pg 261, 270.
8. E. I. Stiefel, K. Matsumoto, *Transition Metal Sulfur Chemistry*, *American Chemical Society Symposium Series*, 653, **1996**, pg 103
9. J. R. Dilworth, J. Hui, *Adv. Inorg. Chem.*, **1993**, 40, 411.
10. D. H. Nguyen, H. F. Hsu, M. Millar, S. A. Koch, *J. Am. Chem. Soc.*, **1996**, 118, 8963.
11. L. L. Maisela, A. M. Crouch, J. Darkwa, I. A. Guzei, *Polyhedron*, **2001**, 20, 3189.
12. V. C. Pensado, V. G. Benitez, S. H. Ortega, R. A. Toscano, D. M. Morales, *Inorg. Chim. Acta*, **2006**, 359, 4007.
13. T. F. Baumann, J. W. Sibert, M. M. Olmstead, A.G. M. Barrett, B.M. Hoffman, *J.*

-
- Am. Chem. Soc.*, **1994**, *116*, 2639.
14. R. J. Puddephatt, *Chem. Soc. Rev.*, **1983**, *12*, 99.
 15. H.Q. Liu, Q. T. Lui, B. S. Kang, L. R. He, J. Xiu. Lu, *Sci. Sin. Ser.*, **1988**, *1*, 10.
 16. M. C. Hall, J. A. Jarvis, B. T. Kilbourn, P. G. Owston, *J. Chem. Soc. Dalton Trans.*, **1972**, 1554.
 17. F. L. Jiang, G. W. Wei, X. J. Huang, M. C. Hong, *J. Coord. Chem.*, **1992**, *25*, 185.
 18. R.Cao, X. J. Lei, Z. Y., Huang, M. C. Hong, H. Q. Liu, *J. Coord. Chem.*, **1992**, *25*, 165.
 19. R. CIO, M. Hong, F. Jiang, B. Kang, X. Xie, *Polyhedron*, **1996**, *15*, 2670.
 20. D. E. T. Wilton-Ely, A. Schier, N. W. Mitzel, H. Schmidbaur, *J. Chem. Soc., Dalton Trans.* **2001**, 113.
 21. R. J. Puddephatt, in *Gold-Progress in Chemistry, Biochemistry and Technology*, Ed. H. Schmidbaur, John Wiley & Sons, Inc, New York, **1999**.
 22. D. de Vos, P. Clements, S. M. Pyke, D. R. Smyth, E. R. T. Tiekink, *Metal Based Drugs*, **1999**, *6*, 31.
 23. P. Pyyko, A. Bauer, A. Schier, H. Schmidbaur, *J. Chem. Soc. Dalton Trans.*, **1997**, 4753.
 24. M. Preisenberger, A. Bauer, A. Schier, H. Schmidbaur, *Z.Naturforsch*, **1998**, *53b*, 781.

-
25. M. Freytag, P.G. Jones, *Chem. Commun.*, **2000**, 277.
26. S. Esperas, *Acta. Chem. Scand, Ser. A*, **1976**, 30, 527.
27. H. Schmidbaur, A. Wohlleben, F. Wagner, O. Orama, G. Huttner, *Chem. Ber.*, **1977**, 110, 1748
28. H. G. Raubenheimer, J. G. Toerien, G. J. Kruger, W. Van Zyl, P. oliver, *J. Organomet. Chem.*, **1994**, 466, 291.
29. S. Wang, J. P. Fackler, Jr, *Inorg. Chem.*, **1990**, 29, 4404.
30. R. A. Bell, J. R. Kramer, *Environ. Toxicol. Chem.*, **1999**, 18, 9.
31. S. Wang , J. P. Fackler, Jr, *Organometallics*, **1988**, 7, 2415.
32. R. C. Elder, M. K. Eidness, *Chem. Rev.*, **1987**, 87, 1027.
33. R. V. Parish, B. P. Howe, J. P. Wright, J. Mack, R. G. buckely, *Inorg. Chem.*, **1996**, 35, 1659.
34. S. P. Fricker, *Metal Based Drugs*, **1999**, 6, 291.
35. O. Crespo, M. C. Gimeno, P. G. Jones, A. Laguna, M. D. Villacampa, *J. Chem. Soc. Dalton Trans.*, **1997**, 2963.
36. J. Vicente, M. T. Chicote, M. D. Bermudez, P. G. Jones, G. M. Sheldrick, *J. Chem. Soc., Dalton Trans*, **1986**, 2361.
37. M. B. Dinger, W. Henderson, *J. Organomet. Chem.*, **1998**, 560, 233.

-
38. M. Bardaji, P. G. Jones, A. Laguna, M. Laguna, *Organometallics*, **1995**, *14*, 1310.
39. L. J. McCaffery, W. Henderson, B. K. Nicholson, J. E. Mackay, M.B. Dinger, *J. Chem. Soc. Dalton Trans.*, **1997**, 2577.
40. J. A. S. Howell, *Polyhedron*, 2006, *25*, 2993.
41. P. J. Costa, M. J. Calhorda, *Inorg. Chim. Acta*, **2006**, *359*, 3617.
42. L. J. Larson, E. M. McCauley, B. Weissbart, D. S. Tinti, *J. Phys. Chem.*, **1995**, *99*, 7218.
43. D. F. Shriver, P. W. Atkins, C.H. Langford, *Inorganic Chemistry*, Oxford University Press, **1990**, pg 450.
44. Q. J. Pan, H. X. Zhang, *Organometallics*, **2004**, *23*, 5198.
45. R. Narayanaswamy, M. A. Young, E. Parkhurst, M. Ouellette, R. C. Elder, A. E. Bruce, *Inorg. Chem.*, **1993**, *32*, 2506.
46. V. W. Yam, K. M. Wong, L. L. Hung, N. Zhu, *Angew. Chem. Int. Ed*, **2005**, *44*, 3107.
47. A. Volger, H. Kunkely, *Coord. Chem. Rev.*, **2001**, *489*, 219.
48. D. Li, X. Hong, C. M. Che, W.C. Lo, S. M. Peng, *J. Chem. Soc., Dalton Trans*, **1993**, 2929.
49. V. W. Yam, *Acc. Chem. Res*, **2002**, *35*, 555.

-
50. F. G. Herring, G. Hwang, K. C. Lee, F. Mistry, P. C. Phillips, H. Willner, F. Aubke, *J. Am. Chem. Commun.*, **1992**, 114, 1271.
51. R. D. Rakhimov, K.P. Butin, K. I. Grandberg, *J. Organomet. Chem.*, **1994**, 464, 253.
52. J. G. M. Warren, A. M. Roelobsen, G. H. W. Ipskamp, *Inorg. Chem.*, **1989**, 28, 968.
53. K.P. Butin, R.D. Rakhimov, V. P. Dyadchenko, O.A. Yenyukova, *Metalloorg. Khim.*, **1989**, 2, 1401.
54. (a) S. E. Livingstone, *Quart. Rev. Chem. Soc.*, **1965**, 19, 386. (b) R. S. Nyholm, J. F. Skinner, M.H. B. Stiddard, *ibid.*, **1968**, 38. (c) K. A. Jensen, *Anorg. Chem.*, **1944**, 252, 227. (d) P. Woodward, L. F. Dahl, E. W. Abel, B. C. Crosse, *J. Amer. Chem. Soc.*, **1965**, 87, 5251. (e) R. G. Hayter, F. S. Humiec, *J. Inorg. Nucl. Chem.*, **1964**, 26, 807. (f) J. Ruiz, J. Giner, V. Rodriguez, *Polyhedron*, **2000**, 19, 1627.
55. F. A. Cotton, G. Wilkinson, *Advanced. Inorganic Chemistry.*, 5th Ed, Wiley: New York, **1988**, pg 917-937.
56. A. Miedanar, R. C. Haltiwanger, D.L. Du Bois, *Inorg. Chem.*, **1991**, 30, 417.
57. M. G. Fitzpatrick, L. R. Hanton, D. A. McMorran, *Inorg. Chem.*, **1995**, 34, 4821.
58. A. J. Downard, A. M. Bond, A. J. Clayton, L. R. Hanton, D. A. McMorran, *Inorg. Chem.*, **1996**, 35, 7684.

-
59. C. Y. Chiou, T. C. Chou, *J. Organomet. Chem.*, **2002**, 87, 1.
60. A. Hodgson, L. R. Jordan, *Anal. Chem.*, **1999**, 398, 43.
61. K. Li, I. A. Guzei, J. Darkwa, *Polyhedron*, **2003**, 22, 805.
62. M. Y. Darensbourg, T. Tuntulani, J. H. Reibenspies, *Inorg. Chem.*, 1994, **33**, 611.
63. J. Darkwa, *Inorg. Chim. Acta*, **1997**, 257, 137.
64. R. J. Angelici, *Polyhedron*, **1997**, 16, 3073.
65. A. K. Fazlur-Rahman, J. G. Verkade, *Inorg. Chem.*, **1992**, 32, 5331.
66. Y. M. Hsiao, S. S. Chojnacki, P. Hinton, J. H. Reibenspies, M. Y. Darensbourg, *Organometallics*, **1993**, 12, 870.
67. J. Darkwa, *Inorg. Chim. Acta*, **1997**, 257, 137.
68. G. J. Kubas, *Inorg. Chem.*, **1979**, 18, 1.
69. T. Loucka, *J. Electroanal. Chem.*, **1971**, 31, 319.
70. D. A. Outka, R. J. Madix, G. B. Fischer, C. DiMaggio, *Langmuir*, **1986**, 2, 406.
71. I. R. Moraes, M. Weber, F. C. Nart, *Electrochimica. Acta*, **1997**, 42, 617.
72. M. S. Thomas, *M.Sc. dissertation, University of the North, South Africa*, **1999**.
73. J. Valentine, D. Valentine Jr, J. P. Collman, *Inorg. Chem.*, **1971**, 10, 219.
74. J. J. Levison, S. D. Robinson, *Inorg. Chem.*, **1968**, 4, 407.

-
75. S. Cenini, A. Mantovani, A. Fusi, M. Keubler, *Gazz. Chim.*, **1975**, *105*, 255.
76. C. Y. Chiou, T. C. Chou, *Sens and Actuat. B* , **2002**, *87*, 1
77. (a) N. Imanaka, Y. Yamaguchi, G. Adachi, J. Shiokawa, *J. Electrochem. Soc.*, **1985**, *132*, 2519 ,(b) N. Rao, C. M. Bleek, J. Schoonamn, O. T. Sorensen, *Solid-State Ionics*, **1992**, *30*, 53, (c) Y. Yan, N. Miura, N. Yamazoe. *J. Electrochem. Soc.*, **1996**, *143*, 609 , (d) J. M. Skeaff, A. A. Dubreuil, *Sens and Actuat.*, **1993**, *10*, 161.
78. H. E. Maruyama, Y. Saito, Y. Matsumoto, Y. Yano, *Solid-State Ionics*, **1985**, *17*, 281.
79. W. R. Barger, H. Wohltjen, A. W. Snow, *Solid-State Sens., and Actuat.*, **1984**, p.410
80. D. C. Thornton, A. R. Bandy, F. H. Tu, B. W. Blomquist, G. M. Mitchell, *J. Geophys.*, **2002**, *107*, 4632.
81. Y. Matsumi, H. Shigemori, K. Takahashi, *Atm. Environ.*, **2005**, *39*, 3177.
82. F. W. Koehler, G. W. Small, R. J. Combs, R. B. Knapp, R. T. Kroutil, *Vibrat. Spectrosc.*, **2001**, *27*, 97.
83. T. L. Marshall, C. T. Chaffin Jr, R. M. Hammaker, W. G. Fateley, *Environ. Sci. Technol.*, **1994**, *28*, 224A.

-
84. J. Wang, *Analytical Electrochemistry*, second ed., Wiley-VCH, Weinheim, Germany, **2000**.
85. A. Isaac, C. Livingstone, A. J. Wain, R. G. Compton, *Anal. Chem.*, **2006**, 25, 6.
86. A.J. Bard, L.R. Faulkner, *Electrochemical Methods*, Eds. John Wiley & Sons: New York, **1980**. See pages vii-xvi.
87. P. N. Mashazi, *Study of metallophthalocyanines attached onto pre-modified gold surface*, Rhodes University, **2007**, pg 1-42.



CHAPTER 2

2. Experimental Section

2.1. Materials and methods

The starting material tris-chloro-2-phenylpyridinegold(III), [AuCl(PPh₃)] was prepared by literature procedures.^{1,2} Benzyl mercaptans, 2-aminothiophenol, 4-chlorothiophenol, 2-phenylpyridine were supplied by Aldrich. The SO₂ cylinder was obtained from Afrox. All solvents were analytical grade and were dried and purified by refluxing under inert atmosphere over a drying agent; tetrahydrofuran (THF), was distilled from sodium/benzophenone, and dichloromethane (CH₂Cl₂) was distilled from calcium hydride (CaH₂). All solvents were deoxygenated before use. All the reactions were performed under a nitrogen atmosphere in Schlenk type apparatus but work up of the products was done in air since products were air stable in solution and in the solid state. Acetonitrile and dichloromethane (UV grade) and tetrabutylammonium-tetrafluoroborate [*n*-Bu₄N][BF₄] (Aldrich) used for the electrochemical experiments, were used as received.

2.2. Instrumentation

¹H, ¹³C, {¹H} and ³¹P{¹H} NMR spectra were recorded on a Varian Gemini 2000, 300 MHz spectrometer. ¹H NMR data are listed in order of chemical shift (δ, reported in ppm and referenced to the residual solvent peak of CDCl₃ (δ = 7.26) or DMSO (δ = 2.49), and multiplicity, number of protons, assignment, coupling constant (*J* in Hertz) are also

provided in the data. Proton decoupling experiments were used to assist in assignment of carbon and phosphorus. ^{13}C NMR data are listed in order of chemical shift (δ , reported in ppm and referenced to the residual solvent peak of CDCl_3 ($\delta = 77.0$ or DMSO ($\delta = 39.5$), multiplicity (due to C-P coupling) number of carbons, assignment, coupling constant (J , in Hertz) are listed where appropriate. ^{31}P NMR data are listed in the order of chemical shift (δ reported in ppm and referenced to 85% aqueous phosphoric acid ($\delta = 0.00$), number of phosphorus atoms. The following abbreviations are used through the text s = singlet, d = doublet, dd = doublet of doublet t = triplet, m = multiplicity.

Mass spectra were recorded on a Waters API Quatro micro spectrometer at the University of Stellenbosch, South Africa. Elemental analyses were performed by the microanalytical laboratory at the University of Cape Town and X-ray structures were determined by the Structural Department of the University of the Witwatersrand. A Perkin Elmer Lambda 25 UV-vis spectrophotometer was used to perform UV-vis measurements. The samples were measured in quartz cells (1 cm path length) using dichloromethane as reference. Infrared measurements were performed using a Perkin Elmer paragon 1000 FT-IR spectrometer. The samples were measured as KBr pellets.

2.3. Preparation of starting materials

The starting materials were all prepared by literature procedures^{2,3}; and were characterized by ^1H and $^{13}\text{C}\{^1\text{H}\}$ NMR to ensure their purity.

2.3.1. Synthesis of $\text{HAuCl}_4\cdot 4\text{H}_2\text{O}$.

Gold pellets (1.30 g, 0.06 mol) were dissolved in aqua-regia a mixture of (6.50 mL, HCl, 1.69 mL HNO_3) at room temperature. Immediately the mixture was covered with a parafilm and perforated so as to allow no gas to escape. The mixture was left to dissolve over a period of 20 h, until all the gold pellets completely dissolved. The resulting yellowish solution was then evaporated at 80 °C, reducing the solution to 1mL. The solution was allowed to cool in air to form crystals. Yield: 2.03 g, (55%).

2.3.2. Reaction of $\text{HAuCl}_4\cdot 4\text{H}_2\text{O}$ with PPh_3 : formation of

$[\text{AuCl}(\text{PPh}_3)]$.

$\text{HAuCl}_4\cdot 4\text{H}_2\text{O}$ (0.50 g, 1.21 mmol) was dissolved in ethanol (10 mL) and a suspension of PPh_3 (0.64 g, 2.24 mmol) in ethanol (10 mL) was added to the mixture. There was an immediate formation of a yellow precipitate which turned white after 2 min. The reaction was left to run for 40 min at room temperature and the white precipitate isolated by suction filtration and washed with ethanol. Yield: 0.53 g, (88%). ^1H NMR (CDCl_3): δ 7.57 (m, 17H). $^{13}\text{C}\{^1\text{H}\}$ NMR: δ 122.5 (s), 123.1(s), 127.4 (s), 128.4 (s), 129.3 (s), 130.9 (s), 137.3 (s), 141.0 (s), 146.0 (s).

2.3.3. Reaction of $\text{OHC}(\text{C}_6\text{H}_4)\text{OCH}_2(\text{C}_6\text{H}_5)$ with $\text{HS}(\text{C}_6\text{H}_4)\text{NH}_2$: formation of

$\text{HS}(\text{C}_6\text{H}_4)\text{NHCH}(\text{C}_6\text{H}_4)\text{OCH}_2(\text{C}_6\text{H}_5)$.

A mixture of 4-aminothiophenol (0.30 g, 2.40 mmol) and 4-(hexyloxy)-benzaldehyde (0.48 mL, 2.39 mmol) was dissolved in ethanol (60 mL), the solution was stirred at room temperature for 24 h. A cream -yellow precipitate was isolated by suction filtration and washed with ethanol. Yield: 0.5 g, (43%). ^1H NMR (CDCl_3): δ 8.35 (s, 1H), 7.82 (d, 2H, $^2J_{\text{HH}} = 8.4$ Hz, phenyl), 7.52 (d, 2H, $^2J_{\text{HH}} = 2.7$ Hz, phenyl), 7.12 (d, 2H, $^2J_{\text{HH}} = 8.7$ Hz, phenyl), 6.94 (d, 2H, $^2J_{\text{HH}} = 9$ Hz, phenyl), 4.01 (t, 2H, $^3J_{\text{HH}} = 15.0$ Hz, CH_2), 1.83 (t, 2H, $^3J_{\text{HH}} = 15.0$ Hz, CH_2), 0.99 (t, 3H, $^3J_{\text{HH}} = 12.0$ Hz, CH_3).

2.3.4. Reaction of $[\text{PdCl}_2(\text{MeCN})_2]$ with 2-phenylpyridine: formation of

$[\text{PdCl}_2(2\text{-C}_6\text{H}_5(\text{C}_6\text{H}_4\text{N}))]$

The Palladium salt, $[\text{PdCl}_2(\text{MeCN})_2]$, (0.10 g, 0.38 mmol) was dissolved in dichloromethane (20 mL) and stirred for ca. 2 min until all solids dissolved. 2-phenylpyridine (0.18 g, 0.08 mmol) was added, and precipitation occurred immediately. The reaction was left to stir for 6 h and brown precipitate formed was isolated by filtration. Yield: 0.12 g, (48%). ^1H NMR ($\text{DMSO-}d_6$): δ 8.70 (d, $^2J_{\text{HH}} = 5.3$ Hz, py), 8.01 (m, 1H, py), 7.66 (m, 3H, phenyl). $^{13}\text{C}\{^1\text{H}\}$ NMR (CDCl_3): δ 123.1(s), 127.4 (d, $^2J_{\text{CP}} = 60.0$ Hz), 128.4(s), 129.3 (s) 130.9 (s), 137.3 (s), 141.0 (s), 146.0 (s).

2.4. Preparation of complexes

2.4.1. Reactions of chloro-triphenylphosphinegold(I) with mixed thiolate compounds

2.4.1.1. Reaction of [AuCl(PPh₃)] with benzyl mercaptan: formation of



To a dichloromethane solution (20 mL) of benzyl mercaptan (11.8 μl , 0.10 mmol) was added [AuCl(PPh₃)] (0.10 g, 0.20 mmol) excess silver(I) oxide (0.04 g, 0.20 mmol) and the solution stirred for about 2 h. The silver salt was filtered off and the filtrate was concentrated to ca. 2 mL, the product was precipitated by adding excess hexane. A white solid was isolated by suction filtration. Yield: 0.029 g, (50%). ¹H NMR (CDCl₃): δ 7.55 (m, 17H, phenyl), 7.13 (d, 2H, ²J_{HH} = 7.5 Hz), 4.18 (s, 2H, CH₂). ³¹P {¹H} NMR; δ 35.5 (s, PPh₃). ¹³C {¹H} NMR (CDCl₃): δ 33.6 (s, CH₂), 126.5(s), 128.6(d, J_{CP} = 30 Hz, PH), 131.8 (s), 134.3(d, J_{CP} = 60.0 Hz, phenyl). IR (KBr pellet, cm⁻¹): 3056 (b), 1583 (s), 1474 (s), 1434 (s), 1303 (s), 1259 (s), 1186 (s), 1106 (s), 1018 (s), 993 (s), 931 (s), 818 (s), 760 (s), 712 (s), 616 (s). Anal. Calc for C₂₅H₂₃PSAu: C, 46.72; H, 3.77; S, 4.80 %; Found: C, 45.70; H, 3.46; S, 3.51%.

2.4.1.2. Reaction of [AuCl(PPh₃)] with 2-aminothiophenol: formation



To a dichloromethane solution (20 mL) of 2-aminothiophenol (10.8 μl , 0.10 mmol) was added [AuCl(PPh₃)] (0.10 g, 0.20 mmol), excess silver(I) oxide (0.04 g, 0.20 mmol) and the solution stirred for about 2 h. The silver salt formed was filtered off and the filtrate concentrated to ca. 2 mL. The product was precipitated as a white solid by adding excess

hexane (20 mL). A white solid was isolated by suction filtration. Yield: 0.038 g, (50%). ^1H NMR (CDCl_3): δ 7.43 (d, 1H, $^2J_{\text{HH}} = 7.5$ Hz, C_6H_4), 7.41-7.52 (m, 15H, phenyl), 7.10 (t, 1H, $^2J_{\text{HH}} = 30.0$ Hz, C_6H_4), 6.69 (td, 1H, $^3J_{\text{HH}} = 7.8$ Hz, $^3J_{\text{HH}} = 20.7$ Hz, C_6H_4), 3.71 (s, 1H, NH_2). $^{31}\text{P}\{^1\text{H}\}$ NMR ; δ 36.4 (s, PPh_3). $^{13}\text{C}\{^1\text{H}\}$ NMR (CDCl_3): δ 123.8 (s), 124.5 (s), 127.7 (s), 129.2 (s), 131.0 (s), 143.4 (s), 144.9 (s), 153.0 (s). ESI (m/z, %, assignment): 459 (100, $[\text{AuPPh}_3]^+$), 583 (20, $[\text{M}^+]$), 1042 (47 $[\text{M}^+ - \text{AuPPh}_3]^+$). (IR KBr pellet, cm^{-1}): 3048 (b), 1605 (s), 1474 (s), 1474 (s), 1430 (s), 1306 (s), 1252 (s), 1181 (s), 1161 (s), 1022 (s), 989 (s), 807 (s), 780 (s), 768 (s).

2.4.1.3. Reaction of $[\text{AuCl}(\text{PPh}_3)]$ with 4-chlorothiophenol: formation of

$[\text{Au}(4\text{-SC}_6\text{H}_4\text{Cl})(\text{PPh}_3)]$ (3)

To a dichloromethane solution (20 mL) of 4-chlorothiophenol (0.02 g, 0.10 mmol), was added $[\text{AuCl}(\text{PPh}_3)]$ (0.10 g, 0.20 mmol), excess silver(I) oxide (0.04 g, 0.20 mmol), whereupon the solution became cream white, which was stirred for 2 h. The silver salt was filtered off and the filtrate was concentrated to ca. 2 mL, the product was precipitated by adding excess hexane. A grey solid was isolated by suction filtration. Yield: 0.028 g (46%). ^1H NMR (CDCl_3): δ 7.25 (d, 2H, $^2J_{\text{HH}} = 7.2$ Hz, C_6H_4) 7.50 (m, 17H, phenyl, C_6H_4). $^{31}\text{P}\{^1\text{H}\}$ NMR δ : 35.8 (s, PPh_3). $^{13}\text{C}\{^1\text{H}\}$ NMR (CDCl_3): δ 128.0 (s), 128.5 (s), 129.2 (d, $^2J_{\text{CP}} = 30.0$ Hz), 131.9 (d, $^2J_{\text{CP}} = 9.0$ Hz), 133.7 (s), 134.1 (s), 134.3 (s). (KBr pellet, cm^{-1}) 3056 (b), 1583 (s), 1474 (s), 1303 (s), 1259 (s), 1186 (s), 1106 (s), 1018 (s), 931 (s), 818 (s), 789 (s), 706 (s), 692(s), 616(s). Anal Calc for $\text{C}_{24}\text{H}_{20}\text{ClPSAu}$: C, 43.59; H, 3.22; S, 5.32 %. Found: C, 42.82, H, 3.08: S, 5.25%.

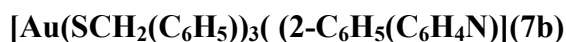
2.4.2. Reactions of Tris-chloro-2-phenylpyridine gold(III).

2.4.2.1. Reaction of $\text{HAuCl}_4 \cdot 4\text{H}_2\text{O}$ with 2-phenylpyridine: formation of



A solution of 2-phenylpyridine (0.20 g, 1.20 mmol) in water (3 mL), was added to a solution of $\text{HAuCl}_4 \cdot 4\text{H}_2\text{O}$ (0.43 g, 1.28 mmol) in water (5 mL). The yellow precipitate was formed immediately. The yellow precipitated was isolated by suction filtration. Yield: 0.501 g, (86%). ^1H NMR ($\text{DMSO-}d_6$): δ 8.79 (d, 1H, $^3J_{\text{HH}} = 5.4$ Hz, py); 8.29 (m, 1H, py); 8.18 (d, 1H, $^3J_{\text{HH}} = 7.8$ Hz, py); 8.03 (td, 1H, $^3J_{\text{HH}} = 8.4$ Hz, $^3J_{\text{HH}} = 7.8$ Hz, py); 7.72 (t, 2H, $^2J_{\text{HH}} = 3.9$ Hz, phenyl); 7.59 (t, 1H, $^2J_{\text{HH}} = 9.0$ Hz, phenyl). $^{13}\text{C}\{^1\text{H}\}$ NMR ($\text{DMSO-}d_6$): δ 124.2 (s), 125.2 (s), 128.3 (s), 129.8 (s), 131.7 (s), 131.7 (s), 133.5 (s), 144.8 (d, $^2J_{\text{CP}} = 60.0$ Hz) 153.1 (s).

2.4.2.2. Reaction of $[\text{AuCl}_3(2\text{-C}_6\text{H}_5(\text{C}_6\text{H}_4\text{N}))]$ with benzyl mercaptan: formation of



To a Schlenk flask containing dichloromethane (60 mL) was added complex 7 (0.10 g, 0.20 mmol), benzyl mercaptan (76.60 μl , 0.06 mmol) and silver(I) oxide (0.15 g, 0.05 mmol) and the mixture refluxed for 3 h, the silver salt formed was filtered off, and the solvent evaporated under reduced pressure, to give a bright yellow oil which resisted crystallization. Yield: 0.168 g (94%). ^1H NMR (CDCl_3): δ 8.69 (d, 1H, $^2J_{\text{HH}} = 5.4$ Hz, py); 7.98 (d, 1H, $^3J_{\text{HH}} = 1.5$ Hz, py); 7.74 (t, 2H, $^3J_{\text{HH}} = 2.4$ Hz, py), 7.50 (td, 1H, $^3J_{\text{HH}} = 7.8$ Hz, $^3J_{\text{HH}} = 4.8$ Hz, py), 7.20 (m, 17H, phenyl), 3.95 (s, 2H, CH_2). $^{13}\text{C}\{^1\text{H}\}$ NMR (CDCl_3): δ 43.1 (s, CH_2), 122.5 (s), 123.1 (s), 127.4 (d, $^2J_{\text{CP}} = 60.0$ Hz), 128.4 (s), 129.3 (s)

130.9 (s), 137.3 (s), 141,0 (s), 146,0 (s). ESI (m/z, %, assignment):683 (5, [M⁺-AuPhPy]⁺), 353 (5, [PhPyAu]⁺) 156 (100 [PhPy]⁺). IR (KBr pellet, cm⁻¹): 3046 (b), 2964 (s), 1616 9(s), 1536(s), 1489 (s), 1456 (s), 1397 (s), 1325 (s), 1252 (s), 1198 (s), 1022 (s), 862 (s), 789 (s), 760 (s), 660 (s). Anal. Calc for C₃₂H₃₁NS₃Au.: C, 53.18; H, 4.19; N, 1.94 ; S, 12.35 %. Found: C, 53.25; H, 4.60; N, 1.96; S, 12.33 %.

2.5. Crystallographic structure determination

The crystal evaluation and data collection were performed on a Bruker CCD-1000 diffractometer with Mo K_α (λ = 0.71073 Å) radiation and the diffractometer to crystal distance of 4.9 cm. The initial cell constants were obtained from three series of ω scans at different starting angles. The reflections were successfully indexed by an automated indexing routine built in the SMART programme. These highly redundant datasets were corrected for Lorentz and polarization effects. The absorption correction was based on fitting a function to the empirical transmission surface as sampled by multiple equivalent measurements.

A successful solution by direct methods provided most non-hydrogen atoms from the *E*-map. The remaining non-hydrogen atoms were located in an alternating series of least-squares cycles and difference Fourier maps. All non-hydrogen atoms were refined with anisotropic displacement coefficients. All hydrogen atoms were included in the structure factor calculation at idealized positions and were allowed to ride on the neighbouring atoms with relative isotropic displacement coefficients.

2.6. Electrochemistry Studies

Electrochemical studies of the complexes were performed on a BAS-100A potentiostat connected to the computer and controlled by GPES software. Cyclic voltammetry (CV) and square wave voltammetry (OSWV) data were collected using a conventional three-electrode system, with a platinum disc working electrode and platinum wire as the auxiliary electrode. The reference electrode used was a saturated calomel electrode (SCE). The supporting electrolyte used was tetrabutylammonium-tetrafluoroborate which was obtained from Aldrich.

Electrochemical characterization experiments for complex **1** (10^{-3} M) were performed in a mixture of acetonitrile-dichloromethane, containing tetrabutylammonium-tetrafluoroborate (0.10 M) as supporting electrolyte. The solution was placed in a single compartment cell fitted with three with a working electrode, one counter electrode and a reference electrode (SCE). Prior to each scans, the working electrode was polished on alumina slurries rinsed with ionized water following with bubbling of argon to the solution before each electrochemical experiment.

Cyclic voltammogram was run at 100 mV/s scan rate and at -800 - 2000 mV potential scan. The working electrode was polished after each run to avoid adsorption of gold on to the surface of the platinum wire. Immediately after each scan the voltammetric mode was changed to Osteryoung square wave voltammetry.

Sulfur dioxide (SO₂) was then bubbled to the solution in the cell, which the solution changed colour immediately from clear to yellow. Argon was purged through the solution following with run of the cyclic voltammogram and Osteryoung Square Wave Voltammetry respectively at 100 mV/s scan rate and at -800-2000 mV potential scan. Similar procedure was done for complex **2**, **3** and **7b**.

2.7. UV-vis spectroscopy studies

Dichloromethane which is the solvent used to dissolve the complexes was run as a blank. Complex **1** (6 mg) was dissolved in dichloromethane and placed in a Quartz cell. The sample cell was then inserted into the spectrophotometer and the sample run. The sample was run at a wavelength between 200-350 nm. Immediately after the run SO₂ was bubbled through the solution, which changed colour from clear to yellow. The samples run at a wavelength between 200-350 nm.

2.8. Reference:

1. A. Wojcicki, *Adv. Org. Chem.* **1974**, *12*,1823.
2. E. C. Constable, T. A. Leese, *J. Organomet.*,**1989**, *363*, 419.
3. F. A. Nevondo, A.M. Crouch, J. Darkwa, *J. Chem. Soc., Dalton Trans.*, **2000**,
43.

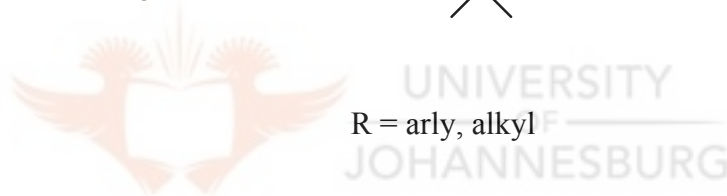
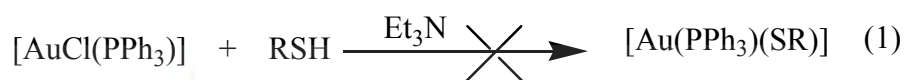


CHAPTER 3

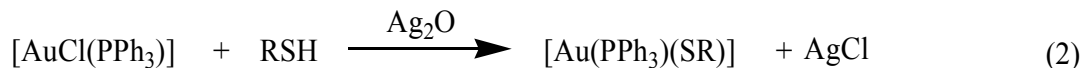
3. RESULTS AND DISCUSSION

3.1. Synthesis of $[\text{Au}(\text{SC}_6\text{H}_4\text{X})(\text{PPh}_3)]$ X = 4-Cl, 2-NH₂, CH₂

In investigating the use of gold and palladium thiolate complexes as sulfur dioxide sensors, two types of thiolate complexes were designed. The complexes were first synthesized *via* the reaction of $[\text{AuCl}(\text{PPh}_3)]$ and an appropriate ligand in the presence of excess triethylamine according to equation 1.



No reaction was observed between the thiol and $[\text{AuCl}(\text{PPh}_3)]$. This could be attributed to the fact that the electron shell of a gold atom is short of one electron and chlorine atom has many electrons in its outer shell, these results in gold and chlorine forming a strong bond which requires an abstraction of Cl. Thus second attempt was to synthesize the complexes by reacting $[\text{AuCl}(\text{PPh}_3)]$ with the appropriate thiol in a 1:1 mole ratio as reported by Bardaji *et al.*¹ equation (2). This method involves the use of Ag_2O that removes the Cl bound to gold.



(R = CH₂C₆H₄ (**1**), 2-C₆H₄(NH₂) (**2**), 4-ClC₆H₄ (**3**), 4-hexyloxyC₆H₄N(CH)C₆H₄) (**7a**))

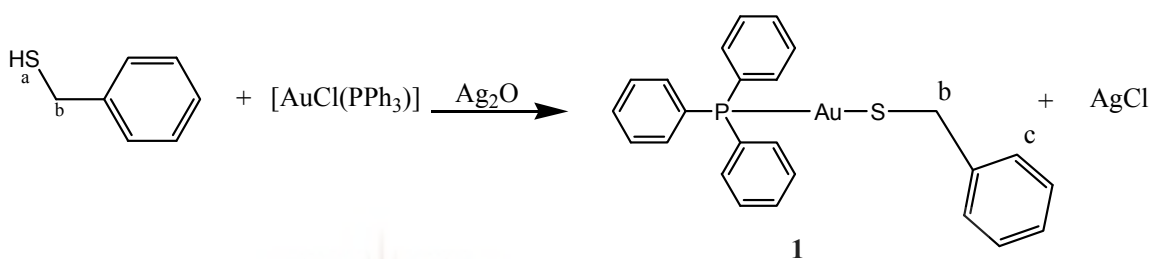
Bardaji *et al.*¹ reported that 2-aminobenzenethiol, with acetylacetonato derivative of gold(I) [Au(acac)(PPh₃)] is able to deprotonate the thiol; which results in the loss of the protonated acac. This results in the thiolate formed coordinating to the corresponding gold(I) fragment, which is known as the acac method.¹ Parish *et al.*² reported that substitution by a hard ligand requires abstraction of Cl by silver ions for ligand substitution of the Au-Cl bonds to proceed.

All the reactions in equation (2) were generally complete within 2 h and the yields were between 40-65%. The complexes were characterised by a combination of ¹H, ³¹P and ¹³C NMR, IR spectroscopy as well as elemental analysis.

3.1.1. Characterisation by NMR spectroscopy

A typical ¹H NMR spectrum is that of **1** (Fig. 3.1) which clearly shows the formation of the desired product. The presence of the phenyl protons belonging to the PPh₃ group and benzyl thiolato group were observed. The peaks for PPh₃ appeared at 7.53 ppm as a multiplet and a peak for H_c appears as a doublet at 7.43 ppm, while the peak at 4.21 ppm was assigned to the CH₂ group of the thiolate ligand (Scheme 3.1). Based on the integration of peaks in the spectrum the multiplet at 7.43 ppm and 7.54 ppm were assigned to 17H, which are due to the protons of the phenyl rings bearing the phosphorus atom and the phenyl protons of the thiolate ligand. Additional evidence of complexation

is the shift of the phosphorus peak in the $^{31}\text{P}\{^1\text{H}\}$ NMR spectrum from 34.0 ppm in $[\text{AuCl}(\text{PPh}_3)]$ to 35.7 ppm for the thiolate complex. A distinct singlet peak at 4.21 ppm for the thiolate moiety proves that the thiolate ligand, contrary to the appearance of a doublet at 3.67 ppm (CH_2) and triplet at 1.74 ppm (SH_a) in benzyl thiolate is bound to the gold.



Scheme 3.1: Synthesis of $[\text{Au}(\text{SCH}_2(\text{C}_6\text{H}_5)(\text{PPh}_3)]$ (**1**).

The $^{13}\text{C}\{^1\text{H}\}$ NMR spectrum of **1** clearly differentiated between the aromatic region and the CH_2 , which appears downfield of the spectra at 126.4 ppm, while the CH_3 appears up field at 34.0 ppm. The carbons of the phenyl ring are clearly seen at 126.5, 128.6, 131.8 and 134.3 ppm, with the C_b appearing at 34.0 ppm. (Scheme 3.1)

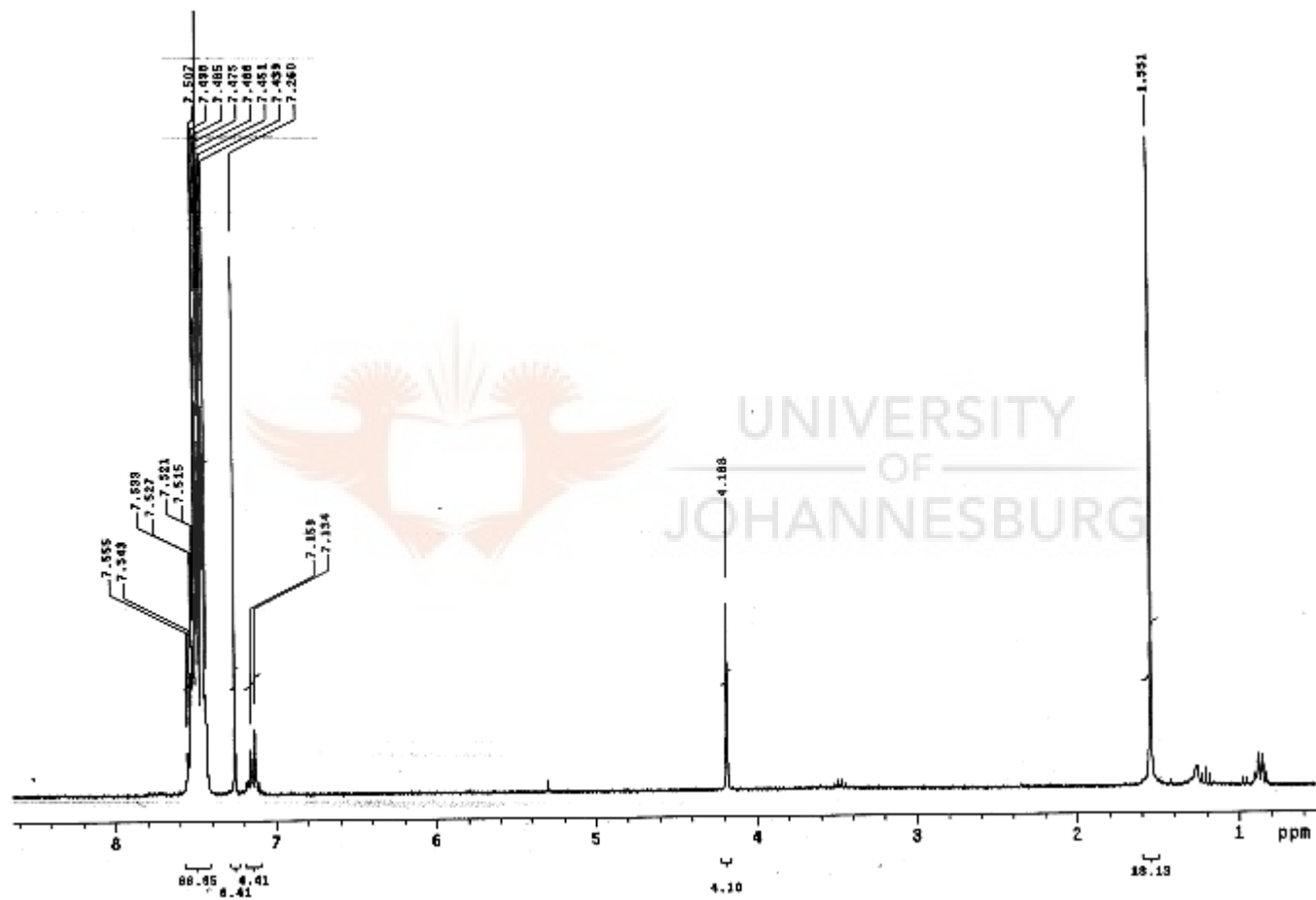
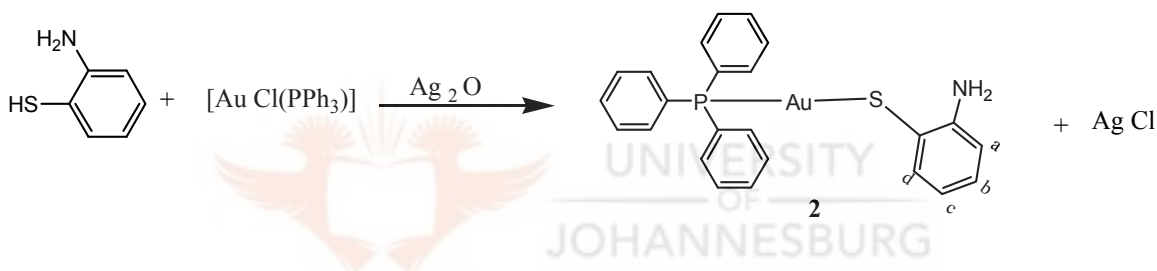


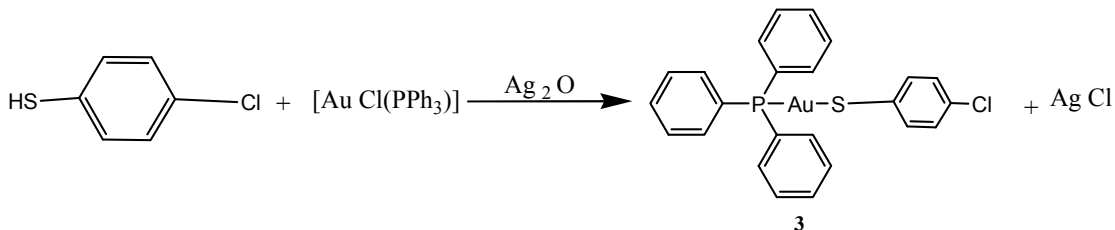
Figure 3.1: ^1H NMR spectrum of $[\text{Au}(\text{SCH}_2(\text{C}_6\text{H}_5)(\text{PPh}_3)]$ (1). * = H_2O

Similarly, the $^{31}\text{P}\{^1\text{H}\}$ NMR spectrum of **1**, shows a shift of the phosphorus peak to 36.6 ppm from 34.0 ppm of the starting material $[\text{AuCl}(\text{PPh}_3)]$, signifying complexation. However, there is no significant changes in the ^1H and $^{13}\text{C}\{^1\text{H}\}$ NMR spectra of **2** and thus are similar to those of the starting materials. A peak (hump) at 3.73 ppm is due to NH_2 protons and those between 6.73 and 7.56 ppm are due to the thiolate protons in **2** ($\text{H}_a, \text{H}_b, \text{H}_c, \text{H}_d$) (Scheme 3.2). The spectroscopic data acquired are in agreement with those reported by Bardaji and co-workers.¹



Scheme 3.2: Synthesis of $[\text{Au}(2\text{-SC}_6\text{H}_4\text{NH}_2)(\text{PPh}_3)]$ (**2**).

The $^{31}\text{P}\{^1\text{H}\}$ NMR spectrum of **3** is similar to those of **1** and **2**. However, the ^1H NMR spectrum exhibits a doublet at 7.25 ppm and a multiplet at 7.56 ppm, (Fig. 3.2) which are due to the two protons of the 4-chlorothiophenol and the rings of triphenylphosphine respectively.



Scheme 3.3: Synthesis of $[\text{Au}(4\text{-SC}_6\text{H}_4\text{Cl})(\text{PPh}_3)]$ (**3**).

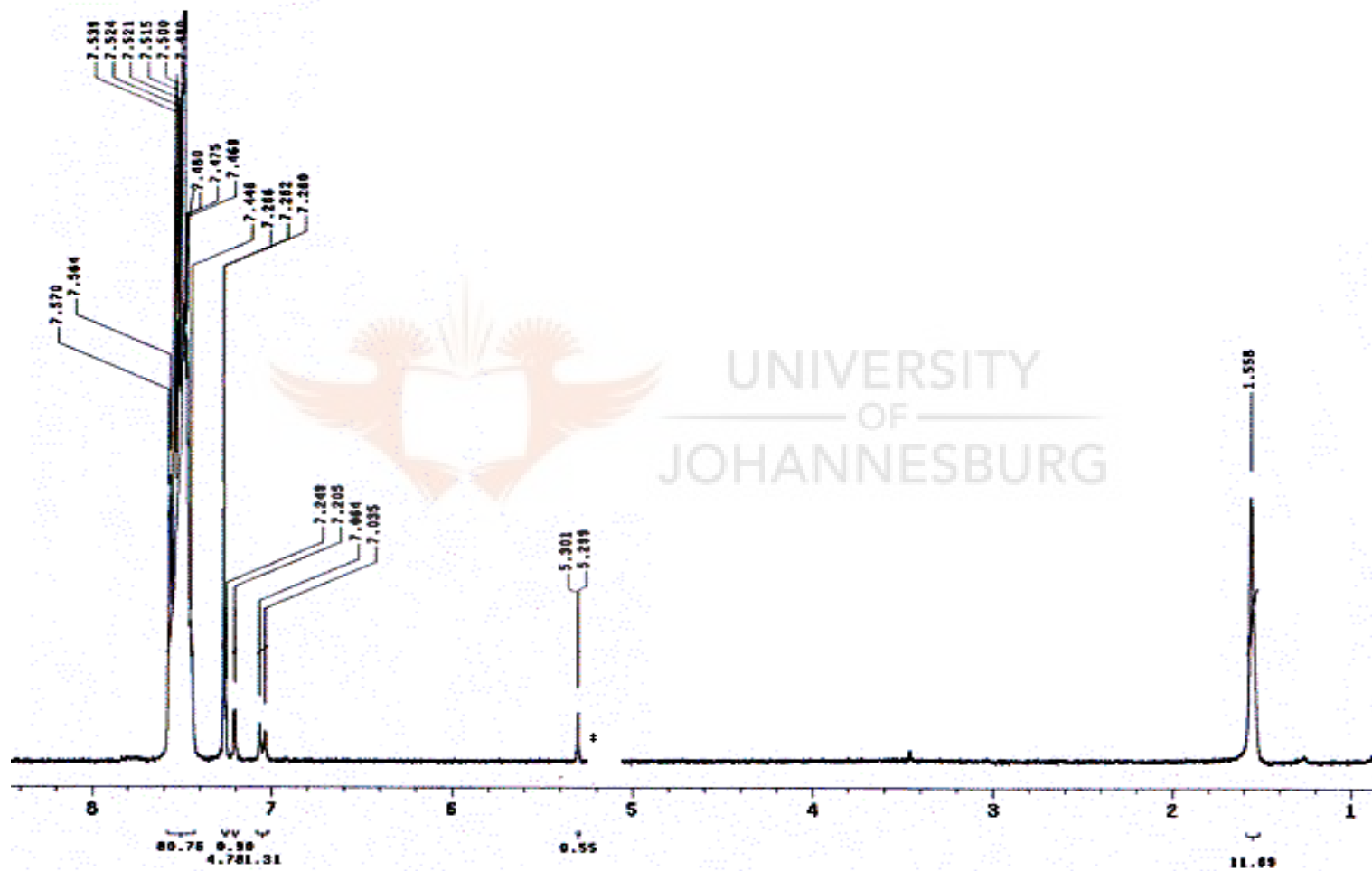
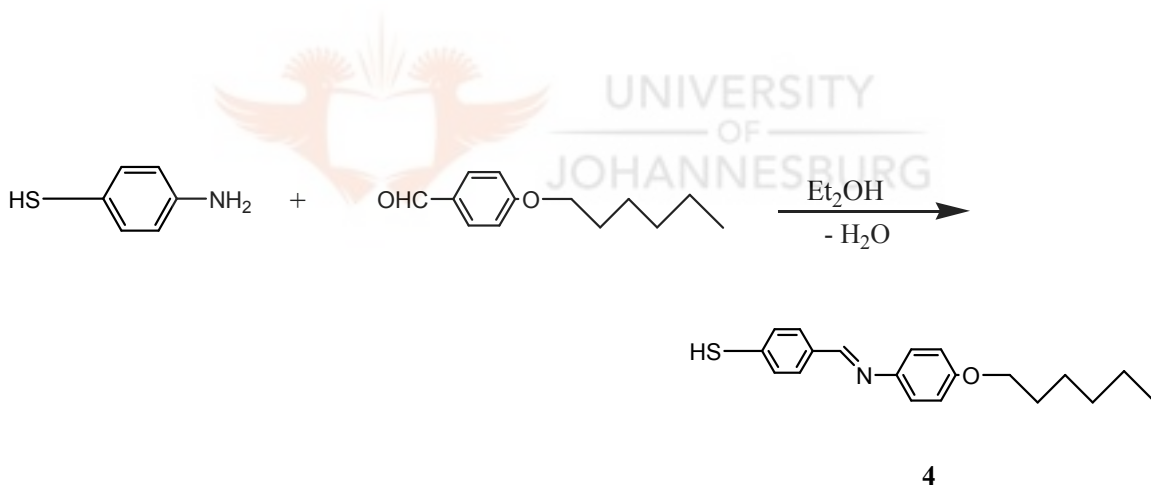


Figure 3.2 : ^1H NMR spectrum of $[\text{Au}(4\text{-SC}_6\text{H}_4\text{Cl})(\text{PPh}_3)]$ (3).

The ligand 4-hexyloxyC₆H₄N(CH)C₆H₄ (**4**) was prepared by condensation of equimolar amounts of 4-aminothiophenol and 4-(hexyloxy)-benzaldehyde (Scheme 3.4.) in ethanol Scheme 4. This condensation reaction is the common route for the formation of imine bonds³ and the product was precipitated as a yellow solid within 30 mins but the reaction was left to run for 24 h to ensure that the reaction is complete. ¹H and ¹³C{¹H} NMR spectroscopy were used to characterize the Schiff base compound isolated. The presence of an imine group was confirmed by ¹H NMR spectroscopy, with the imine proton appearing at 8.48 ppm. This is comparable to those of similar compounds synthesized by Nevondo *et al.*⁴

(HSC₆H₄NCCH)C₆H₄X-4, X = F, Cl, Br, SMe and Me).⁵



Scheme 3.4. Synthesis of 4-hexyloxyC₆H₄N(CH)C₆H₄ (**4**).



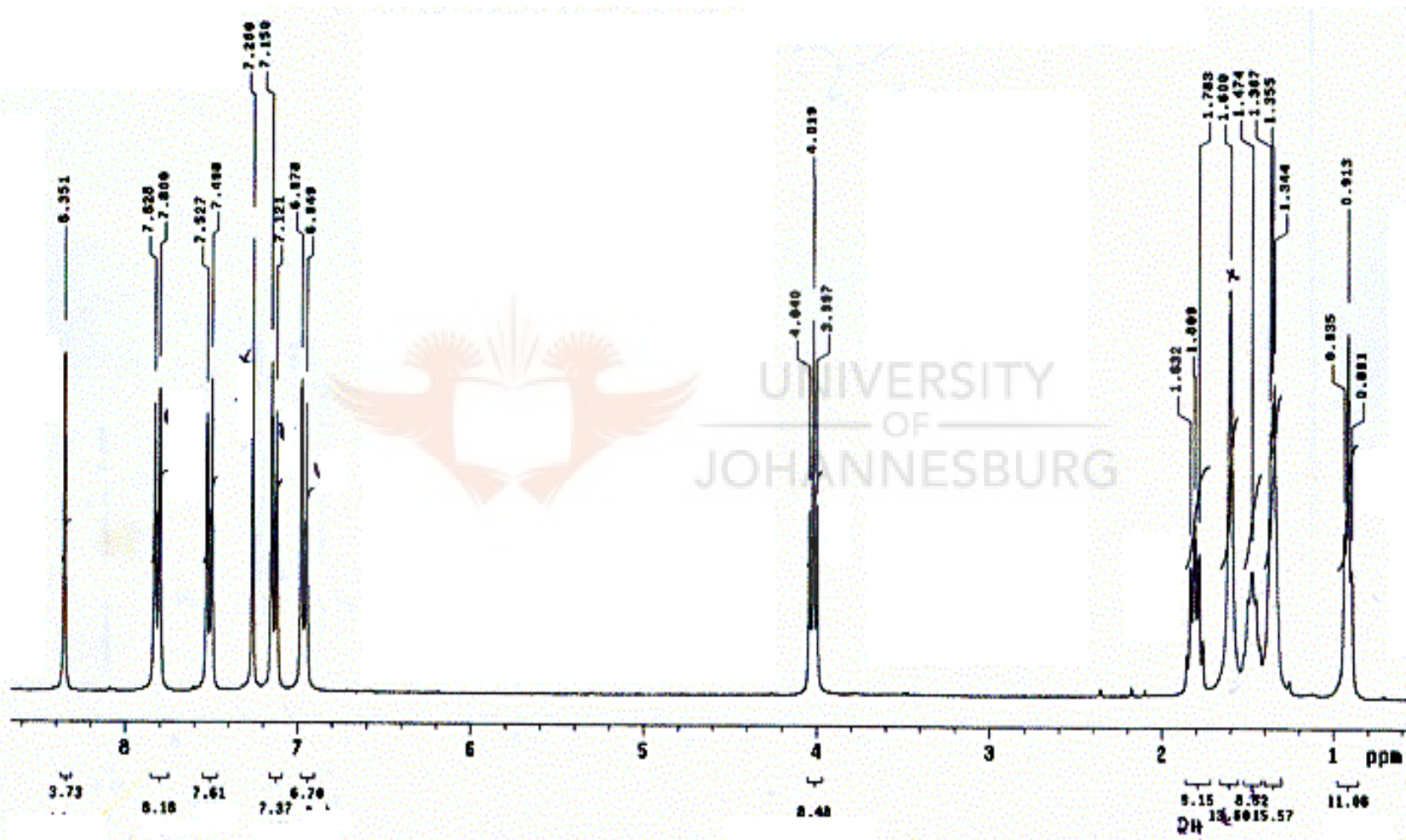
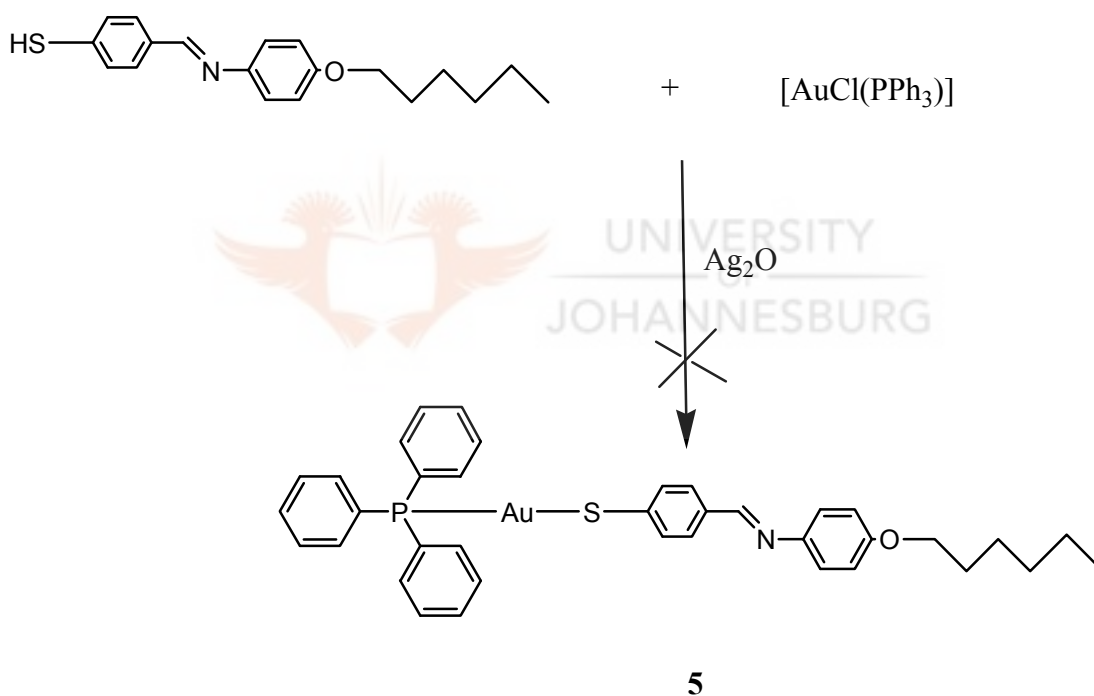


Figure 3.3 : ¹H NMR spectrum of 4-hexyloxyC₆H₄N(CH)C₆H₄ (4).

With complex **5** there were no significant changes in ^1H and $^{31}\text{P}\{^1\text{H}\}$ NMR chemical shifts between what was isolated as a product and the starting materials. This suggests that there may not have been a reaction between $[\text{AuCl}(\text{PPh}_3)]$ and the 4-hexyloxy $\text{C}_6\text{H}_4\text{N}(\text{CH})\text{C}_6\text{H}_4$. Furthermore thin-layer chromatography (TLC) and mass spectrometry were run, which proved that there was no reaction between $[\text{AuCl}(\text{PPh}_3)]$ and 4-hexyloxy $\text{C}_6\text{H}_4\text{N}(\text{CH})\text{C}_6\text{H}_4$.



Scheme 3.4: Synthesis of 4-hexyloxy $\text{C}_6\text{H}_4\text{N}(\text{CH})\text{C}_6\text{H}_4$ (**5**).

3.1.2. Characterization by Infrared spectroscopy

The IR spectra of all the complexes showed the phenyl ring signals, which include the triphenylphosphine and the thiolato ligand, with stretching frequencies around 3000 cm^{-1} and bending frequencies around 1500 and 500 cm^{-1} . The absence of a thiol (SH) peak, which appears around $2550\text{-}2600\text{ cm}^{-1}$ as strong peak, was evidence of complexation

between triphenylphosphine gold(I) chloride and thiol ligands. Complexation was also proven by appearance of a C-S peak between 1050 and 1200 cm^{-1} as a strong peak (Fig. 3 4).

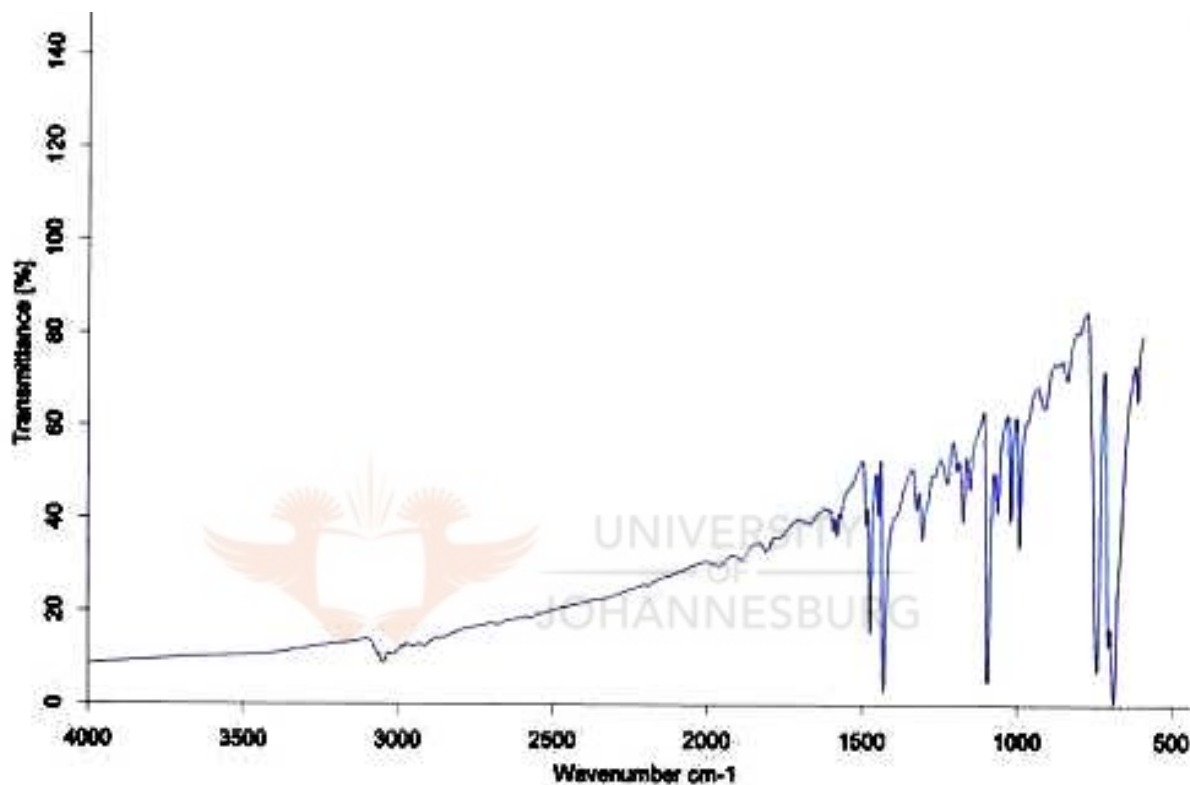


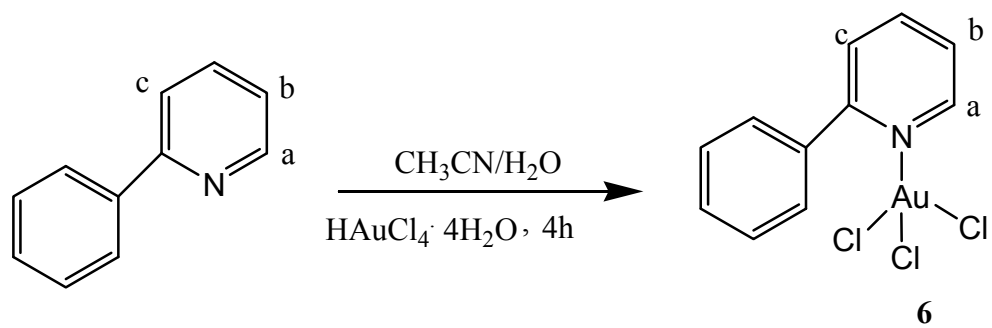
Figure 3.4: IR spectrum of $[\text{Au}(4\text{-SC}_6\text{H}_4\text{Cl})(\text{PPh}_3)]$ (**3**) as a KBr pellet.

Detailed characterization of the synthesized complexes all confirmed the structures and the purity of the synthesized ligands and complexes. The Infrared (IR) also confirmed the formation of the thiolated complexes. When absences of thiol (SH) peak were absent. spectrometry ($M^+ = m/z$) showed the molecular peak corresponding to the molecular weights of the synthesized complexes, even though there were other fragments.

3.2. Synthesis of gold(III) thiolate complexes

Firstly, synthesis of the tris-chloro-2-diphenylpyridine gold(III) complex (**6**) was attempted by reacting $\text{HAuCl}_4 \cdot 4\text{H}_2\text{O}$ with 2-diphenylpyridine in acetonitrile but there appeared to have been no reaction. Interestingly in an acetonitrile-water (5:1) mixture at room temperature for 4 h, the same reaction gave a yellow precipitate in moderate yields. Fuchita *et al.*⁶ reported the same reaction in ethanol or dichloromethane using 3:1 molar ratio of ligand to $\text{HAuCl}_4 \cdot 4\text{H}_2\text{O}$. However, the product first formed is a salt $[\text{LH}][\text{AuCl}_4]^-$ L= 2-phenylpyridine, but it is not clear whether the hydrated water molecule in $\text{HAuCl}_4 \cdot 4\text{H}_2\text{O}$ is the proton source for the formation of the salts, which had to be further refluxed. Complex **7** was prepared by a method used by Constable *et al.*⁷ because of its simplicity. The method is a direct reaction of the 2-phenylpyridine with $\text{HAuCl}_4 \cdot 4\text{H}_2\text{O}$ in acetonitrile-water (5:1) which leads to $[\text{AuCl}_3(\text{L})]$, L = 2-phenylpyridine.

From the ^1H NMR spectrum obtained, there was a clear indication of complexation between the gold salt and the ligand because there was a shift from 8.65 ppm to 8.79 ppm of the H_a . The peaks of **6** H_a , H_b and H_c appeared at 8.79, 8.29 and 8.21 ppm respectively. H_a and H_c appearing as doublet and H_b as a triplet. (Fig. 3.5). The same pattern of ^1H NMR peaks was observed by Constable *et al.*⁷ with the proton peaks appearing at 9.62, 8.44 and 8.00 ppm respectively. The difference in the position of the peaks can be attributed to the different deuterated solvents used in running the spectra. The spectrum of **7** was run in d^6 -DMSO whilst that of Constable *et al.*⁷ was run in CDCl_3 . The structure of **6** was confirmed by X-ray crystallography (Fig. 3.5).



Scheme 3.6: Synthesis of $[\text{AuCl}_3(2\text{-C}_6\text{H}_5(\text{C}_6\text{H}_4\text{N}))]$ (**6**).



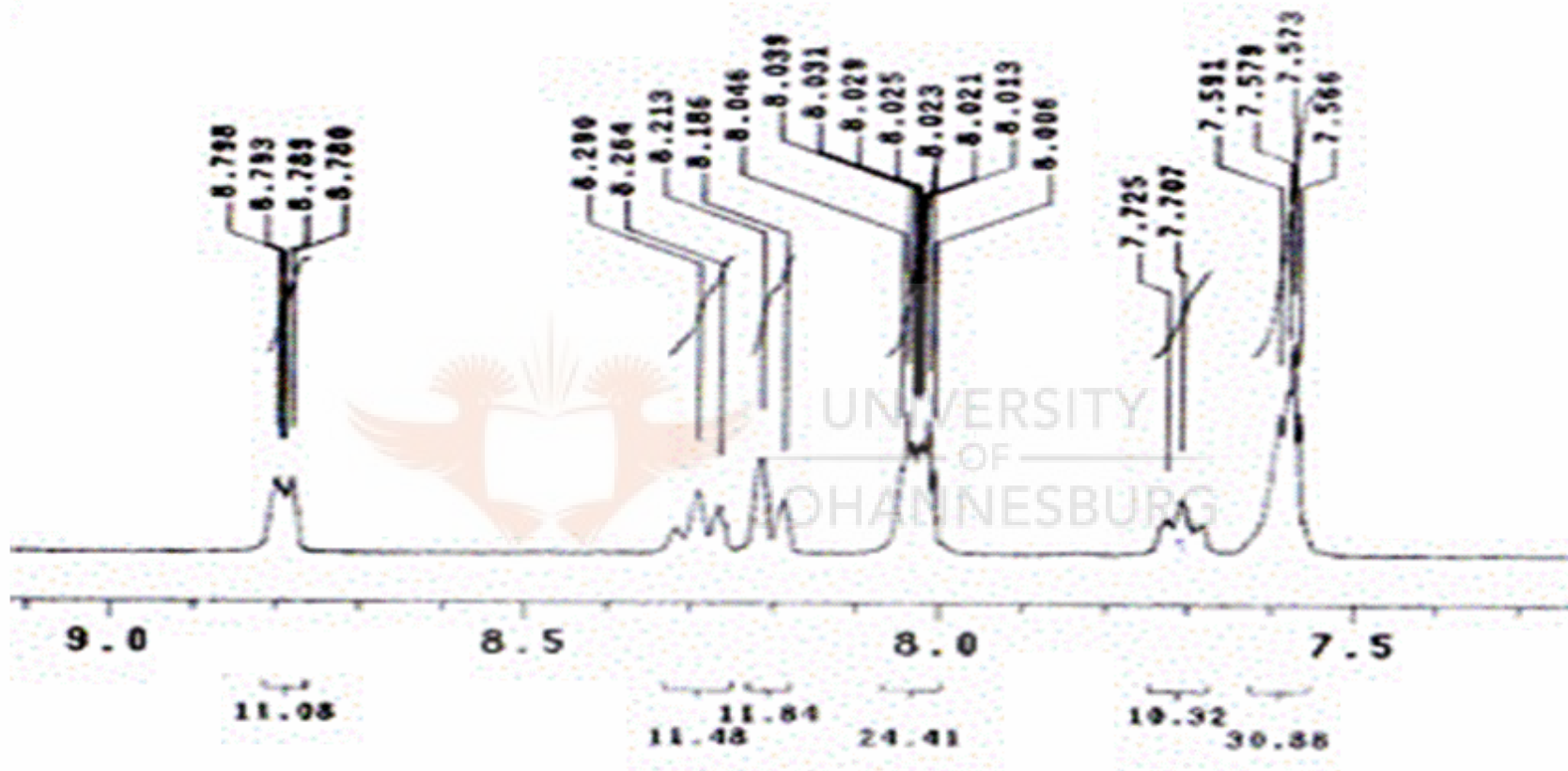


Figure 3.5: ^1H NMR spectrum of $[\text{AuCl}_3(2\text{-C}_6\text{H}_5(\text{C}_6\text{H}_4\text{N}))]$ (6).

3.2.1. Molecular structure of **6**

Even though the gold(III) starting material has been known in the literature,⁸ suitable crystals for single crystal X-ray crystallography of **6** were grown by slow evaporation of acetonitrile-water mixture and used to determine the solid state structure of complex **6**. The coordination around the Au was found to be a distorted square-planar, resulting from coordination of the Cl₃AuN donor set, which produces angles at the metal centre in the range 89.2(2)-179.2(6)°. The bond angles around the metal is close to linearity along the N(1)-Au(1)-Cl(2) bond (179.2(2)°. The phenyl ring of the ligand is twisted by 56.6 (3) with respect to the pyridyl ring. The bond distances and angles are in the same range and correspond to the expected values reported by Zhang *et al.*⁸ Selected bond distances and angles with their estimated standard deviation are listed in Table 3.2 below in comparison with that by Zhang *et al.*⁸

Table 3.1 : Crystal data and structure refinement for 7

Empirical formula	$C_{11}H_9AuCl_3N$
Formula weight	458.51
Temperature/ K	173(2) K
Wavelength/Å	0.71073
Crystal system	Triclinic
Space group	P-1
a/Å	8.1426(12)
b/Å	9.0772(14)
c/Å	10.1716(15)
$\alpha/^\circ$	66.079(9)
$\beta/^\circ$	83.369(9)
$\gamma/^\circ$	68.055(9)
V/ Å ³	636.70(17)
Z	2
Dc/ Mg m ⁻³	2.392
Crystal size/ mm ³	0.58 x 0.42 x 0.28
Absorption correction	Empirical with SADABS
T _{max} /T _{min}	0.1320/0.0572
R(F) (%) [I > 2σ(I)]	0.1412
R(w F ²) ^a (%) (all data)	0.0523

Table 3.2 Selected bond lengths (Å) and bond angles (°) for tris-chloro-2-phenylpyridinegold(III) with estimated standard deviations (e.s.d.s) in parentheses.

Bond distances (Å) (present study)		Bond distances (Å) Literature ⁸	
N(1)-Au(1)	2.039(8)	N(1)-Au(1)	2.035(5)
Cl(2)-Au(1)	2.039(8)	Cl(2)-Au(1)	2.258(2)
Cl(1)-Au(1)	2.26(2)	Cl(1)-Au(1)	2.268(2)
Cl(3)-Au(1)	2.66(2)	Cl(3)-Au(1)	2.280(2)
Bond angles (°) (present study)		Bond angles(°) Literature ⁸	
N(1)-Au(1)-Cl(2)	179.7(2)	N(1)-Au(1)-Cl(2)	179.6(1)
N(1)-Au(1)-Cl(1)	89.8(2)	N(1)-Au(1)-Cl(1)	90.2(1)
N(1)-Au(1)-Cl(3)	89.2(2)	N(1)-Au(1)-Cl(3)	88.2(7)
Cl(2)-Au-Cl(1)	90.43(10)	Cl(2)-Au-Cl(1)	90.2(1)
Cl(2)-Au(1)-Cl(3)	90.59(9)	Cl(2)-Au(1)-Cl(3)	90.2(2)
Cl(1)-Au-Cl(3)	177.98(8)		177.6(5)

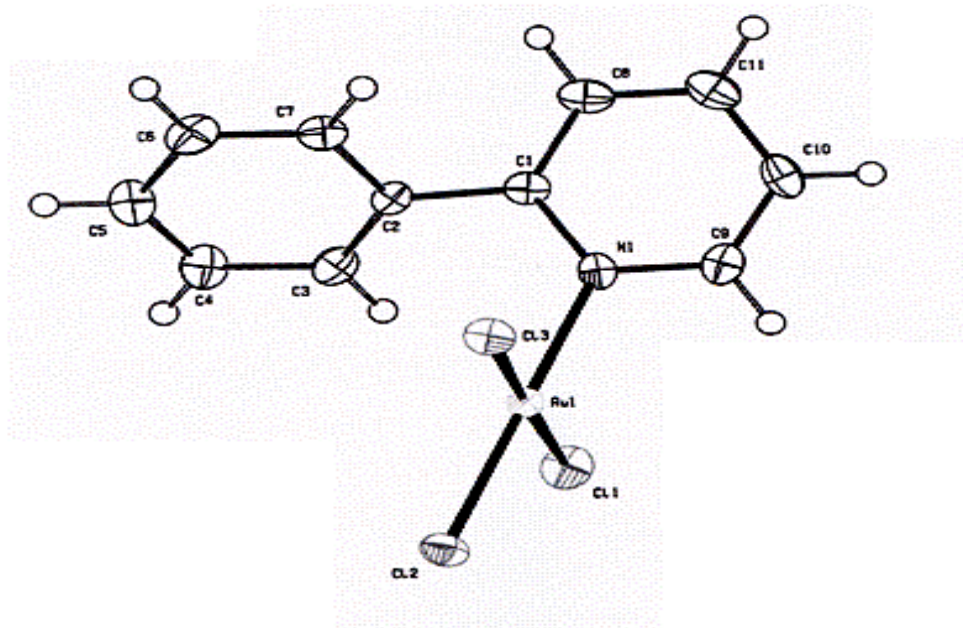
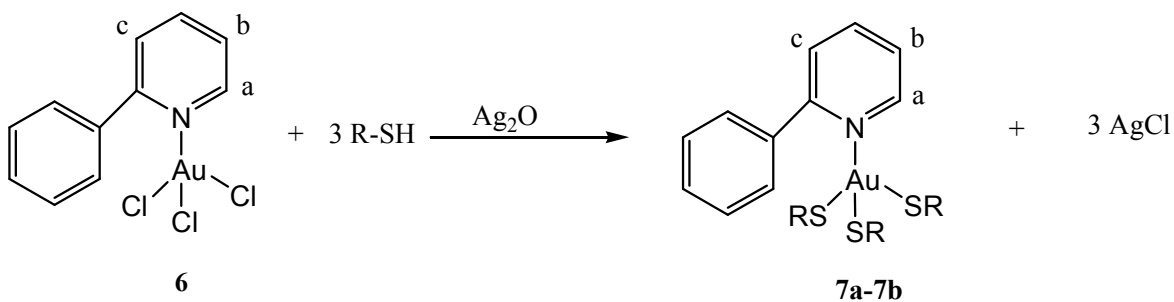


Figure 3.6: Molecular structure of complex $[\text{AuCl}_3(2\text{-C}_6\text{H}_5(\text{C}_6\text{H}_4\text{N}))]$ (6).

3.2.2. Synthesis of $[\text{Au}(\text{SR})_3(2\text{-C}_6\text{H}_5(\text{C}_6\text{H}_4\text{N}))]$ ($\text{R} = \text{CH}_2\text{C}_6\text{H}_5$ (**7b**)).



Scheme 3.7: Synthesis of 2-phenylpyridinegold(III) thiolate complexes.

Complexes **7a-7b** were synthesized by reacting complex **6** with various substituted thiols in the presence of silver(I) oxide, using 1:3 complex to thiol ratios (Scheme 3.7). The reactions were generally allowed to stir under reflux for 3 h to ensure complete reaction. The products were isolated from the salt by-product, by filtration. Reactions with 4-[(4-hexyloxy-phenylimino)-methyl]benzenethiol (**7a**) resulted in a maroon solution but after 1 h the color of the solution changed to green. The change in color is suspected to be due to hydrolysis of the ligand back to the starting materials, 4-aminothiophenol and 4-(hexyloxy)benzaldehyde).

This was confirmed from the ^1H NMR spectrum which had a peak at 9.81 ppm. The spectrum of an authentic 4-(hexyloxy)-benzaldehyde has a peak at 9.81 ppm. Changes of the substituents in the thiolato ligands had no significant influence on the electronic environment of either 2-phenylpyridine ring or the thiolate ligands, as their ^1H NMR chemical shifts were not significantly affected.

The ^1H NMR spectrum of **7b** (Fig. 3.7) clearly differentiated between the 2-diphenylpyridine and benzyl mercaptan ligand. All the characteristic peaks of 2-phenylpyridine which appears between 7.24 ppm and 8.87 ppm were clearly identified, with H_a as a doublet at 8.87 ppm, H_b as a triplet at 7.97 ppm and H_c as a doublet at 7.88 ppm, with additional peaks of the benzyl ring of the thiol at 7.29 ppm. Evidence of the reaction between benzyl mercaptan and **6** to give **7b** was deduced from the appearance of the CH_2 protons as a singlet at 3.60 ppm in the complex compared to the doublet in benzyl mercaptan (Fig. 3.7). More evidence was shown by the high intensity of the peak CH_2 compared to the intensity of the peak H_a , as the reaction is done at a ratio of 3:1 (benzyl mercaptan: **6**). Similar ^1H NMR spectrum has been reported by Fan *et al.*¹⁰ for related complexes, 2-phenylpyridine gold(III) complexes with thiol ligands. The observed ^1H NMR peaks for H_a , H_b and H_c at 8.94, 8.36 and 7.24 ppm respectively, compared to complex **7b**'s which were reported at 8.87, 7.97 and 7.88 ppm respectively.

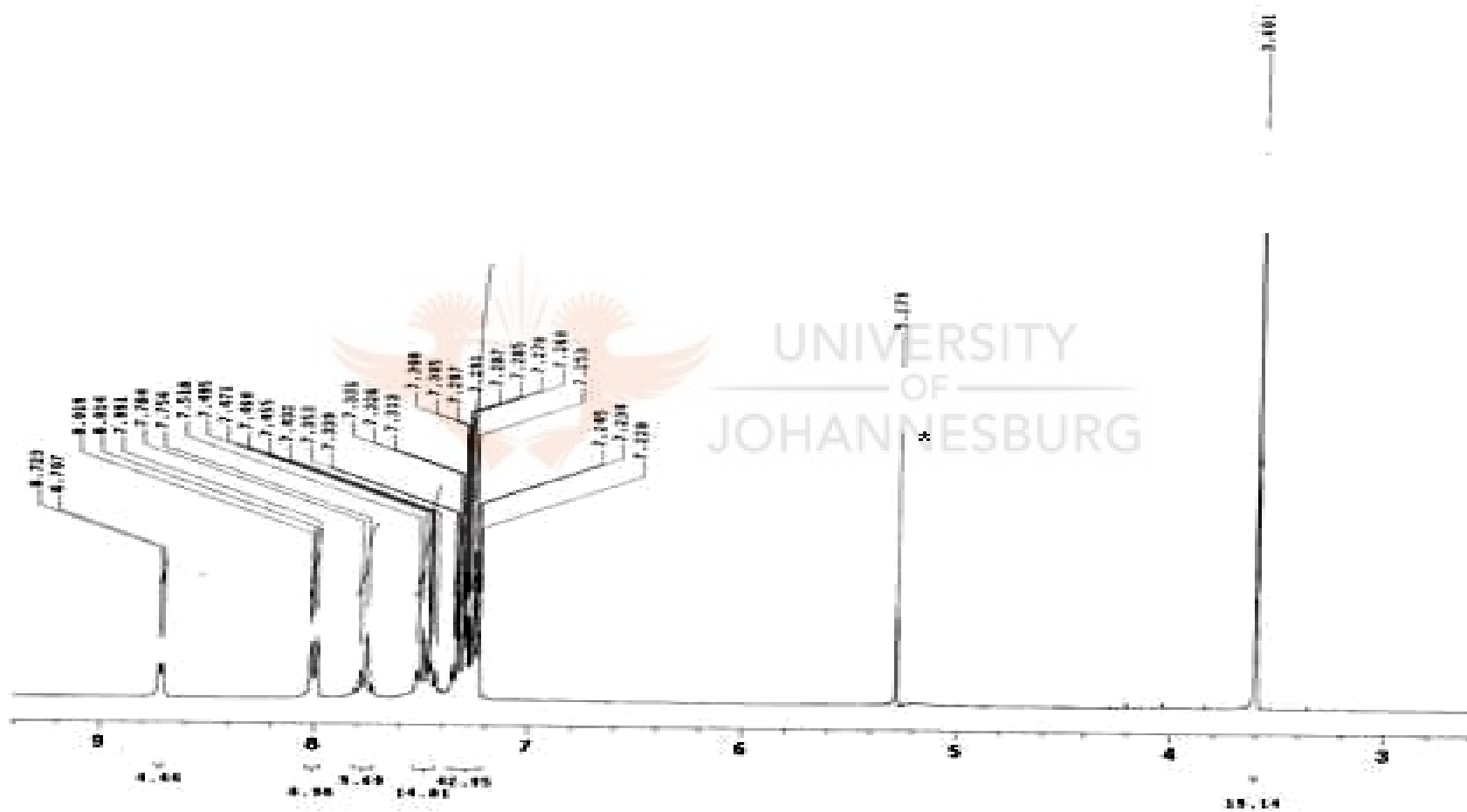


Figure 3.7: ¹H NMR spectrum of [Au(SCH₂(C₆H₅))₃(2-C₆H₅(C₆H₄N))] (**7b**). * = CH₂Cl₂

Fan *et al.*¹⁰ previously reported the synthesis of gold(III) complexes of the type $[\text{AuCl}_2(\text{ppy})]$ (ppy = 2-phenylpyridine), with 2,3-mercapato-1-propanol in dichloromethane-methanol at room temperature, which gave a mixture of two isomers. These thiolate gold(III) complexes were found to be more stable and more soluble in organic solvents.¹⁰ The thiolate gold(III) complex **7b** was also obtained as a soluble and stable compound. The spectroscopic data obtained confirm the synthesis of the complexes. The ^1H and ^{13}C NMR displayed a pattern which was consistent with different environments of all protons of the thiol and the starting material, thus confirming complexation.

3.3. Synthesis of palladium(II) complexes

Gold(III) has an isoelectronic outer structure (d^8) with platinum(II) and palladium(II) and likewise forms square planar complexes,¹¹ it is therefore not surprising that such complexes would have similar reactivity. For instance platinum and nickel thiolato complexes readily react with SO_2 , binding reversibly to a sulfur atom of the thiolate ligand due to weak sulfur-sulfur interaction.¹²

In preparing 2-phenylpyridinepalladium(II) chloride, it was found that when 2 moles of 2-phenylpyridine was reacted with 1 mole of $[\text{Pd}(\text{Cl}_2)(\text{MeCN})_2]$, a complex in which one mole of 2-phenylpyridine crystallized with 2-phenylpyridine palladium(II) chloride was obtained. This was confirmed by X-ray crystallography (Fig. 3.8). This showed that 2 molecules of 2-phenylpyridine bonded with a PdCl_2 unit, with a third molecule of the

ligand co-crystallizing with the product. The molecular structure exhibits a distorted square planar geometry about the palladium.

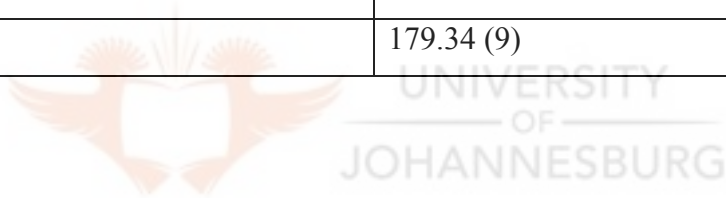
The environment consists of two chlorine atoms in trans disposition to the metal and the two nitrogen atoms of the pyridine rings. The Pd-Cl (2.3025 (16) and 2.3095(17) Å) distances are typical for palladium square planar complexes (Pd-Cl from 2.276 to 2.326 Å).¹³ Moreover the Pd-N_{py} bond distances 2.0054(4)Å are of the same order as those reported in the literature¹⁴ (Pd-N_{py} from 1.971 to 2.141 Å).¹⁵ The angles N-Pd-N and Cl-Pd-Cl are likely to be compared. The Cl-Pd-Cl and N-Pd-N angle (179.34 (9)° and 178. (9) (2) respectively) deviate a little from linearity. The pyridine and chlorine angles are also considerably smaller and bigger [N(1)-Pd-Cl(1), 92.03 (13)°, N(2)-Pd-Cl(1), 88.30 (12)°, N(1)-Pd-Cl (2), 88.61(13)°, N(2)-Pd-Cl(2), 91.06 (12)°] than the ideal values(90°) of square planar geometry. Other bond length and angle data of interest are summarised in Table 3.4.

Table 3.3: Crystal data and structure refinement for **8**

Empirical formula	C ₃₄ H ₂₈ Cl ₂ N ₂ Pd
Formula weight	641.88
Temperature/ K	173(2)
Wavelength/Å	0.71073
Crystal system	Triclinic
Space group	PI
a/Å	24.9108(6)
b/Å	15.2114(4)
c/Å	7.3007(2)
α/°	90
β/°	92
γ/°	90
V/Å ³	2764.74(12)
Z	4
D _c / Mg m ⁻³	1.542
Crystal size/ mm ³	0.1x 0.1 x 0.2
Absorption correction	Empirical with SADABS
T _{max} /T _{min}	0.9729/0.9657
R(F) (%) [I[I>2σ(I)]]	0.0428
R(w F ²) ^a (%) (all data)	0.1269

Table 3. 4. Selected bond lengths (Å) and bond angles (°) for dichloro-bis-2-phenylpyridinepalladium(II) with estimated standard deviations (e.s.d.s) in parentheses.

Bond distances (Å)	
Pd-N(1)	2.005(4)
Pd-N(2)	2.030 (4)
Pd-Cl (1)	2.3025 (16)
Pd-Cl(2)	2.3095(17)
Bond angles (°)	
N(1)-Pd-N(2)	178.9(2)
N(1)-Pd-Cl(1)	92.03 (13)
N(2)-Pd-Cl(1)	88. 30 (12)
N(1)-Pd-Cl (2)	88. 61(13)
N(2)-Pd-Cl(2)	91.06 (12)
Cl(1)-Pd-Cl(2)	179.34 (9)



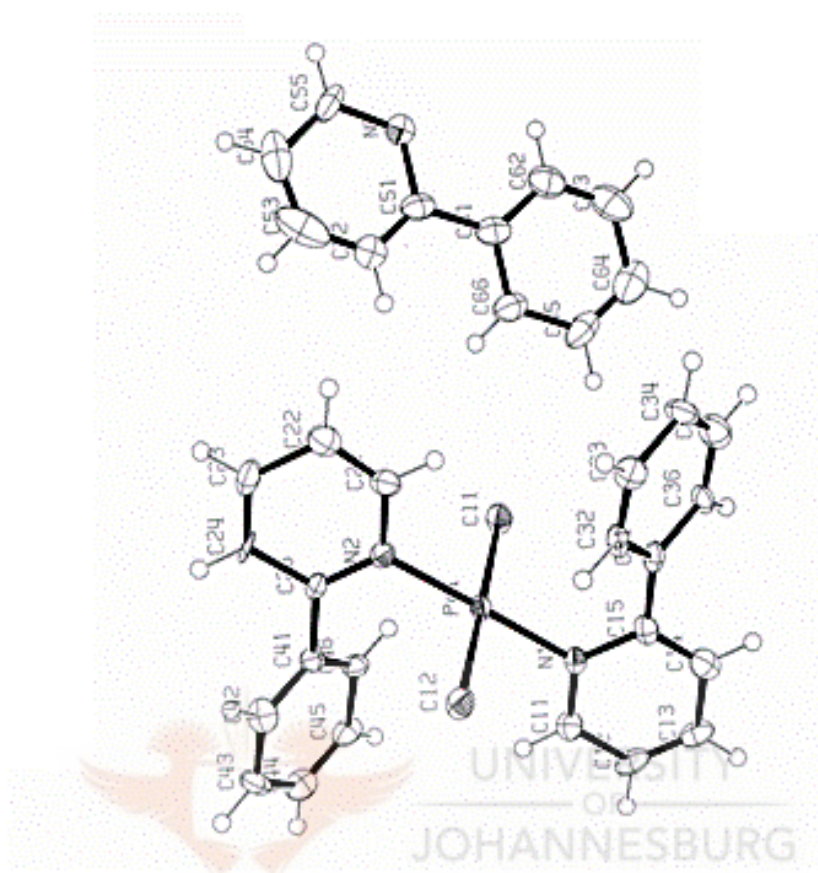


Figure 3.8: Molecular structure of $[\text{PdCl}_2(2\text{-C}_6\text{H}_5(\text{C}_6\text{H}_4\text{N}))]$ (**8**).

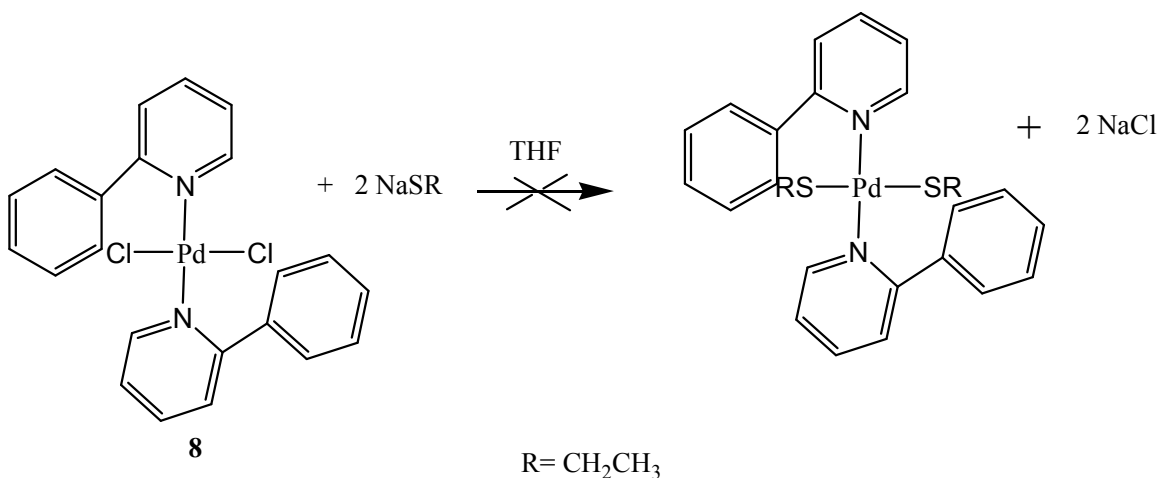
3.3.1. Synthesis of palladium(II) thiolate complexes

Initially the thiols and palladium(II) complex was reacted in the presence of excess Et₃N as a base, but the Et₃N was unable to effect a reaction between the thiol and the (2-phenylpyridine)Pd(II) chloride. The thiols were therefore reacted with a stronger base, NaH in order to convert them into sodium salts of general formula NaSR, where R is the rest of the thiolate molecule (equation 3).



(R = aryl, alkyl)

The sodium salt was successfully prepared but the final palladium product was intractable. The reason for the unsuccessful results could be due to the steric effect, which is caused by the phenyl rings on the pyridine preventing the binding of the thiolate ligands to the palladium centre as in (Scheme 3.7). Steric crowding at the metal centre is usually assumed to inhibit associatively activated reactions and to facilitate dissociatively activated reactions. Bulky groups can block the approach of attacking nucleophiles, but the reduction of coordination number in a dissociatively activated reaction can relieve the crowding in the activated complex.¹⁶



Scheme 3.7: Synthesis of [Pd(SR)₃(2-C₆H₅(C₆H₄N))].

As observed in the crystal structure that the ligand co-crystallises with the palladium complex. This phenomenon could also explain why the thiol could not react with the palladium chloride starting material.

3.4. ELECTROCHEMICAL STUDIES

3.4.1. Introduction: An overview

The redox chemistry of binuclear gold(I) phosphine complexes containing aliphatic dithiolate ligands have been recently investigated by using electrochemical, chemical and photochemical techniques.¹⁷ These complexes are related to auranofin, an orally active anti-arthritis drug containing triethylphosphine and tetraacetylthioglucose.¹⁸ Cyclic voltammetry experiments of auranofin showed two irreversible anodic processes near 600 mV and 1500 mV. The oxidation process showed that only one electron is transferred per two Au, P, or S sites.¹⁹

These molecules readily undergo oxidation addition reactions to form gold(I) to gold(III) complexes. Anderson, *et al.*²⁰ also reported the oxidation of $[\text{AuCl}(\text{PPh}_3)]$, which undergoes oxidation at 1500 mV vs ferrocene/ferrocinium.²¹ The oxidation is assigned as involving the gold(I/III) couple on the basis of electrochemical and spectrochemical studies. In addition, Anderson *et al.* also suggested that the ligands themselves may undergo oxidation at low positive potentials. It is important to note that free thiolate anions, such as p-thiocresolate, oxidize near 1500 mV. These electrochemical studies demonstrate that gold, phosphine and sulfur ligands may have redox sites.²⁰

As gold(III) has an isoelectronic outer structure (d^8) with platinum(II) and palladium(II) and likewise forms square planar complexes,¹¹ it is therefore not surprising that such complexes would have similar reactivity. The redox chemistry of palladium is dominated by two-electron conversions between palladium(0), palladium(II) and palladium(IV) species.²¹ Mononuclear palladium(I) complexes are rare because disproportionation to palladium(II) and palladium(0) is usually thermodynamically and kinetically favourable.²² Initial experiments have revealed that the palladium(II) complexes exhibit only single two-electron reduction step when cyclic voltammetry is carried out at room temperature in acetonitrile using scan rates.²³ However, for the nickel system the potential separation between the two reduction steps was found to depend on the solvent and electrode kinetics of the nickel(I,0) couple appeared significantly slower than those of the nickel(II,I) couple.²⁴ thus it is anticipated that the correct choice of experimental conditions might lead to either nickel(II,I) or nickel(I,0).

In this section, we describe how electrochemical techniques have been used to monitor various metal thiolate sensors for sulfur dioxide. There are several methods and instruments that are available to monitor levels of sulfur dioxide. These methods include chromatography,²⁵ capillary isotachopheresis,²⁶ Fourier transform infrared spectrometry,²⁷ pulsed laser photo acoustic detection,²⁸ and chemi-luminescence.²⁹ These methods are based on expensive conventional UV or IR spectroscopy instrumentation in which the gases must be conditioned before analysis.²⁵ It was expected that our studies may introduce an easier and cheaper means to monitor the levels of sulfur dioxide in the environment.

3.5. Redox chemistry of gold thiolate complexes

3.5.1. Oxidative process of [AuCl(PPh₃)]

Electrochemical studies of the complexes were undertaken and the data is presented below. The instrument used was a BAS-100A potentiostat connected to the computer with a platinum working electrode and platinum wire as the auxiliary electrode and SCE as reference electrode. The supporting electrolyte used was tetrabutylammonium-tetrafluoroborate [*n*-Bu₄N][BF₄]

The first experiment performed was the cyclic voltammetry of [AuCl(PPh₃)] to establish a baseline of the electrochemistry of phosphine gold(I) complexes. The results of cyclic voltammetry experiments of [AuCl(PPh₃)] are shown in Fig 3.9. Figure 3.9 is the current-voltage responses for 10⁻³ M of [AuCl(PPh₃)] in tetrabutylammonium-tetrafluoroborate [*n*-Bu₄N][BF₄] and dichloromethane-acetonitrile solutions at scan rates 100 mV/s. The

CV shows one anodic peak process, which occurs at 1690 mV (vs. SCE). The redox peak is found to be irreversible, which means there is no reduction peak coupled with the peak at all scan rates, concentration and switching potentials. The redox processes are assigned as involving the gold(I/III) couple. The same redox peaks were reported by Anderson *et al.*²⁰ that [AuCl(PPh₃)] undergoes oxidation at 1600 mV. Rakhimov *et al.*³⁰ suggests that the oxidation of [AuCl(PPh₃)] at 1600 mV (vs. SCE) involves phosphine. But Anderson explained that the phosphine can only be observed as a shoulder at 1330 mV in the presence of AuCl⁻ during the formation of [AuCl(PPh₃)], which is due to a free phosphine equation (4).



The shoulder is due to reduction of a species formed by oxidation of [AuCl(PPh₃)], but it is not well defined by cyclic voltammetry but is more pronounced in a thin layer cyclic voltammogram, since diffusion of any electrogenerated products away from the electrode is reduced.²⁰

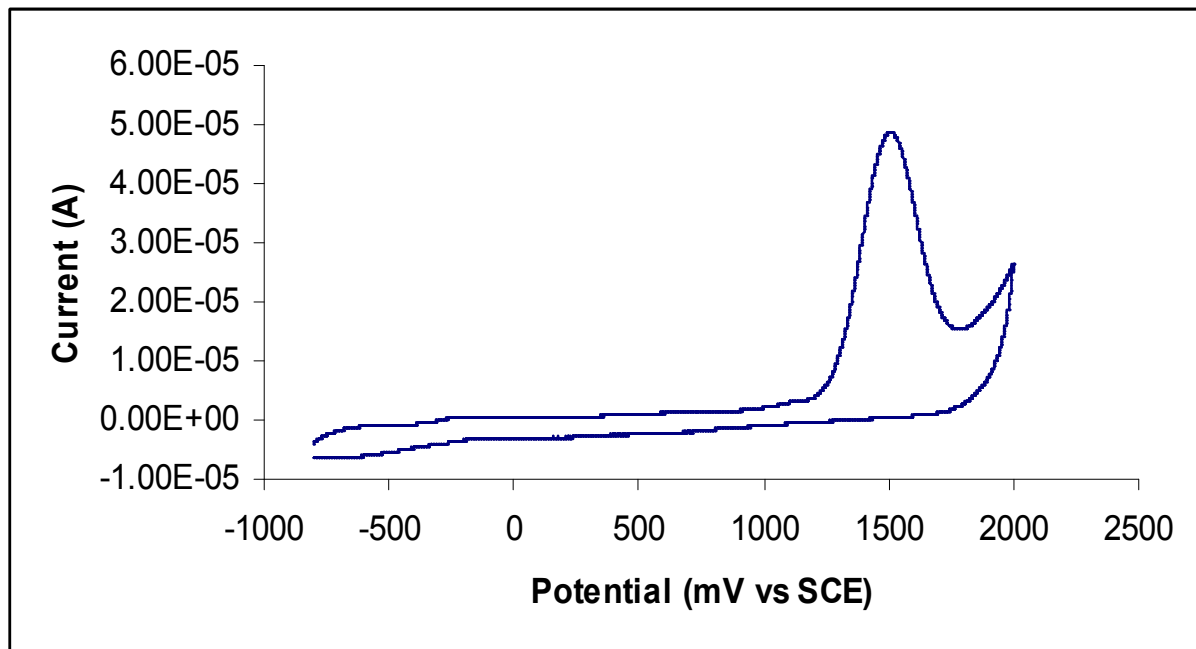


Figure 3.9: Cyclic Voltammetry of 10^{-3} M solution of $[\text{AuCl}(\text{PPh}_3)]$ in acetonitrile-dichloromethane, 0.10 M $[\text{n-Bu}_4\text{N}][\text{BF}_4]$ at 100V/s: potential scan from -800 - 2000 mV

Figure 3.10 shows the electron-transfer mechanism for gold complexes that have been studied.²⁰ The species $[\text{AuX}_4]^-$ X = Cl, ClO and $[\text{Au}(\text{PPh}_3)]\text{Cl}$ can be generated from one another by redox processes. As shown, the nature of ligands coordinated to gold(I) species have a significant influence on the electro-chemical properties.²⁰

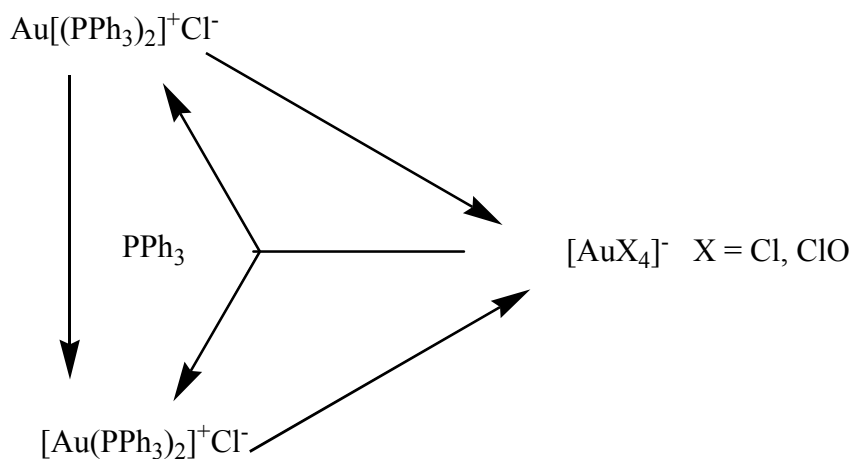
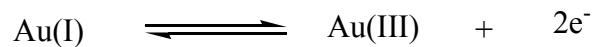


Figure 3.10. Electron-transfer scheme for $\text{K}[\text{AuCl}_4]$, $[\text{Au}(\text{PPh}_3)]\text{Cl}$ and



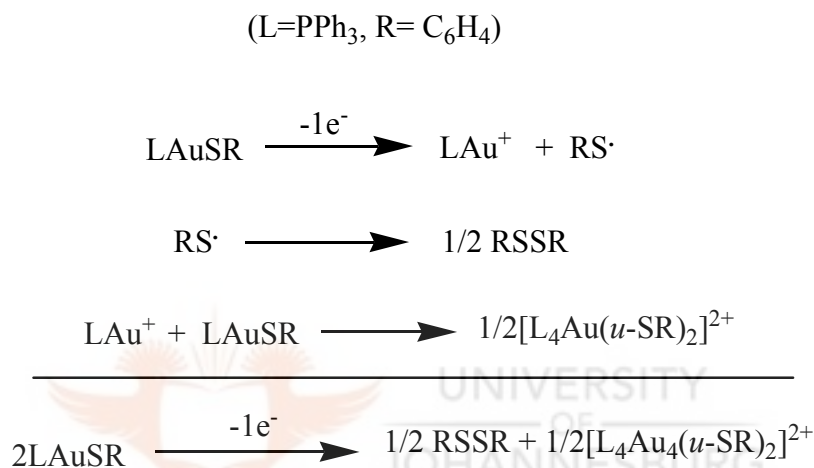
3.5.2. Oxidative process of gold(I) and gold(III) thiolate complexes

Figure 3.11 shows CV results of $[\text{Au}(\text{SCH}_2(\text{C}_6\text{H}_4)(\text{PPh}_3)]$ (**1**), the results were obtained using the instrument BAS-100A potentiostat connected to the computer and controlled by GPES software, with a platinum working electrode and platinum wire as auxiliary electrode and SCE as reference electrode. The supporting electrolyte used is tetrabutylammonium-tetrafluoroborate $[n\text{-Bu}_4\text{N}][\text{BF}_4]$.

The CV shows one anodic peak process, which appears at 1630 mV (vs SCE). The redox peak is found to be irreversible, which means there is no reduction peak coupled with the peak at all scan rates, concentration and switching potential. The redox process is assigned as involving the gold(I/III) couple, the redox observed for complex **1** is similar to the results obtained for [AuCl(PPh₃)]. The difference is a new unresolved peak that appears at 329 mV. The peak is due to the thiolate ligand bound to the gold. It is important to note that free thiolate anions, such as p-thiocresolate, are known to oxidize near 0 mV (vs. SCE).

The thiol p-thiocresol, oxidizes near 1000 mV. Mohamed *et al.*¹⁸ explained that change of concentration as well as of electrolyte has an effect on resolution of peaks; the data demonstrated that the CV wave-shapes for phosphine gold thiolate complexes are sensitive to the type of electrode as well as to solvent owing to the effects of adsorption at the electrode. The investigation explained that changing the electrolyte (PF₆⁻ vs. BF₄⁻) would have an effect. The results obtained suggested the PF₆⁻ anion is not as efficient as BF₄⁻ in keeping the electrode clear of oxidation products, leading to an increase in filming rate and thus leading to a great oxidation in the current response. The data also described that the increase in concentration of an analyte leads to great response of oxidation process.¹⁸

The oxidation sequence of the gold thiolate complex is illustrated in Scheme 3.9. One electron oxidation of $[\text{Au}(\text{SCH}_2(\text{C}_6\text{H}_4)(\text{PPh}_3)]$ (**1**) results in homolytic cleavage of the Au-S bond and formation of $[\text{Au}(\text{PPh}_3)]^+$ and thiyl radical $\cdot\text{SCH}_2\text{C}_6\text{H}_4$, which rapidly dimerizes to produce disulfide.³¹



Scheme 3.9: Electron transfer of $[\text{Au}(\text{SCH}_2(\text{C}_6\text{H}_5)(\text{PPh}_3)]$

Previous studies on the electronic structure of gold(I) phosphine complexes have assigned the HOMO orbitals of these complexes as having significant sulfur character.³² The cation, $[\text{Au}(\text{PPh}_3)]^+$, reacts with a molecule of the starting mononuclear gold(I) complex to form a digold complex with thiolates bridging two gold(I) centers, which then dimerizes *via* gold-gold bonds to form the observed tetragold cluster (Scheme 3.9). The last step in the mechanism is supported by an independent synthesis of the tetragold cluster. According to the scheme, one electron oxidation of $[\text{Au}(\text{SCH}_2(\text{C}_6\text{H}_4)(\text{PPh}_3)]$ converts the complexes to gold clusters and disulfide. The same results were reported by

Chen *et al.*³¹, comparing oxidation of mononuclear and dinuclear gold(I) phosphine thiolate complexes.

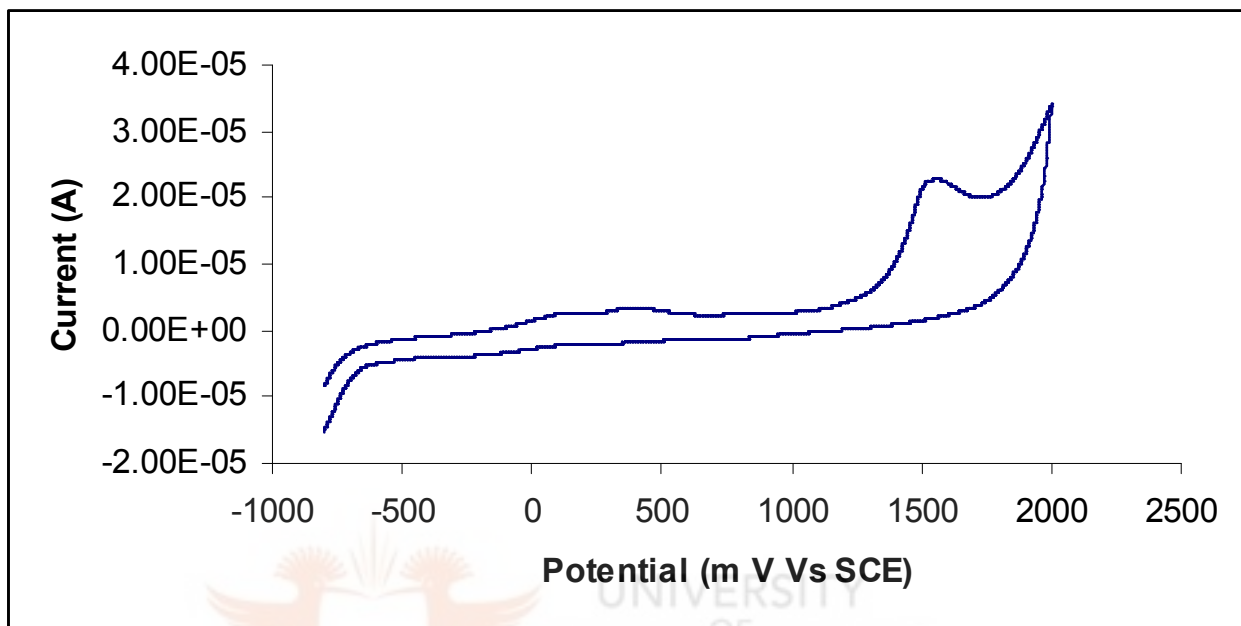


Figure 3.11: Cyclic Voltammetry of 10^{-3} M solution of $[\text{Au}(\text{SCH}_2(\text{C}_6\text{H}_4)(\text{PPh}_3))]$ (**1**) in acetonitrile-dichloromethane, 0.10 M $[\text{n-Bu}_4\text{N}][\text{BF}_4]$. at 100V/s: potential scan from -800- 2000 mV

Similar results for complex **1-7b** were obtained, where one anodic peak and unresolved peak at 1551 mV and 706 mV respectively. The results were obtained for the complexes **1-7b** are summarised in Table 3.5.

3.5.3. Reactions of complexes $[\text{Au}(\text{SR})(\text{PPh}_3)]$, ($\text{R} = \text{CH}_2\text{C}_6\text{H}_5$ (1), $\text{C}_6\text{H}_4\text{NH}_2$ -2 (2), $\text{C}_6\text{H}_4\text{Cl}$ -4 (3), $[\text{Au}(\text{SCH}_2\text{C}_6\text{H}_5)_3\text{2-C}_6\text{H}_5(\text{C}_6\text{H}_4\text{N})]$ (7b) with sulfur

dioxide.

All the complexes readily react with sulfur dioxide, the complexes change colour from clear to yellow immediately upon purging of sulfur dioxide.

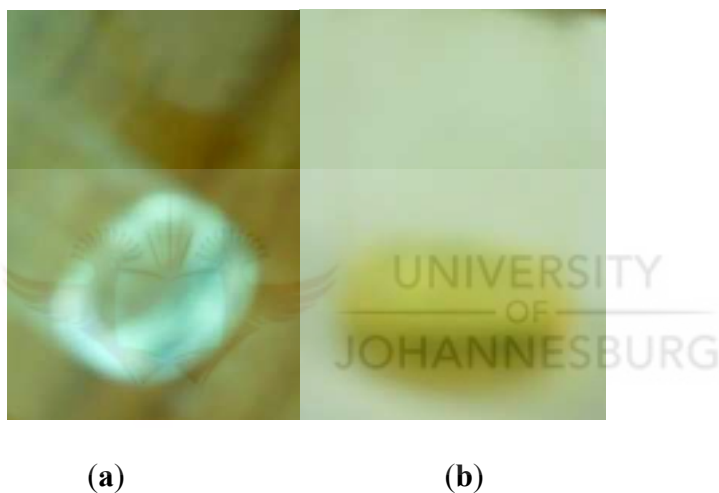
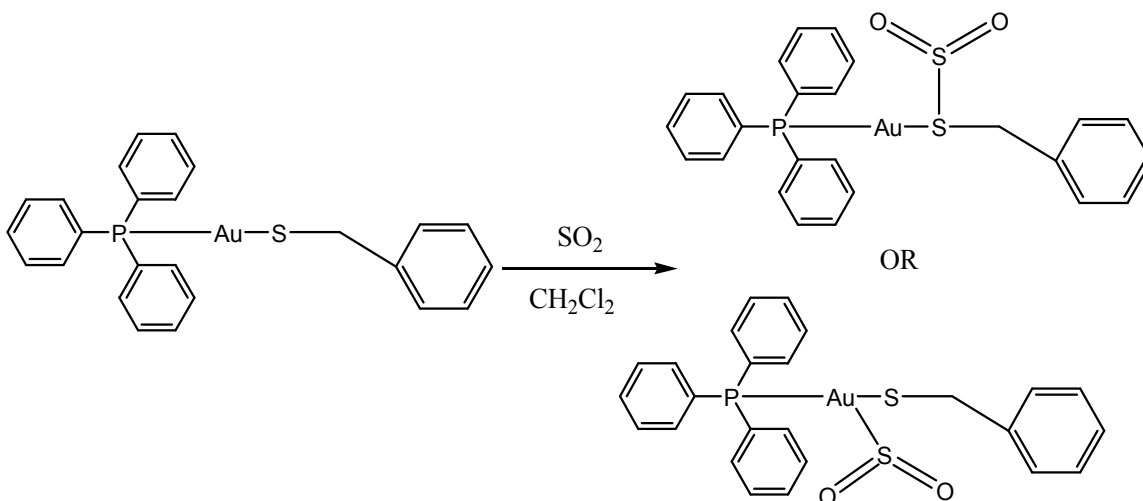


Figure 3.12: Showing the colours of complex **1-7b** before (a) and after reaction with SO_2

The progress of the reaction of these complexes with SO_2 was apparent as their colour changed. Similar colour changes were observed in SO_2 reactions with metal organochalcogene complexes by Kubias and co-workers, where blue solutions of $\text{Cp}_2^*\text{Cr}_2\text{S}_2$ ($\text{Cp} = \eta^5\text{-C}_5\text{Me}_5$) which turned deep red on reaction with SO_2 .³³ There are two possible ways in which the SO_2 can react with the gold complexes (Scheme 3.10). The first is the binding of the SO_2 to the metal, as observed for the nickel square planar complexes,

(dppe)Ni(1,2-BDT) or (dppe)Ni(TDT) (dppe = bis(diphenylphosphine) ethane, 1,2-BDT = 1,2-benzenethiol and TDT = toluenedithiol.³⁴ The second option is the SO₂ binding to the chalcogen atom of the ligand. Binding of SO₂ to the gold should result in change in the chemical environment or chemical shift in the ¹H NMR either shift downfield or upfield, but no such peaks were found for the SO₂ adducts of the complexes, this could therefore show that the SO₂ is not bound to the gold.

The second option for SO₂ is to bind to the sulfur atom as the only option; this is possible and could result from the nucleophilicity of the Au-SR moiety.³³ Kubias have independently demonstrated that the metal-SR moiety can bind SO₂ with the thiolato sulfur behaving as Lewis base. Therefore, binding of SO₂ to the ligand results in a reduction of the electron density at the metal centre as the ligand donates electron in the empty d-orbital's of the SO₂ ligand, which results in backbonding to the phosphorus (PPh₃) to compensate for any electron density that it would have lost to the metal during the SO₂ binding. Based on the above discussion the SO₂ adducts could be formulated as [Au(S(SO₂))(C₆H₄X)(PPh₃)], where X = 4-Cl, 2-NH₂ and CH₂. Unfortunately attempts to obtain crystals of the gold complexes have been elusive, due to the very facile manner in which the SO₂ desorbs.



Scheme 3.13 . Show possible ways SO_2 could react with the complex

Table 3.5 summarizes the results from this study of oxidation of gold(I) phosphine and gold(III) complexes bound to sulfur ligands. Figure 3.13, shows the CV results of the complexes with sulfur dioxide. Upon purging of sulfur dioxide to the solution, the redox peak at 1551 mV also increases in current and the peak at 706 mV also increase in current, and appearance of new peak at 143 mV. Because of the new peak at 143 mV, we suspected that the sulfur dioxide might be undergoing oxidation with the platinum electrode.

Table 3.5: Cyclic Voltammetry data for gold(I) phosphine and gold(III) thiolate complexes.

Complex	Oxidation potential		
	Au ^I /Au ^{III}	S-S(disulfide)	SO ₂ /SO ₄ ²⁻
[AuCl(PPh ₃)l	1690 mV		
1	1630 mV	329 mV	290 mV
2	1551 mV	706 mV	143 mV
3	1740 mV	870 mV	978 mV
7b	1513 mV	122 mV	204 mV

Reference electrode: SCE, solvent mixture: (CH₂Cl₂:CH₃CN) (1:3 molar ratios)

The substituents of the thiolate ligand also seem to have some effect on the CV peaks. The thiolato signals for the series of compounds of formula [Au(SC₆H₄X)(PPh₃)] where X = 4-Cl, 2-NH₂ and CH₂ can be compared. Changing the X-group and keeping other ligands the same showed that the complex containing more electrons with drawing X= 4-Cl, 2-NH₂ and CH₂ was difficult to oxidize. Thus the order of difficulty in oxidizing the complexes was Cl > CH₂ > NH₂ with potential values of 1740 mV, 1630 mV and 1551 mV versus SCE for Cl, CH₂, NH₂ respectively. Even with the formation of S-S (disulfide) the same trend was observed.

A CV experiment of the platinum electrode with electrolyte and SO₂ was run. The results showed the same peak at 143 mV (Fig 3.13). The reaction of SO₂ at electrochemical interface is complicated, since the oxidation and reduction of dissolved SO₂ takes place at about the same potential.

The oxidation product of dissolved SO₂ at platinum electrodes has been proposed initially to be ditionate.³⁵ Audry and Voinov³⁶ postulated that the reaction proceeds via ditionate as intermediate on smooth platinum electrodes. Samec and Weber³⁷ have also studied the SO₂ oxidation on gold electrodes and have proposed the adsorbed SO₂ as reaction intermediate and the formation of S(VI) as the oxidation product generating HSO₄⁻ in acidic solutions.³⁷

The results were in good agreement with the early findings of Seo and Sawyer that the electron transfer precedes via a two electron at 400 mV on gold electrodes.³⁸ Moraes and Weber also reported that during electrochemical adsorption of SO₂ at fixed potential below 700 mV on platinum electrodes cathodic current flows, showing that during the adsorption an oxidation reaction takes place and the SO₂ residues are irreversibly adsorbed.³⁹ The results obtained in this study are in agreement with the one reported in the literature.

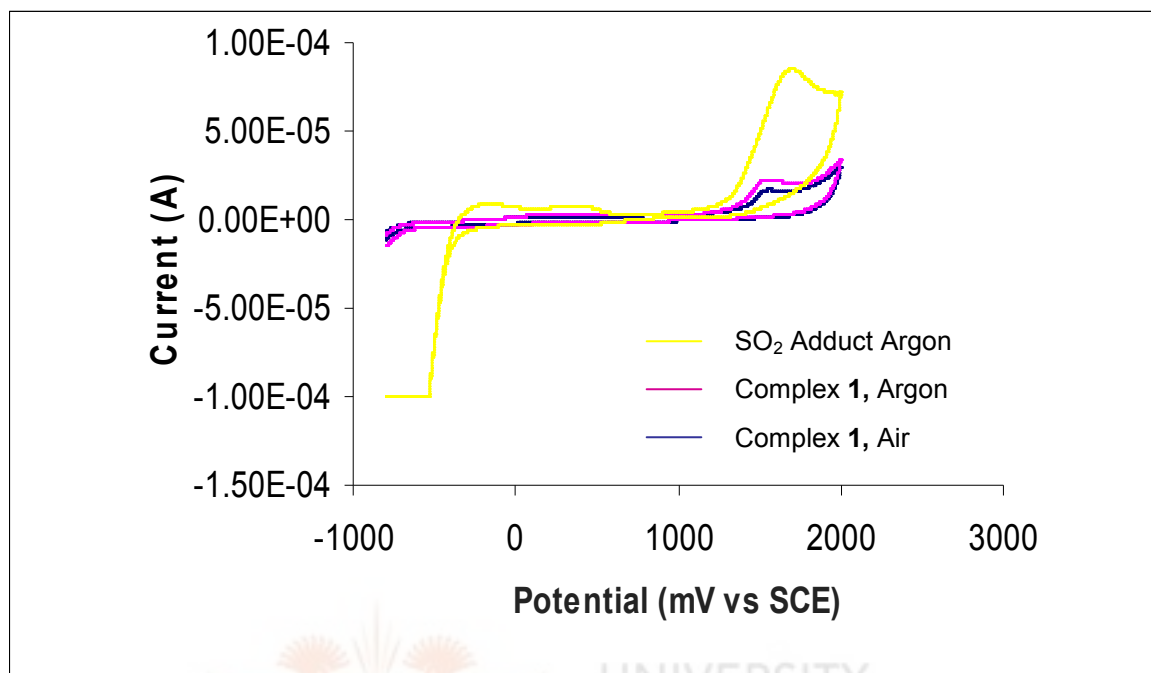


Figure 3.13: Cyclic Voltammetry of 10^{-3} M solution of $[\text{Au}(\text{SCH}_2(\text{C}_6\text{H}_4)(\text{PPh}_3)]$ in acetonitrile - dichloromethane, 0.10M $[n\text{-Bu}_4\text{N}][\text{BF}_4]$ at 100 mV/s: potential scan from -800 - 2000 mV

Osteryoung Square Wave Voltammetry (OSWV) was performed on the complexes **1-7b** before and after purging of SO₂. The OSWV peaks were certainly broadened, but there was no clear cut indication towards the thiol and the SO₂ peaks. The gold(I)/gold(III) peak was clearly demonstrated. The use of coordinating solvent acetonitrile (CH₃CN) and BF₄N as supporting electrolyte could mask some key features of the CV. Reports by Geiger and co-workers⁴⁰ mentioned that poorly resolved peaks in CH₃CN/ 0.10 M [*n*-Bu₄N][BF₄] often becomes well resolved in the system of uncoordinative dichloromethane and poorly nucleophilic salt [*n*-Bu₄N][BC₆F₅)₄] as supporting electrolyte.⁴⁰ Efforts were made to show the peaks clearer by plotting the voltammogram from 0 mV to 1500 mV(Fig. 3.15).

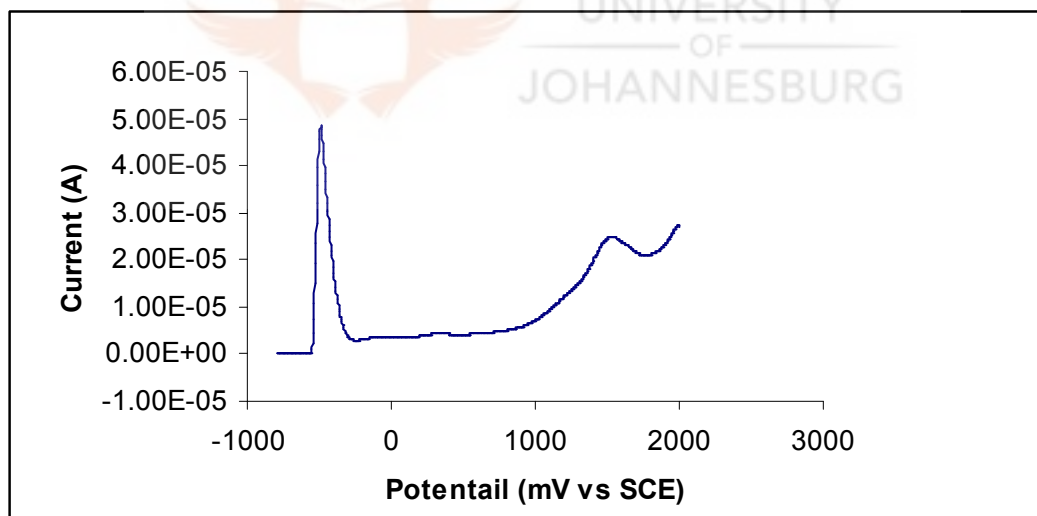


Figure 3.14: Osteryoung Square Wave Voltammetry of 10⁻³ M solution of [Au(SCH₂(C₆H₄)(PPh₃))] in acetonitrile -dichloromethane, 0.10 M [*n*-Bu₄N][BF₄] at 100 mV/s: potential scan from -800 - 2000mV

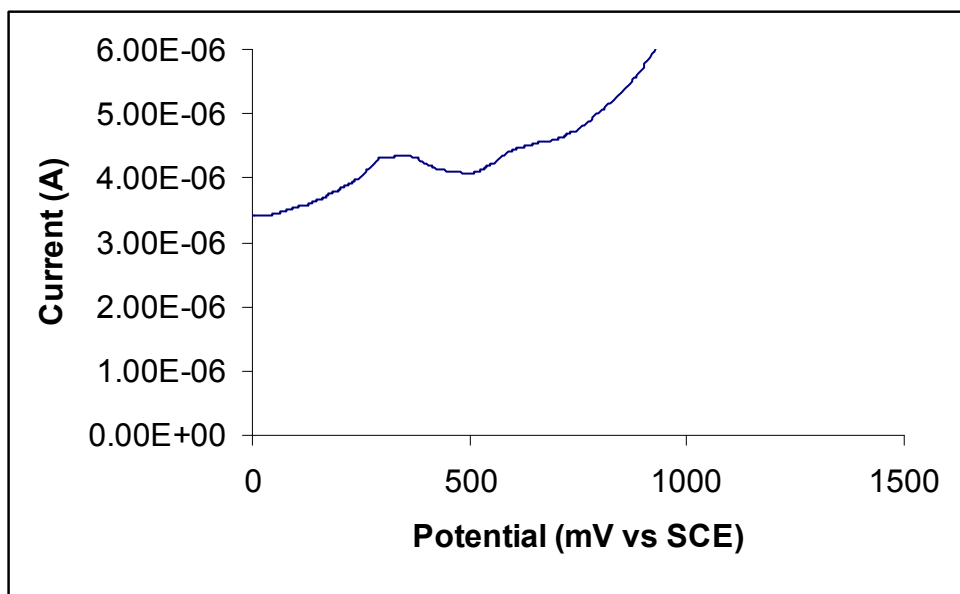


Figure 3.15: Osteryoung Square Wave Voltammetry of 10^{-3} M solution of $[\text{Au}(\text{SCH}_2(\text{C}_6\text{H}_4)(\text{PPh}_3)]$ in acetonitrile /dichloromethane, 0.10 M $[\text{n-Bu}_4\text{N}][\text{BF}_4]$ at 100 mV/s: potential scan from 0 to 1000 mV



3.6. Palladium thiolate complexes

The palladium complex involved in the study was synthesized as described elsewhere.⁴¹ As gold(III) has isoelectronic outer structure (d^8) with platinum and palladium, these complexes would be expected to have similar reactions. This phenomenon led to investigating the reaction of palladium thiolate complexes with SO_2 , thus comparing them to the gold thiolate complexes.

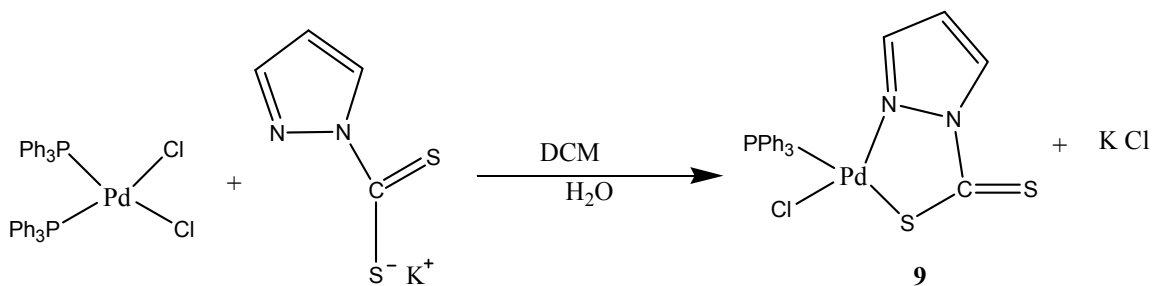


Figure 3.16. Structure of palladium thiolate complex

Complex **9** was synthesized by reacting pyrazole salt with palladium chloride in dichloromethane and water in a biphasic reaction, the reaction took 15 min to complete. The product obtained was isolated using a separating funnel and the solution was evaporated to get the desired product.

The results of Cyclic Voltammetry experiments of **9** are shown in (Fig. 3.17) is the current-voltage responses for 10^{-3} M of Pd complexes in tetrabutylammonium-tetrafluoroborate [*n*-Bu₄N][BF₄] and dichloromethane solutions at scan rates 100 mV/s. The CV shows one anodic peak process at 1076 mV. The redox peak is also found to be irreversible when comparing with gold thiolate complexes. Umakoshi and co-workers also observed one anodic peak with complex [Pd₂(pyt)₄] pyt = pyridine-2-thiol, which was irreversible at 500 mV using scan rate $v = 50$ mV/s, Umakoshi explained that the irreversible behaviour, is observed even at scan rate of 500 mV/s, which indicates a rapid decomposition of the one-electron-oxidation product [Pd₂(pyt)₄]⁺.⁴²

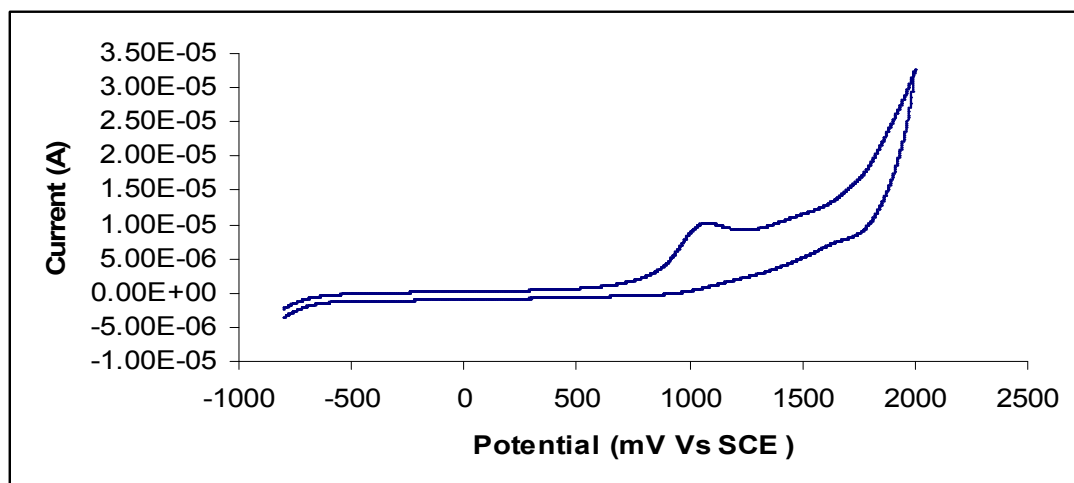


Figure 3.17 : Cyclic Voltammetry of 10^{-3} M solution of complex **9** in acetonitrile - dichloromethane, 0.10 M $[n\text{-Bu}_4\text{N}][\text{BF}_4]$ at 100 mV/s: potential scan from -800 to 2000 mV

Upon purging of SO_2 through the solution, no change of colour was observed but there was shift of peak from 1076 mV to 1089 mV and the appearance of a new peak at 1324 mV (Fig. 3.18). The shift of the peak and new peak is due to the binding of SO_2 to the sulfur atom of the ligand or to the metal and also peak at 143 mV. Similar peak shifts were also observed with the gold complexes. The palladium thiolate complexes were then seen to react the same way as the gold thiolate complexes with SO_2 , as it is expected that palladium(II), platinum(II) and gold(III) has isoelectric outer structure and form square planar complexes.

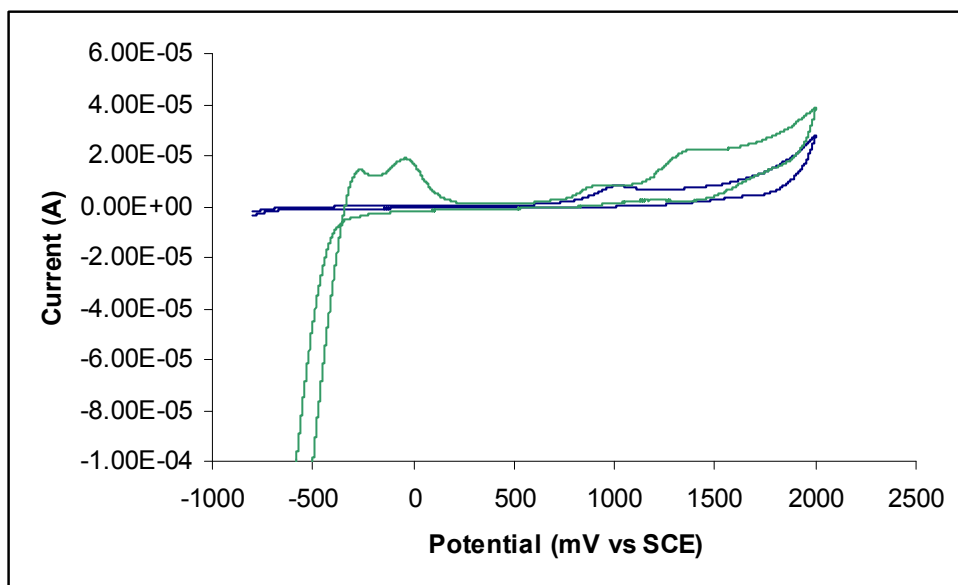


Figure 3.18. Cyclic Voltammetry of 10^{-3} M solution of complex **9** in acetonitrile-dichloromethane, 0.10 M $[n\text{-Bu}_4\text{N}][\text{BF}_4]$ at 100 mV/s: potential scan from -800-2000mV

Table 3.6: Cyclic Voltammetry Data for palladium(II) thiolate complexes.

Before SO ₂		After SO ₂	
Complex	Pd(II)/ Pd(0)	Pd(II)/ Pd(0)	S-S
9	1076 mV	1089 mV	1324 mV

There are three main catalytic behaviour that can be involved in electrochemical reactions, which are (i) a peak potential shift to less or higher potential; (ii) enhanced peak currents; (iii) higher slope at inclining part of the peak and better defined peak shape wave can be observed.⁴³ The results obtained in this study when SO₂ is reacted with gold complexes shows enhancement (increase in current) of the gold peak at 1551 mV, this is because the SO₂ reacts with the gold metal because there was no change with the thiolate

peaks. But when SO₂ is reacted with the palladium complex there is a shift and also an appearance of a new peak, which can be concluded that the SO₂ reacts with the ligand and the metal.

3.7. Visible and Ultraviolet Spectroscopy Studies

Ultraviolet studies were performed as another form of monitoring whether the complexes [Au(SR)(PPh₃)], (R = CH₂C₆H₅ (**1**), C₆H₄NH₂ (**2**), C₆H₄Cl (**3**), [Au(SCH₂C₆H₅)₃ 2-C₆H₅ (C₆H₄N)] (**7b**) react with sulfur dioxide. Ultraviolet spectra are recorded by irradiating a sample with the UV light of continuously changing wavelength. When the wavelength of light corresponds to the amount of energy required to excite a π electron to a higher level, energy is absorbed. The absorption is detected and displayed on a chart that plots wavelength versus radiation absorbed.⁴⁴ The wavelength of radiation necessary to cause an electronic excitation in an unsaturated molecule depends on the nature of the π electron system in the molecule. As the rule energetically favoured electron promotion will be from the highest occupied molecular orbital (HOMO) to the lowest unoccupied orbital (LUMO), and the resulting species is called excited state.⁴⁴

Before purging of SO₂ to the complex, UV-Vis spectra exhibited characteristic absorptions in the B band region (UV region) at around 200-400 nm, arising from the deeper π - π^* transitions, a sharp peak at 227nm and a broad peak around 250nm are observed. After addition of SO₂ to the complex, the B bands (broad peak) of all the complexes shift to higher energy from 250nm to 286nm (Fig 3.19), and there was no shift of the 227nm peak. Electrons in the vast majority of molecules fall into one of the three

classes: σ electrons, π electrons and non-bonding electrons called n electrons. The third class plays no role in the bonding of atoms into molecules. In chemical terms a single bond between atoms such as C-C, C-H, O-H, contains σ electrons, a multiple bond, C=C, C=N, contains π electrons, while atoms to the right of carbon in the periodic table, notably nitrogen, oxygen, and the halogens, possess n electrons. In general the σ electrons are mostly firmly bound to the nuclei and hence require a great deal of energy to undergo transition, while the π and n electrons require less energy, the n electrons usually requires less than the π .⁴⁵

When the SO₂ is added to the complex it donates electrons to the complex making energy of excitation of electrons less. The shift of the broad peak can be attributed to π - π^* and n - π^* transition (attributed to the non-bonding of sulfur electron (n)). This appears near the broad line of the near and far ultraviolet. The broad band at 286nm is due to weak π - π^* transition, which can be assigned to conjugation and also n - π^* transition, which can be assigned to the bonding to the conjugated system sulfur. π - π^* and n - π^* transition both increases considerably in wavelength and intensity.

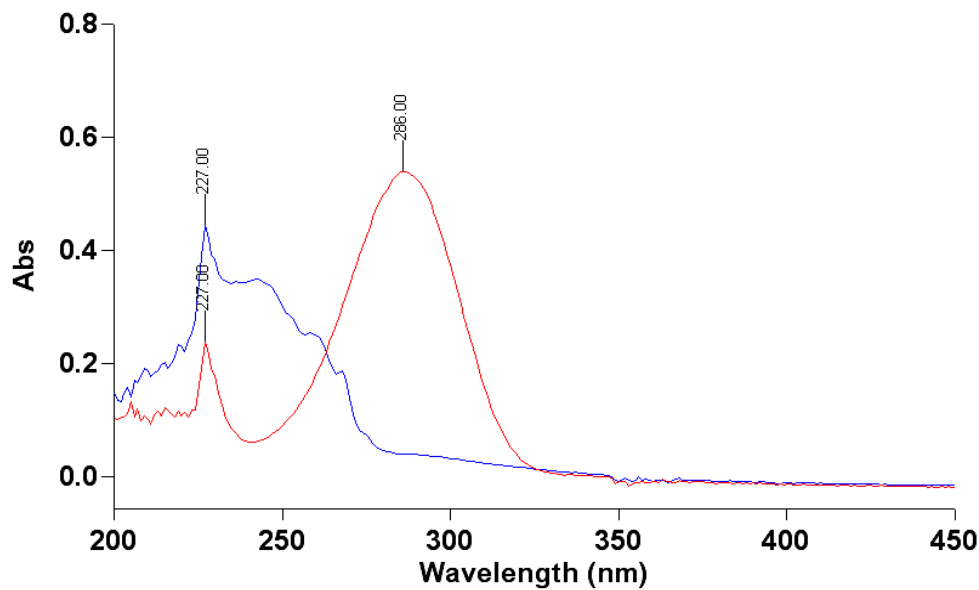


Figure 3.19: UV-VIS spectra of gold(I) phosphine thiolate complexes, with sulfur dioxide (blue-Before, Red- After purging of SO₂)

Matsumi *et al.*⁴⁶ reported that absorption of SO₂ in wavelength region appears from 215-450 nm. It was also reported that fluorescent of aromatic, unsaturated compounds with chemical bonds appears around 220 nm. The data obtained in the study is in agreement with the one reported, because a peak between 250-350 nm after purging of SO₂ is observed.

The ¹H NMR spectra of all the complexes **1-7b** displayed a pattern which was consistent with different environments of all protons of the thiol ligands and the starting materials. ¹³C{¹H} NMR was in agreement with the ¹H NMR. The ³¹P{¹H} NMR spectra of the gold(I) phosphine thiolate complexes displayed a pattern consisting of a singlet, corresponding to the expected phosphine peak.

The Infrared (IR) also confirmed the formation of the thiolated complexes. The absence of thiol (SH) peak and the formation of thiolated (Au-S) were observed. The mass spectrometer ($M^+ = m/z$) showed the molecular peak corresponding to the molecular weight of the synthesized complexes, even though there were lots of fragments.

The electrochemical studies of gold and palladium complexes exhibited the peaks due to either gold or palladium metal. The CV experiments also showed the ligand peaks even though these peaks were not as pronounced as the metal based peaks. The reaction of the gold and palladium complexes with SO_2 were also monitored using cyclic voltammetry. The introduction of SO_2 in the solution containing gold-thiolated complexes exhibited an increase in current densities typical of the catalytic processes. The palladium complexes showed a shift peak potential and this was also typical of the catalytic reaction.

The reactions were further monitored by UV-vis spectroscopy. All the gold thiolated complexes were found to react with sulfur dioxide. The absorption maxima in the UV-vis spectra of the complexes shifted after SO_2 reactions. The change of colour of the solution was also observed upon bubbling of sulfur dioxide gas. This was also in agreement with the results of the UV-vis which clearly indicated the effect of SO_2 when bubbled into the solution of gold-thiolated complexes.

3.8. References:

1. M. Bardaji, M. J. Calhorda, P. J. Costa, *Inorg. Chem.*, **2006**, *45*, 1059.
2. R.V. Parish, P.W. Jonathan, G. R. Pritchard, *J. Organomet. Chem.*, **2000**, *596*, 165.
3. X. Yang, C. Stern, J. J. Marks, *J. Am. Chem. Soc.*, **1994**, *116*, 10015.
4. F. A. Nevondo, A.M. Crouch, J. Darkwa, *J. Chem. Soc., Dalton Trans.*, **2000**, 43.
5. A. Houlton, J. Silver, D. Cunningham, *J. Chem. Soc., Dalton Trans.*, **1992**, 2235.
6. Y.Fuchata, H. Ieda, A. Kayama, J. Nagaoko, H. Kwano, *J. Chem. Soc., Dalton Trans.*, **1998**, 4095
7. E. C. Constable, T. A. Leese, *J. Organomet.*, **1989**, *363*, 419.
8. X. P. Zhang, G. Yang, L. Wang , S. W. Ng, *Acta Cryst.*, **2007**. *63*, 1582.
9. D. Fan, C.T. Yang, J. D. Ranford, J.J. Vittal, *J. Chem. Soc. Dalton Trans.*, **2003**. 4749.
10. D. Fan, C.T. Yang, J. D. Ranford, J. J. Vitta, P. L. Lee, *Dalton Trans*, **2003**, 3376
11. R. Cameron, R. T. Skerlj, *J. Organomet. Chem.*, **2003**, *57*, 67.
12. M. A. Mazid, M.T. Razi, P. J. Sadler, *Inorg. Chem.*, **1981**, *20*, 2872.
13. A. Panella, J. Pons, J. Garcia-Anton, X. Solans, M. Font-Bardia, J. Ros, *Inorg. Chim, Acta*, **2006**, *359*, 4477.
14. A. Panella, J. Pons, J. Garcia-Anton, X. Solans, M. Font-Bardia, J. Ros, *Inorg. Chim, Acta*, **2006**, *359*, 2343.
15. R. Mathieu, G. Esquius, N. Lugan, J. Ros, *Eur. J. Inorg. Chem.*, **2001**, 2683.
16. F. A. Cotton, G. Wilkinson, *Advanced Inorganic Chemistry* , 5th ed., Wiley , New York, **1988**, pg 917-937

17. T. Jiang, G. Wei, C. Turmel, A. E. Bruce, *Metal Based Drugs*, **1994**, *1*, 5.
18. A. A. Mohamed, A. E. Bruce., *Metals Based Drugs*, **1999**, *6*, 4.
19. A. J. Blake, A. Taylor, A. Schroder, *J. Chem. Soc. Chem. Commun.*, 1993, *14*, 1092.
20. J. E. Anderson, S. M. Sawtelle, C. E. McAndrews, *Inorg. Chem.*, **1999**, *29*, 2627.
21. F. A. Cotton, G. Wilkinson, *Advanced Inorganic Chemistry*, 5th ed., Wiley, New York, **1988**, pg 917-937.
22. K. Broadley, G. A. Lane, N. G. Connelly, W. E. Geiger, *J. Am. Chem. Soc.* **1987**, *109*, 402.
23. D. L. Du Bois, A. Miedaner, R. C. Haltiwanger, *J. Am. Chem. Soc.*, **1991**, *113*, 8753.
24. A. J. Downard, L. R. Hanton, R. L. Paul, *J. Chem. Soc., Chem. Commun.*, **1992**, 235.
25. M. Nonomuraac, T. Hobob, *J. Chromatogram*. A836, **1999**, 107..
26. N. Knapp, R. T. Kroutil, *Vibrat. Spectrosc.*, **2001**, *27*, 97.
27. M. A. Gondal, J. Mastromarino, *Appl. Opt.*, **2001**, *40*, 2010.
28. H. Y. Xu, K. M. Wang, D. N. Wang, Q. C. Li, *J. Chem. Chin. Univ.*, **1998**, *19*, 1401.
29. H. Li, Q. Wang, J. Xu, W. Zhang, *Sensors and Actuators*, **2002**, *87*, 18..
30. R.D. Rakhimov, K.P. Grandberg, *J. Organomet. Chem.*, **1994**, *464*, 253.
31. J. Chen, T. Jiang, G. Wei, A. Ahmend, M. C. Homrighausen, K. Bauer, R. M. Mitchell, *J. Am. Chem. Soc.*, **1999**, *121*, 9225.

32. W. B. Jones, J. Yaun, R. Narayanaswamy, M. A. Young, M. R. M. Bruce, *Inorg. Chem.*, **1995**, *34*, 1996.
33. P. G. Eller, G. J. Kubas, *J. Am. Chem. Soc.*, **1997**, *99*, 4346.
34. J. Darkwa, *Inorg. Chim. Acta*, **1997**, *257*, 142.
35. A. J. Appleby, B. Pichon, *J. Electroanal. Chem.*, **1979**, *95*, 59.
36. C. Audry, M. Voinov, *Electrochim. Acta.*, **1980**, *25*, 299.
37. Z. Samec, J. Weber, *Electrochim. Acta.*, **1975**, *20*, 403.
38. E. T. Seo, D. T. Sawyer, *Electrochim. Acta.*, **1965**, *10*, 239.
39. I. R. Moraes, M. Weber, F. C. Nart, *Electrochim. Acta.*, **1997**, *42*, 617.
40. W. L. Davis, R. F. Shango, H. G. E. Langner, J. C. Swarts, *Polyhedron*, **2005**, *24*, 1611.
41. M. B. Dinger, W. Hendeson, B.K. Nicholson, W. T. Robinson, *J. Organomet. Chem.*, **1998**, *560*, 169.
42. K. Umakoshi, A. Ichimura, I. Kinoshita, S. Ooi, *Inorg. Chem.*, **1990**, *29*, 4005.
43. P. N. Mashazi, P. Westbroek, K. I. Ozoemena, T. Nyokong, *Electrochim. Acta*, **2007**, *53*, 1858.
44. J. McMurry, *Fundamentals of Organic Chemistry*, 4th ed, Brooks ;Cole, **1998**, pg 417.
45. C. N. Banwell, E. M. McCash, *Fundamentals of Organic Chemistry*, 4th ed., Brooks;Cole, pg 189.
46. Y. Matsumi, H. Shigemori, K. Takahashi, *Atmso. Env.*, **2005**, *39*, 3177.

CHAPTER 4

CONCLUSIONS

Gold thiolates complexes with general formula $[\text{Au}(\text{SC}_6\text{H}_4\text{X})(\text{PPh}_3)]$ X= Cl, NH₂, CH₂ and $[\text{Au}(\text{SCH}_2(\text{C}_6\text{H}_4)_3(2\text{-C}_6\text{H}_5(\text{C}_6\text{H}_4\text{N})))]$ were prepared by deprotonation of the thiol ligands and their subsequent reactions with $[\text{AuCl}(\text{PPh}_3)]$ and $[\text{AuCl}_3(2\text{-C}_6\text{H}_5(\text{C}_6\text{H}_4\text{N}))]$. The yields were generally moderate to high, ranging from 50 - 70%. The structures of gold(III) precursor, $[\text{AuCl}_3(2\text{-C}_6\text{H}_5(\text{C}_6\text{H}_4\text{N}))]$ and palladium(II) precursor, $[\text{Pd}(\text{Cl}_2)(2\text{-C}_6\text{H}_5(\text{C}_6\text{H}_4\text{N}))]$ as proposed from physical and analytical data were confirmed by single crystal X-ray diffraction studies. Both were found to have a distorted square planar geometry around the gold and palladium metal centre. Detailed characterization of the synthesized complexes all confirmed the structures and the purity of the synthesized ligands and complexes. Several methods of characterization such: NMR, Mass spectrometer, Elemental analysis, UV-vis spectroscopy and Infrared spectroscopy were employed.

It is quite clear that in forming of gold(I)/(III) and palladium(II) thiolates with the thiols used in these reaction, a stronger base is needed to effect the reactions. Surprisingly it was also observed that a simple 2:1 ratio reaction of 2-phenylpyridine and PdCl₂ reaction does not give the expected results. Further experiments and investigation will be pursued in finding a stronger base that could give positive results.

The ^1H NMR spectra of all the complexes **1-7b** displayed a pattern which was consisted with different environments of all protons of the thiol ligands and the starting materials. $^{13}\text{C}\{^1\text{H}\}$ NMR was in agreement with the ^1H NMR. The $^{31}\text{P}\{^1\text{H}\}$ NMR spectra of the gold(I) phosphine thiolate complexes displayed a pattern consisting of a singlet, corresponding to the expected phosphine peak.

The Infrared (IR) also confirmed the formation of the thiolated complexes. The absence of thiol (SH) peak and the formation of thiolated (Au-S) were observed. The mass spectrometer ($\text{M}^+ = m/z$) showed the molecular peak corresponding to the molecular weight of the synthesized complexes, even though there were lots of fragments.

The electrochemical studies of gold and palladium complexes exhibited the peaks due to either gold or palladium metal. The CV experiments also showed the ligand peaks even though these peaks were not as pronounced as the metal based peaks. The reaction of the gold and palladium complexes with SO_2 were also monitored using cyclic voltammetry. The introduction of SO_2 in the solution containing gold-thiolated complexes exhibited an increase in current densities typical of the catalytic processes. The palladium complexes showed a shift peak potential and this was also typical of the catalytic reaction. The reactions were further monitored by UV-vis spectroscopy. All the gold thiolated complexes were found to react with sulfur dioxide. The absorption maxima in the UV-vis spectra of the complexes shifted after SO_2 reactions. The change of colour of the solution was also observed upon bubbling of sulfur dioxide gas. This was also in agreement with

the results of the UV-vis which clearly indicated the effect of SO₂ when bubbled into the solution of gold-thiolated complexes. This clearly indicates that metal thiolates can be used as potential sensors for SO₂. Noting that detailed electrochemistry studies should be performed.

